ANALYTICAL CONSIDERATIONS OF THE STRETCHED EXPONENTIAL/POWER LAW EXPONENTIAL RELATIONS USED FOR TIME-RATE DECLINE CURVE ANALYSIS

A Thesis

by

ALVARO DAVID BETANCOURT SANCHEZ

Submitted to the Office of Graduate and Professional Studies of
Texas A&M University
in partial fulfillment of the requirements for the degree of

MASTER OF SCIENCE

Chair of Committee,	Thomas A. Blasingame
Committee Members,	I. Yucel Akkutlu
	Maria A. Barrufet
	Peter Valkó
Head of Department,	A. Daniel Hill

August 2017

Major Subject: Petroleum Engineering

ABSTRACT

Since their introduction to the petroleum literature in 2008/2009, the stretched exponential (SE) and the power-law exponential (PLE) relations have become the "conservative" standard for time-rate (decline curve) analysis of well performance data from low/ultra-low permeability reservoirs. The origins of the SE relation can be traced to Rudolf Kohlraush circa 1854; however, its use as an expression for time-rate production data analysis essentially began in 2009 with Valkó. The PLE time-rate relation, on the other hand, was derived empirically (and independently) from observations of well performance data by Jones in 1942 and by Ilk and Blasingame in 2008. To date, there is no "proof" of the SE/PLE from a theoretical basis; however, there are many references devoted to the characteristic functions which have been proposed or derived from the given form of these relations.

In this work, we attempt to provide analytical and semi-analytical bases/relations for the SE/PLE functional form to deliver insight on its mathematical behavior and to offer an understanding of its performance as a production forecasting tool. Our first approach consists on approximating the SE/PLE relation by a truncated sum-of-exponentials providing that the SE/PLE model behave as a linear superposition of exponentially decaying functions. For completeness, we extend this work to approximate the hyperbolic and modified hyperbolic time-rate relations with this mentioned sum-of-exponentials function.

Next, we develop numerical approximations of the SE/PLE relation in the Laplace domain using three approaches — using the Taylor series expansion, the Laguerre quadrature, and applying the methodology proposed by Blasingame which transform a piecewise power-law function into the Laplace domain. Our goal in this section is to use the Laplace transform and the convolution identity to resolve the SE/PLE decline model in the Laplace domain with the perspective that there may be some sort of diagnostic capability or another sort of mathematical identity, which in the process, may arise.

The last part of this work is devoted to "reverse engineer" the flowing bottomhole pressure required to generate a specific SE/PLE case using numerical reservoir simulation. By means of the pseudosteady-state flow equation, the material balance equation, and a prescribed time-rate model (for our case, the SE/PLE, and the hyperbolic time-rate relations), we are able to get a mathematical expression for the flowing bottomhole pressure as a function of time. This mathematical model will be compared against well performance obtained from numerical reservoir simulation. This part of the "reverse engineering" approach provides a "proof of concept" of the validity of the SE/PLE time-rate relation and corroborates the derived functional form of the flowing bottomhole pressure.

ACKNOWLEDGEMENTS

I would like to thank my committee chair, Dr. Thomas A. Blasingame for teaching me that "perfection is the standard," for his patience during these past two years and for making me feel that I have an "advisor" that I can count on and trust.

I want to express my gratitude to my advisory committee members, Dr. I. Yucel Akkutlu, Dr. Maria A. Barrufet and Dr. Peter Valkó, for their valuable teachings through my studies at Texas A&M.

Finally, I would like to thank and acknowledge all the people in the "Blasingame Research Group" for their friendship and support.

CONTRIBUTORS AND FUNDING SOURCES

Contributors

This work was supervised by a thesis committee consisting of Professor Thomas A. Blasingame and Professors I. Yucel Akkutlu, Maria A. Barrufet and Peter Valkó of the Petroleum Engineering Department.

All work for the thesis was completed by the student, in collaboration with Professor Thomas A. Blasingame of the Petroleum Engineering Department.

Funding Sources

Graduate study was supported by a scholarship from Secretaría de Educación Superior, Ciencia, Tecnología e Innovación of the Republic of Ecuador.

TABLE OF CONTENTS

LIST OF FIGURES

LIST OF TABLES

CHAPTER I

INTRODUCTION

I.1 Motivation

The stretched exponential (SE) relation (and the power-law exponential (PLE) relation by extension) have been used to model various physical phenomena since the nineteenth century. In the petroleum industry, the SE/PLE relation has been the "conservative" standard for decline curve analysis of production data from low/ultra-low permeability (unconventional) reservoirs. Although empirical in nature, the SE/PLE relation has proven effective in describing oil and gas production from transient to boundary-dominated flow regimes. The motivation of this work comes from this accurate performance of the SE/PLE relation. However, to date, has no formal proof and raises questions about the fundamental principles that govern its behavior. We attempt to provide analytical and semi-analytical insight/bases on the SE/PLE relation as our primary goal, opening the path for subsequent research to understand the fundamental principles that yield this particular and elegant mathematical expression for well performance.

I.2 Objectives

The primary objective of this work is to provide analytical and semi-analytical bases/relations for the SE/PLE relation and to deliver insight on its mathematical behavior as a mechanism for production forecasting and estimated ultimate recovery (EUR) computation. To achieve this primary objective, we provide the following supporting or specific objectives:

- To derive semi-analytical approximations for the SE/PLE relation in terms of exponential series. For the SE relation, the exponential series formulation has been suggested by many authors, and in many different fields, the goal of this objective is to prove this formulation (if possible).
- To generate the SE/PLE rate solution in the Laplace domain so that this relation can be solved for the pressure response function. In short, to create SE/PLE pressure solution(s) in the real domain.
- To "reverse engineer" the bottomhole pressure profile required to generate a specific SE/PLE case. This requires the use of a reservoir model and depends (very) heavily on the well configuration and the particular flow regime (*i.e.*, transient, pseudosteady-state, or a transition regime).

I.3 Statement of the Problem

Ilk et al. (2008) developed the PLE time-rate decline model from empirical observations to analyze well performance data from low/ultra-low permeability reservoirs where production exhibits a non-hyperbolic behavior. This model is based on the observed behavior of the decline coefficient (Eq. 1.1), which starts as a decaying power-law function transitioning to a constant value at later times (D_∞) giving the traditional exponential decline relation. This characteristic provides the PLE relation the ability to model transient to

boundary-dominated flow behavior. The PLE decline parameter model is specifically given as,

$$D = -\frac{1}{q}\frac{dq}{dt} = D_\infty + n\hat{D}_i t^{n-1} \quad \text{.....(1.1)}$$

Integrating Eq. 1.1 we obtain the time-rate relation for the PLE decline model as follows,

$$q(t) = \hat{q}_i \exp[-D_\infty t - \hat{D}_i t^n], \quad \text{.....(1.2)}$$

where $\hat{q}_i$ is the initial rate coefficient, D_∞ is the terminal decline coefficient, $\hat{D}_i$ is the decline coefficient, and n is the time exponent.

Valkó (2009) introduced the SE decline model in the petroleum literature (Eq. 1.3) while working on an extensive production data set from the Barnett Shale. Valkó stated that this model is completely empirical — as is the original Arps' decline models. The mathematical expression for the SE decline model is given by,

$$q(t) = \hat{q}_i \exp\left[-\left[\frac{t}{\tau}\right]^n\right], \quad \text{.....(1.3)}$$

where $\hat{q}_i$ is the initial production rate, n is the time exponent, and τ is the "characteristic time" or time coefficient. The stretched exponential decline (SE) model is identical to the power-law exponential (PLE) model when the terminal decline coefficient, D_∞, is equal to zero (*i.e.*, neglecting the terminal exponential decline that Ilk et al. (2008) employed to represent boundary-dominated flow behavior). Assuming $D_\infty = 0$, Eq. 1.2 becomes,

$$q(t) = \hat{q}_i \exp[-\hat{D}_i t^n] \quad \text{.....(1.4)}$$

By inspection, Eq. 1.3 and Eq. 1.4 are equivalent if the decline coefficient for the PLE model is given by,

$$\hat{D}_i = \left[\frac{1}{\tau}\right]^n \quad \text{.....(1.5)}$$

Eq. 1.4 is our base mathematical expression. Transforming Eq. 1.4 into a dimensionless form, we define the following dimensionless variables for rate and time:

$$q_D = \frac{q(t)}{\hat{q}_i}, \quad \text{.....(1.6)}$$

$$t_D = \frac{t}{\hat{D}_i^{-1/n}}, \quad \text{.....(1.7)}$$

and substituting these relations into Eq. 1.4 to yields,

$$q_D(t_D) = \exp[-t_D^n] \quad \text{.....(1.8)}$$

Eq. 1.8 is the dimensionless form of the SE/PLE decline model. For reference, we present, graphically, the behavior of Eq. 1.8 for various time exponent, n, values in **Fig. 1.1.**

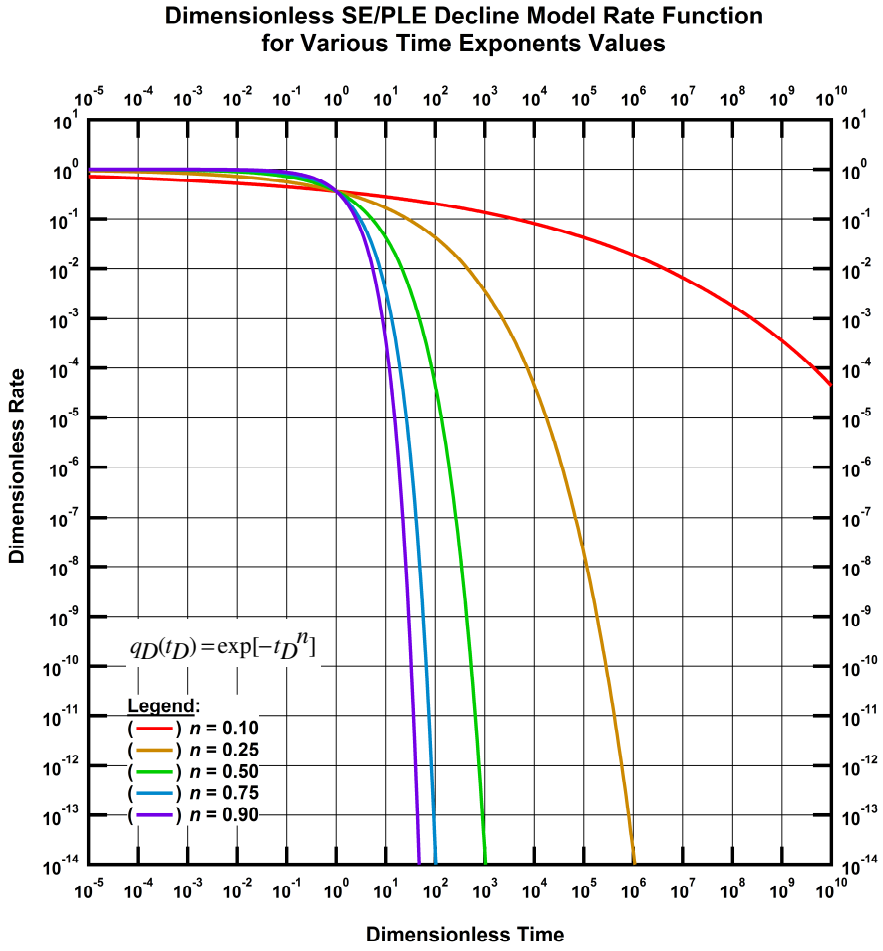

Figure 1.1 — Dimensionless rate functions, various SE/PLE Cases.

Approximation by Sum-of-Exponentials:

Our efforts are focused on the approximation of the SE/PLE by a sum-of-exponentials function. In particular, we propose that the SE/PLE model behaves as a linear superposition of exponentially decaying functions — given mathematically as,

$$q_D(t_D) \equiv \sum_{i=1}^{\infty} a_i \exp[-c_i t_D] \,, \quad \text{.....(1.9)}$$

where the a_i and c_i parameters in Eq. 1.9 are the coefficients to be determined. Considering Eq. 1.9, for a given value of the time exponent n, there is a particular approximation by sum-of-exponentials (*i.e.*, a specific set of a_i and c_i coefficients). Another issue is that we cannot determine an infinite number of coefficients, and we will need to establish a minimum number of coefficients that can be determined. In this sense, Eq. 1.9 is now written as an approximation,

$$q_D(t_D) \approx \sum_{i=1}^{i_{\max}} a_i \exp[-c_i t_D] \,, \quad \text{.....(1.10)}$$

For completeness, the approximation by sum-of-exponentials is extended to the cases of the hyperbolic (HYP) and modified-hyperbolic (MH) decline models. The original dimensionless hyperbolic decline model is given, by Arps, as,

$$q_D(t_D) = \frac{1}{[1+bt_D]^{1/b}} \quad \text{.....(1.11)}$$

The so-call dimensionless modified-hyperbolic (MH) decline model is given by,

$$q_D(t_D) \equiv \begin{cases} \dfrac{1}{[1+bt_D]^{1/b}} & (D_D < D_{Dlim}) \\ q_{Dlim} \exp[-D_{Dlim}[t_D - t_{Dlim}] & (D_D \geq D_{Dlim}) \end{cases} \qquad \begin{aligned} q_{Dlim} &= [D_{Dlim}]^{1/b} \\ t_{D\lim} &= \frac{1}{b}\left[\left[\frac{1}{q_{Dlim}}\right]^{b} - 1\right] \\ D_{Dlim} &= D_{lim}/D_i \end{aligned} \quad \text{.....(1.12)}$$

An example of the time-rate decline models considered in this work (exponential, hyperbolic, modified-hyperbolic, and power-law exponential time-rate models) are shown in dimensionless format in **Fig. 1.2**.

Laplace Transform of the SE/PLE Functions:

The Laplace transform has been widely used in the petroleum literature to solve flow problems that are not well-posed for real domain solutions. The primary advantage of the Laplace transform is that it can be used to reduce certain partial differential equations into a form where an analytical solution can be obtained in the Laplace domain. The "trick" then becomes the inversion of the Laplace domain solution into the real domain, and this often requires the use of (approximate) numerical inversion algorithms.

Another application of the Laplace transform that is very popular in the petroleum literature is the practice to resolve variable-rate/variable-pressure drop problems in using the convolution identity — which in the real domain is a "convolution" integral, but in the Laplace domain, this identity becomes a multiplication of

two functions in the Laplace domain. Our goal is to use the Laplace transform and the convolution identity to resolve the SE/PLE decline model in the Laplace domain with the perspective that there may be some sort of diagnostic capability or another sort of mathematical identity which may arise. Also, we can use the convolution identity to try to establish if the SE/PLE decline model has some unique relationship with either a constant rate or constant pressure formulation.

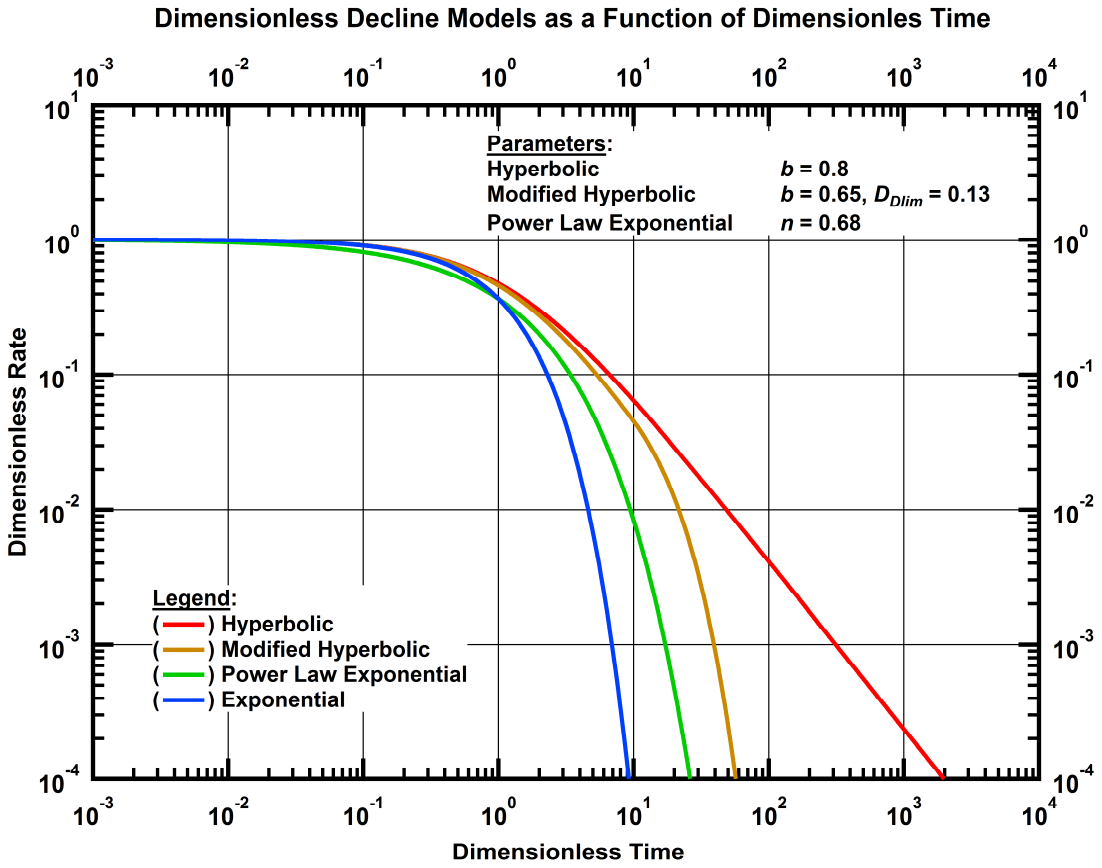

Figure 1.2 — Dimensionless rate function, various time-rate models (exponential, hyperbolic, modified-hyperbolic, and power-law exponential).

In particular, the constant rate/constant pressure formulation in the Laplace domain is given as,

$$\bar{p}_{Dcr}(u) = \frac{1}{u^2 \bar{q}_{Dcp}(u)} \quad \text{.....(1.13)}$$

In simple language, there is no direct Laplace transform of the general form of Eq. 1.8 (*i.e.*, for a general value of the time exponent, n) — except for very specific cases (*e.g.*, n = 1/2 or 1). To develop a comprehensive understanding of the behavior of Eq. 1.8 in the Laplace domain, we will test three different

numerical approaches in order to find an approximation in Laplace domain:

- Approximate the SE/PLE relation by Taylor series expansion, and then take the Laplace transform.
- Use the Laguerre quadrature formulation to transform a general function into the Laplace domain.
- Use the Blasingame (1995) approach to take the Laplace transform of a piecewise power-law function.

Prediction of Flowing Bottomhole Pressure (assuming pseudosteady-state flow behavior):
Using known solutions (*i.e.*, reservoir models), we substitute the SE/PLE decline model as flowrate for a variety of cases to establish the flowing bottomhole pressure trends. This is a "reverse engineering" problem because we know the properties of the reservoir, and we are attempting to determine if there are any unique features of the bottomhole pressure response generated using an imposed SE/PLE flowrate model. As an example, for the case of an imposed exponential decline flowrate model, the bottomhole pressure response during pseudosteady-state is constant (this can be easily derived from the material balance relation and the pseudosteady-state flow relation).

Using a similar concept as the derivation of the exponential decline flowrate relation, we will begin with the oil material balance relation and the oil pseudosteady-state flow relation, these are,

$$\overline{p} = p_i - m_{o,pss}\, N_p \quad \left[\text{where } m_{o,pss} = \frac{B_o}{B_{oi}}\frac{1}{Nc_t}\right] \text{ (oil material balance relation), and} \qquad (1.14)$$

$$\overline{p} = p_{wf} + b_{o,pss}\, q_o \quad \left[\text{where } b_{o,pss} = 141.2\frac{\mu_o B_o}{kh}\left[\frac{1}{2}\ln\left[\frac{4}{e^{\gamma}}\frac{1}{C_A}\frac{A}{r_w^2}\right] + s\right]\right]$$

(oil pseudosteady-state flow relation) ..... (1.15)

Combining Eq. 1.14 and Eq. 1.15 we obtain,

$$p_{wf} = p_i - b_{o,pss}\, q_o - m_{o,pss}\, N_p \qquad (1.16)$$

Eq. 1.16 is rigorous for pseudosteady-state flow in an undersaturated black-oil reservoir. We now begin the "reverse engineering" process by using the SE/PLE flowrate and cumulative production profiles, where these relations are given as,

$$q_o(t) = \hat{q}_{oi}\exp[-\hat{D}_i t^n] \text{ (SE/PLE flowrate relation)} \qquad (1.17)$$

$$N_p(t) = \hat{q}_{oi}\frac{\hat{D}_i^{-1/n}}{n}\left[\Gamma\left[\frac{1}{n}\right] - \Gamma\left[\frac{1}{n}, \hat{D}_i t^n\right]\right] \text{ (SE/PLE cumulative production relation)} \qquad (1.18)$$

Finally, substituting Eq. 1.17 and Eq. 1.18 into Eq. 1.16 we obtain,

$$p_{wf} = p_i - b_{o,pss}\,\hat{q}_{oi}\exp[-\hat{D}_i t^n] - m_{o,pss}\,\hat{q}_{oi}\,\frac{\hat{D}_i^{-1/n}}{n}\left[\Gamma\left[\frac{1}{n}\right] - \Gamma\left[\frac{1}{n}, \hat{D}_i t^n\right]\right] \quad \text{.....(1.19)}$$

As with Eq. 1.16, Eq. 1.19 is rigorous for the conditions of pseudosteady-state flow behavior in an undersaturated black-oil reservoir. While there is no empiricism in Eq. 1.19, we would have to adhere specifically to the stated conditions for an exact solution. Our "reverse engineering" approach will be to impose Eq. 1.17 (*i.e.*, the SE/PLE flowrate relation) on a numerical reservoir simulation model, and validate the pressure profile given by Eq. 1.19. We will also use simplified models to represent these generated pressure profiles to assess whether or not we can establish a time-dependent, flowing bottomhole pressure condition that will produce the SE/PLE time-dependent flowrate profile.

I.4 Organization of the Thesis

This thesis manuscript is organized in chapters with the following structure: Chapter I provides the introductory section which includes a brief motivation statement for this work, the general and specific objectives to achieve, and a comprehensive description of the problems at hand. Chapter I serves as an outline of our work which will be further developed in following chapters.

Chapter II presents in detail the literature reviewed and analyzed for the topics presented in this work, starting with the history of the stretched exponential function, following with the historical and modern time-rate analysis in the petroleum literature. Chapter III covers the main study of the stretched exponential (SE)/power-law exponential (PLE) function. In this chapter, we divide our work into three categories: first the SE/PLE approximation by sum-of-exponentials function, followed by the Laplace transform of the SE/PLE model, to finalize with the prediction of the flowing bottomhole pressure response that a specific SE/PLE case would generate.

Finally, Chapter IV provides a summary of the study, detailed concluding remarks, and recommendation statements. Closing this manuscript, we have the nomenclature and references sections which are followed by four appendices. Appendix A presents the dimensionless hyperbolic, modified hyperbolic, and power-law exponential decline models approximation by a sum-of-exponentials function. Appendix B describes the Laplace transform of the dimensionless stretched exponential/power-law exponential decline model with $n = 0.50$. Appendix C presents the dimensionless power-law exponential decline model in Laplace domain approximations. Finally, in Appendix D we show the validation of time-rate flow relations assuming pseudosteady-state flow behavior: exponential, hyperbolic, and stretched exponential/power-law exponential cases.

CHAPTER II

LITERATURE REVIEW

II.1 Stretched Exponential Function History

The first introduction of the stretched exponential function is attributed to Rudolf Kohlrausch (1854) when attempting to interpret charge relaxation in a Leiden jar (a device used to store electric charge between two electrodes). His mathematical expression is,

$$Q_t = Q_o \exp[-Bt^{\alpha}] \quad \text{.....(2.1)}$$

Time later, the stretched exponential was "rediscovered" by Williams and Watts (1970), who independently developed an empirical dielectric decay function, given by,

$$\gamma(t) = \exp[-(t/\tau_0)^{\beta}] \text{ ,} \quad \text{.....(2.2)}$$

to model relaxation phenomena of amorphous polymers. Since then, the stretched exponential was also known as the William-Watts function or the Kohlrausch-Williams-Watts function. As an aside, we notice that the stretched exponential is a complementary cumulative distribution for the Weibull density (Weibull 1951), mathematically expressed as,

$$D(x) = 1 - e^{-(x/\beta)^{\alpha}} \text{ ,} \quad \text{.....(2.3)}$$

which has been applied in many science and engineering fields. The mathematical behavior of Eq. 2.3 is presented graphically in **Fig. 2.1.** An essential reference of the stretched exponential function is the one given by Palmer et al. (1984) where they used the stretched exponential as an anomalous relaxation law for strongly interacting glassy materials. Although these researchers mentioned Kohlrausch as the first introduction of the function, their citation mentioned his 1847 work (Kohlrausch 1847). In reviewing this paper (written in German) we could not find a specific mathematical expression related to the stretched exponential. For completeness, we notice that some references mention the work of Friedrich Kohlrausch (1863), the son of Rudolf Kohlrausch, in mechanical relaxation of galvanometric threads as the first introduction of the stretched exponential, mistakenly. Additionally, the phrase "stretched exponential" seems to first appear in the work of Chamberlin et al. (1984) when referring to a functional form to model time decay of the remnant magnetization in spin-glasses; their mathematical expression is given by,

$$\sigma_{TRM} = \sigma_0 \exp[-C(\omega t)^{1-n}/(1-n)] \quad \text{.....(2.4)}$$

In the petroleum literature, Arps (1945) gave, as part of his review of development of decline-curve analysis,

a rate-time model attributed to Jones (1942) as follows,

$$q = q_0 \exp\left[\frac{D_0 t^{1-m}}{100(m-1)}\right], \quad \text{.....(2.5)}$$

Which was defined as an approximation for wells declining at variable rates *whereby the decline-time relationship follows a straight line on log-log paper.* Finally, there is the decline model presented by Valkó (2009) using the stretched exponential for low/ultra-low permeability reservoirs, presented in more detail in the next section.

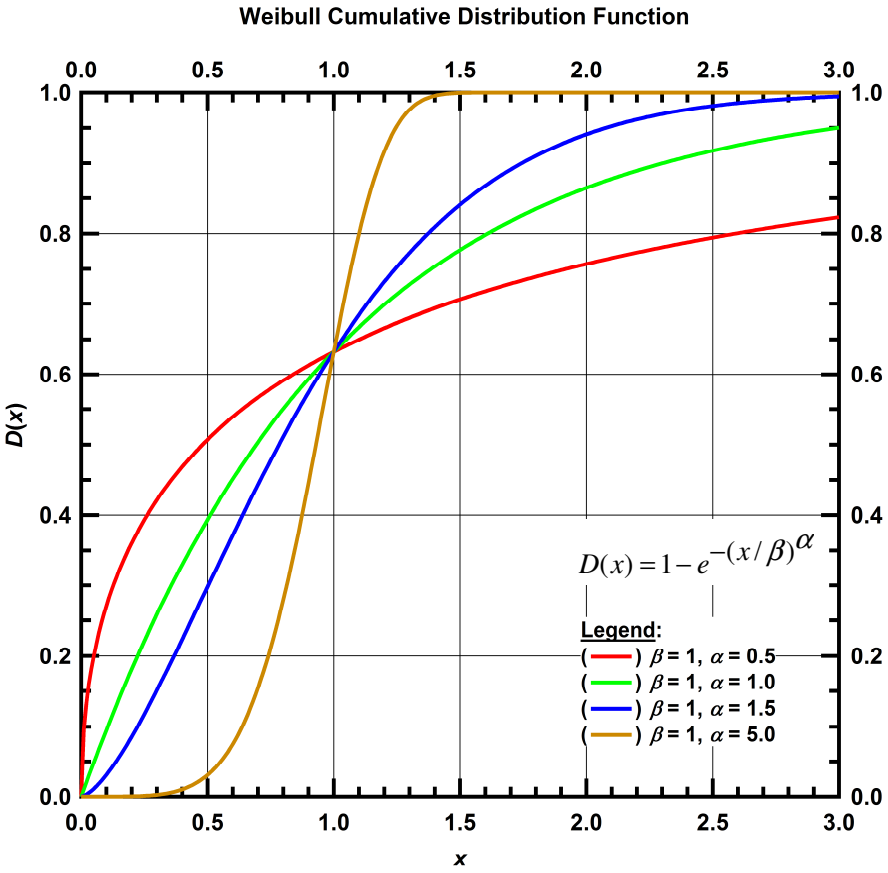

Figure 2.1 — Weibull cumulative distribution function behavior.

II.2 Historic Time-Rate Analysis

Decline curve analysis — better known by its initials DCA — is a methodology, commonly used in the petroleum industry, based on the analysis of historical production rates of oil and gas wells and the extrapolation of their future performance. Using a graphical approach as the preferred diagnostic tool,

stabilized production trends are identified, and rate-time decline models are selected to fit those trends. Once the decline model is calibrated, the extrapolation of rate in future time to an economic limit provides the estimated ultimate recovery (EUR) of the well under analysis. Many time-rate models have been developed since the early twentieth century, and they have evolved to capture contemporary trends in well performance as the industry departs from the conventional to the low/ultra-low permeability unconventional resources. We trace decline curve analysis from the initial attempts to describe well performance to more sophisticated developments in time-rate models.

The beginnings of production data analysis can be traced to the seminal work of Lewis and Beal (1918) in which the authors used their so-called *appraisal curves* to make estimates of future production by constructing percentage decline curves and cumulative percentage curves. Their idea behind using percent flowrate was to compare different wells with different performance by looking at their decline tendency. Additionally, the authors stated that many production records from various wells yield straight lines in a logarithmic plot, making the extrapolation process more straightforward and accurate. Later, Cutler (1924) delivered a broad review — prepared for the US Bureau of Mines — on the estimation of future production and reserves using production-decline curves. The author acknowledges the value — and better accuracy than others to-date methods — of decline models as a forecasting tool whenever adequate data is available. In his work, it was noted that production trends *assume approximately the shape of a hyperbola*; therefore, the extrapolation of production in time could be done linearly in a log-log plot avoiding sources of error.

Johnson and Bollens (1927), acknowledging that there were limitations to extrapolating rate in time when there is no clear straight line in a logarithmic plot, first presented the loss ratio and the loss ratio derivative concepts — mathematically expressed in Eqs. 2.6, and 2.7; which are the basic functions that define the modern decline parameters; *i.e.*: the decline coefficient ($D(t)$) and the decline exponent ($b(t)$) — to overcome the irregularity and lack of accuracy in flowrate data. The authors worked with yearly production data and found the derivatives in a finite difference fashion to extrapolate the loss ratio and then compute future flowrates.

$$\frac{1}{D(t)} = -\frac{q(t)}{dq(t)/dt} \quad \text{.....(2.6)}$$

$$b(t) = \frac{d}{dt}\left[\frac{1}{D(t)}\right] = -\frac{d}{dt}\left[\frac{q(t)}{dq(t)/dt}\right] \quad \text{.....(2.7)}$$

Arps (1945), after assembling a comprehensive compilation of decline-curve analysis developments, presented, "formally", the basic decline relations (*i.e.*, exponential and hyperbolic) to determine the well's most likely future production. His approach was to consider that the most readily accessible variable characteristic of a producing well is its production rate and that by extrapolating this variable — against

time or cumulative production — yields the economic limit of such. Arps noted that the basic reservoir characteristics needed to deal with decline curves are: a close reservoir, pressure is proportional to the amount of remaining oil, and production rates are proportional to reservoir pressure. The empirical character of this approach reflects that future behavior is governed by past performance. The exponential and hyperbolic decline relations are presented in Eq. 2.8, and Eq. 2.9, respectively,

$$q(t) = q_i \exp[-D_i t] , \quad (2.8)$$

$$q(t) = \frac{q_i}{[1 + bD_i t]^{1/b}} , \quad (2.9)$$

where, D_i is the initial decline coefficient, and b is de decline exponent. Arps stated that if the loss ratio is constant or nearly constant, then the well performance is exponential; whereas, if the loss ratios indicate a regular arithmetic series and the derivatives of the loss ratios (b values) are constant, then the well performance is hyperbolic. Additionally, he noted that most hyperbolic decline curves appear to be characterized by decline exponents between 0 and 1, *with the majority between* 0 *and* 0.4. Arps also presented the mathematical expressions for cumulative production time-rate relations for the exponential and hyperbolic decline models as follows,

$$Q(t) = \frac{q_i}{D_i}\left[1 - \exp(-D_i t)\right], \quad (2.10)$$

$$Q(t) = \frac{q_i}{(1-b)D_i}\left[1 - (1 + bD_i t)^{1-1/b}\right] \quad (2.11)$$

Some researchers worked describing the influence that reservoir properties have on decline curves; Gentry and McCray (1978) were some of them. Using numerical simulation they found that relative permeability changes (reservoir heterogeneity) have a significant impact on the decline exponent, b, producing slightly larger values than 1 in some cases, while fluid characteristics have a bearing on the initial flowrate, q_i, and the decline coefficient, D_i. Following this work, Maley (1985) established that the decline exponent, b, often does exceed the value of 1 analyzing low-permeability fractured tight gas wells exhibiting linear flow. Therefore, Arps' equations were unsuitable — and need improvement — to be used in the decline analysis of flowrate from a low-permeability reservoir.

II.3 Modern Time-Rate Analysis

Robertson (1988) proposed a more general time-rate equation, the so-called modified hyperbolic decline model which combine the hyperbolic and exponential expressions. This approach provides a mean to extract uses a hyperbolic trend at early production times, and "splices" an exponential trend at late time to represent a specified "terminal" decline. Additionally, it is noted by the author that the decline exponent (b) exceeding

the value of 1 is most likely associated with multiple strata wells and fractured formations. The author presented the following mathematical expression,

$$q(t) = \frac{q_i(1-\beta)^{1/b}\exp[-at]}{[1-\beta\exp[-at]]^{1/b}}, \quad (2.12)$$

where the parameter a is the asymptotic exponential decline rate, and the parameter β is responsible for several desirable characteristics of Eq. 2.12 and is determined by abandonment pressure and the rock and fluid characteristics. For the range $0 < \beta \leq 1$, decline curves are generated from purely exponential to purely hyperbolic. In contrast to Eq. 2.12, the most common form of the "modified hyperbolic" decline model, given in a piecewise fashion, is expressed by:

$$q(t) = \begin{cases} \dfrac{q_i}{[1+bD_it]^{1/b}}, & D > D_{lim} \\ q_{lim}\exp[-D_{lim}[t-t_{lim}], & D \leq D_{lim} \end{cases}, \quad (2.13)$$

where,

$$q_{lim} = q_i\left[\frac{D_{lim}}{D_i}\right]^{1/b}, \quad (2.14)$$

$$t_{lim} = \frac{[q_i/q_{lim}]^b - 1}{bD_i} \quad (2.15)$$

Ilk et al. (2008) developed a power-law exponential (PLE) decline model relation to analyze well performance data from low/ultra-low permeability reservoirs where production has a non-hyperbolic behavior. This model is based on the observed behavior of the decline coefficient (Eq. 2.16) which starts as a decaying power-law function transitioning to a constant value at later times (D_∞) giving the traditional exponential decline relation (graphically in **Fig. 2.2**).

$$D = -\frac{1}{q}\frac{dq}{dt} = D_\infty + n\hat{D}_i t^{n-1} \quad (2.16)$$

Integrating Eq. 2.16 we obtain the relation for the PLE decline model as follows,

$$q(t) = \hat{q}_i \exp[-D_\infty t - \hat{D}_i t^n] \quad (2.17)$$

In this time-rate model, $\hat{q}_i$ is the initial rate coefficient, D_∞ is the terminal decline coefficient, $\hat{D}_i$ is the decline coefficient, and n is the time exponent.

Later, Valkó (2009), while working on an extensive production history from the Barnett Shale, introduce

the stretched exponential (SE) decline model (Eq. 2.18). Valkó stated that this model is completely empirical — as the original Arps' decline models — yet it is based on *a defining differential equation that is non-autonomous*; additionally, he noted that this model was developed for data where time is periodically taken. The mathematical expression for the SE decline model is given by:

$$q(t) = \hat{q}_i \exp\left[-\left(\frac{t}{\tau}\right)^n\right] \quad \text{.....(2.18)}$$

where $\hat{q}_i$ is the initial production rate, n is the time exponent, and τ is the characteristic number of periods or time coefficient. It is important to note that the stretch exponential decline model is identical to the power-law exponential decline model when the terminal decline coefficient, D_∞, is equal to zero.

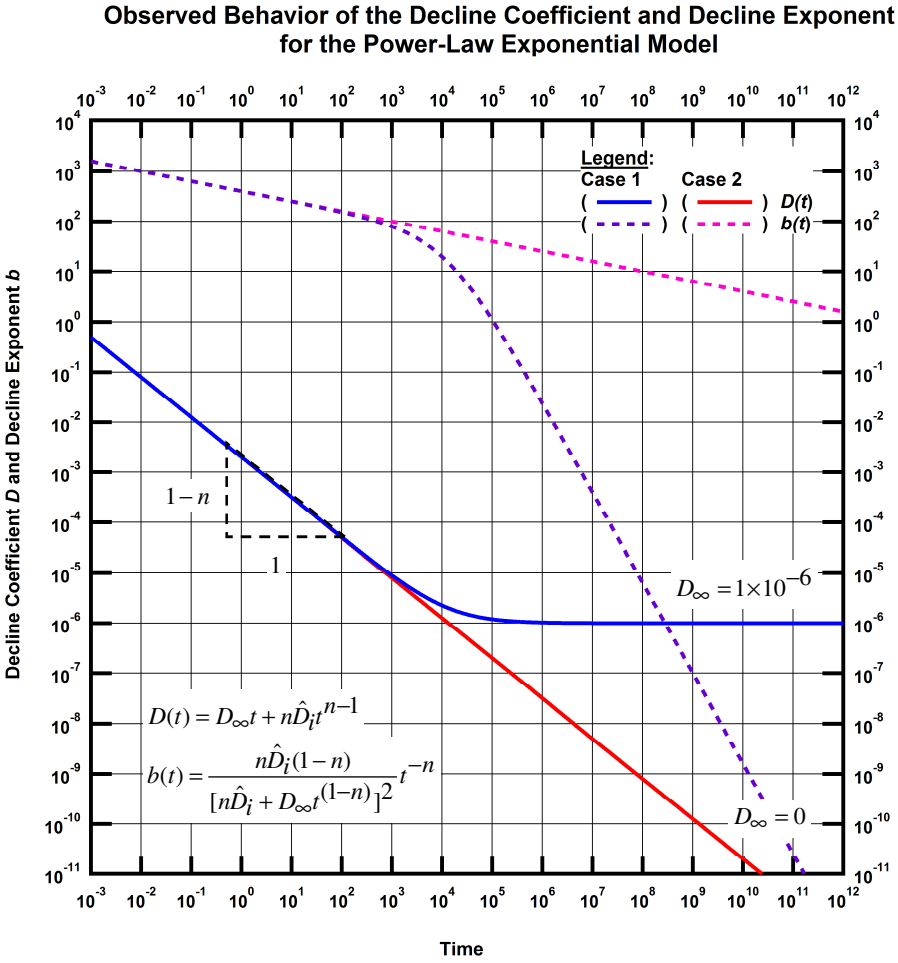

Figure 2.2 — Observed behavior of the decline parameters ($D(t)$ and $b(t)$) for the SE/PLE decline model.

In another publication, Ilk et al. (2010) noted that the stretched exponential model behaves as a superposition of exponential decays; given as follows:

$$q(t) \equiv \sum_{i=1}^{n} q_i \exp[-a_i t] \quad \text{.....(2.19)}$$

Therefore, it can be used to model decaying processes in heterogeneous systems which is the case of low/ultra-low permeability reservoirs. These authors matched the production from a tight gas field with a single, double and four exponential functions and concluded that it seems to fit. As comment, the "superposition of exponential decays" has been pursued by authors working specifically on the stretched exponential model in other fields, Ilk et al. (2010) were just the first to do so in the petroleum literature.

Duong (2011) proposed a novel approach introducing an empirical decline model for fracture-dominated wells in tight and shale gas reservoirs. In his work, the author presents a step-by-step procedure to analyze individual wells by fitting a two-coefficient model — the intercept constant, *a*, and the slope, *m*. on a specialized plot. The time-rate mathematical formulation given by Duong is given as follows:

$$q(t) = q_1 t^{-m} \exp\left[\frac{a}{1-m}\left[t^{(1-m)} - 1\right]\right] \quad \text{.....(2.20)}$$

Clark et al. (2011) proposed — mentioned by the authors as easy to use and capable — a production forecasting model based on a specific subcategory of the generalize logistic growth model called hyperlogistics. The authors used a mathematical expression used in biology (a model for hyperbolic liver regrowth) and adapted it to oil and gas variables where the growth, in this case, is the cumulative production, to give,

$$Q(t) = \frac{Kt^n}{a + t^n} \quad \text{.....(2.21)}$$

Taking the derivative of Eq. 2.21, to obtain flowrate, we have,

$$q(t) = \frac{dQ(t)}{dt} = \frac{Knbt^{(n-1)}}{[a + t^n]^2} \quad \text{.....(2.22)}$$

This model has three parameters: the carrying capacity *K*, the hyperbolic exponent *n*, and the constant *a*. Where the production for low/ultra-low permeability reservoirs exhibits a hyperbolical decline, the logistic growth model matches well performance with good accuracy.

Fulford and Blasingame (2013) presented the transient hyperbolic relation to analyze rate-time well performance from low/ultra-low permeability reservoirs. This model includes an early and late time

hyperbolic behavior which attempts to resemble the flowrate profile in the initial clean-up portion and the transitional and final hyperbolic behavior. The time-rate model is obtained from the transient hyperbolic decline exponent (b) given by,

$$b(t) = b_{\max} - (b_{\max} - b_{\min}) \exp[-\exp[-c(t - t_{eff}) + \exp[\gamma]]] \quad \text{.....(2.23)}$$

where b_{max} is maximum hyperbolic coefficient, b_{min} is the minimum hyperbolic coefficient, t_{elf} is the time to end of linear flow, γ is the Euler-Mascheroni constant, and c is the scaling factor given by $\exp[\gamma]/1.5t_{elf}$. The logistic transition of the b-parameter of this model represents the change between binary states in the reservoir which is proportional to the transition time.

As concluding remarks, we have covered/reviewed the time-rate models commonly used in the petroleum industry. Many/most of the time-rate models are empirical in nature and we note that there have not been a substantial number of studies devoted to the analytical derivation of such models, hence the motivation for this research.

CHAPTER III

STUDY OF THE STRETCHED EXPONENTIAL/POWER-LAW EXPONENTIAL RELATIONS

III.1 Approximation by Sum-of-Exponentials

To begin our development, we recall the dimensionless form of the stretched exponential/power-law exponential (SE/PLE) decline model,

$$q_D(t_D) = \exp[-t_D^n] \quad \text{.....(3.1)}$$

Eq. 3.1 is our base mathematical expression to approximate with the sum-of-exponentials function. For completeness, we recall the dimensionless hyperbolic and modify hyperbolic relations in Eq. 3.2 and Eq. 3.3, respectively. For reference, Appendix A presents in detail how we obtain the dimensionless form of these decline models.

$$q_D(t_D) = \frac{1}{[1+bt_D]^{1/b}} \quad \text{.....(3.2)}$$

$$q_D(t_D) \equiv \begin{cases} \dfrac{1}{[1+bt_D]^{1/b}} & (D_D < D_{Dlim}) \\ q_{Dlim}\exp[-D_{Dlim}[t_D - t_{Dlim}] & (D_D \geq D_{Dlim}) \end{cases} \qquad \begin{aligned} q_{Dlim} &= [D_{Dlim}]^{1/b} \\ t_{D\lim} &= \frac{1}{b}\left[\left[\frac{1}{q_{Dlim}}\right]^b - 1\right] \\ D_{Dlim} &= D_{lim}/D_i \end{aligned} \quad \text{.....(3.3)}$$

As stated before, we focus on the approximation of the SE/PLE by a sum-of-exponentials function; additionally, we extend this work to the hyperbolic and modify hyperbolic decline models. Recalling that the SE/PLE behaves as a linear superposition of exponentially decaying functions, we have this mathematical expression as follows,

$$q_D(t_D) \equiv \sum_{i=1}^{\infty} a_i \exp[-c_i t_D] \quad \text{.....(3.4)}$$

where the a_i and c_i parameters in Eq. 3.4 are the coefficients to be determined.

The primary issue with Eq. 3.4 is that we cannot determine an infinite number of coefficients; hence, we truncate the summation in our work to $i_{max} = 8$, and Eq. 3.4 can be rewritten to give,

$$q_D(t_D) \approx \sum_{i=1}^{i_{\max}} a_i \exp[-c_i t_D] \approx \sum_{i=1}^{8} a_i \exp[-c_i t_D]$$

$$\approx a_1 \exp[-c_1 t_D] + a_2 \exp[-c_2 t_D] + ... + a_8 \exp[-c_8 t_D] \quad \text{.....(3.5)}$$

As comment, Eq. 3.5 is fitted by "brute force" — that is, hand methods were used to establish the initial exponential coefficients, where the first term was approximated, then the next, then the next using a log-log plot of $q_D(t_D)$ versus t_D. Once the hand approach provided "close" estimates, the model and data function were submitted to a non-linear optimization algorithm to obtain the final coefficients. The casual observer may question the "hand approach", but it is important to note that, no matter what product was used to perform the regressions, this problem is so ill-posed that it required the hand manipulation of the coefficients prior to the use of regression.

To complete this work, and once the approximation is obtained, we compute Arps $D(t)$ and $b(t)$ functions (*i.e.*, loss ratio and loss ratio derivative) as an additional test of the regression analysis and to observe the behavior of the sum-of-exponentials function with further mathematical manipulation. The resulting Arps relations, $D(t)$ and $b(t)$, in dimensionless form, when Eq. 3.5 is substituted as the time-rate model are given, respectively, as follows,

$$D_D(t_D) = \frac{\sum_{i=1}^{8} -a_i c_i \exp[-c_i t_D]}{\sum_{i=1}^{8} a_i \exp[-c_i t_D]} \quad \text{.....(3.6)}$$

$$b_D(t_D) = 1 - \frac{\sum_{i=1}^{8} a_i \exp[-c_i t_D] \sum_{i=1}^{8} a_i c_i^2 \exp[-c_i t_D]}{\sum_{i=1}^{8} -a_i c_i \exp[-c_i t_D]} \quad \text{.....(3.7)}$$

Considering Eq. 3.1 and Eq. 3.5, we realize that for a given value of the time exponent, n, there is a particular set of a_i and c_i coefficients; therefore, we contemplate a practical range of n values for the approximation (*i.e.*, n = 0.10, 0.25, 0.50, 0.75, and 0.90). In this sense, we have developed five sum-of-exponentials functions to approximate the SE/PLE time-rate model which are presented in detail in Appendix A. As mentioned, we extend the approximation to the hyperbolic and modify hyperbolic decline models for completeness. This work is also included in Appendix A for reference. The most representative example

is the case for $n = 0.5$; hence, the results for this case are presented here as follows,

- **Figure 3.1** In **Fig. 3.1** we present the dimensionless SE/PLE model for the case of $n = 0.5$ using an eight-term sum-of-exponentials function approximation, where the summation and the eight individual trends are each shown. This plot shows quite clearly that the model is matched extremely well by the approximation.
- **Figure 3.2** In **Fig. 3.2** we present a semilog plot of the a_i and c_i coefficients used to match the SE/PLE $n = 0.5$ case. While the c_i coefficients are monotonically decreasing, which suggests a coherent performance on a term-by-term basis, the a_i coefficients have a somewhat quadratic shape, with the third a_i coefficient being the maximum. It is unclear if this has any mathematical relevance, but this behavior does imply that the a_i coefficient will have an element of uncertain (as these coefficients do not monotonically decrease). Efforts were made to try to ensure monotonicity, but these were not successful in this particular case.
- **Figure 3.3** The Arps $D_D(t_D)$ and $b_D(t_D)$ functions are presented in **Fig. 3.3,** where both the model functions (straight-line trends) and the approximate functions (oscillating curves) agree reasonably well — well enough to suggest that the eight-term sum-of-exponentials approximation is sufficient for the prediction of $q_D(t_D)$, but less so for the Arps $D_D(t_D)$ and $b_D(t_D)$ functions. The oscillatory nature of the sum-of-exponentials approximations for the $D_D(t_D)$ and $b_D(t_D)$ functions suggests the need for more terms in the approximation, but attempts to increase the number of terms lead to worse results, most likely due to numerical issues.

As a closure statement, we believe that the sum-of-exponentials concept is valid for the representation of the SE/PLE decline model, but due to numerical effects, this problem is poorly posed for such approximations. As our work has shown, eight-term sum-of-exponentials approximation is sufficient for the prediction of $q_D(t_D)$.

III.2 Laplace Transform of the Stretched/Power-Law Exponential Function

The Laplace transform has been widely used in the petroleum literature to solve flow problems that are not well-posed for real domain solutions. The primary advantage of the Laplace transform is that it can be used to reduce certain partial differential equations into a form where an analytical solution can be obtained in the Laplace domain. The "trick" then becomes the inversion of the Laplace domain solution into the real domain, and this often requires the use of (approximate) numerical inversion algorithms.

Another application of the Laplace transform that is very popular in the petroleum literature is its use to resolve variable-rate/variable-pressure drop problems in using the convolution identity — which in the real domain is a "convolution" integral, but in the Laplace domain this identity becomes a multiplication of two

functions in the Laplace domain.

Our goal is to use the Laplace transform and the convolution identity to resolve the SE/PLE decline model in the Laplace domain with the perspective that there may be some sort of diagnostic capability or other sort of mathematical identity which, in the process, may arise.

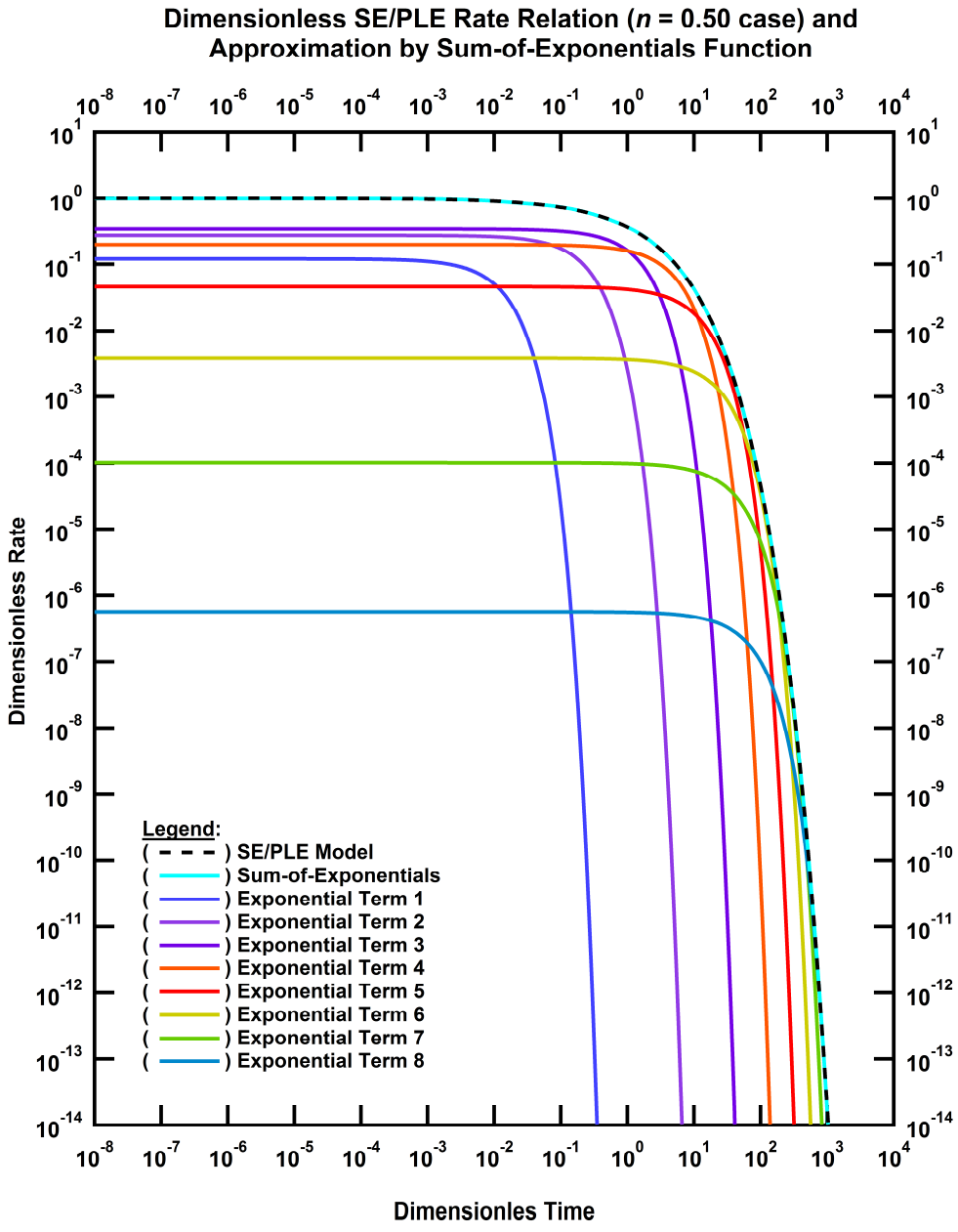

Figure 3.1 — Dimensionless rate functions for the sum-of-exponentials approximation for the n = 0.5 SE/PLE case.

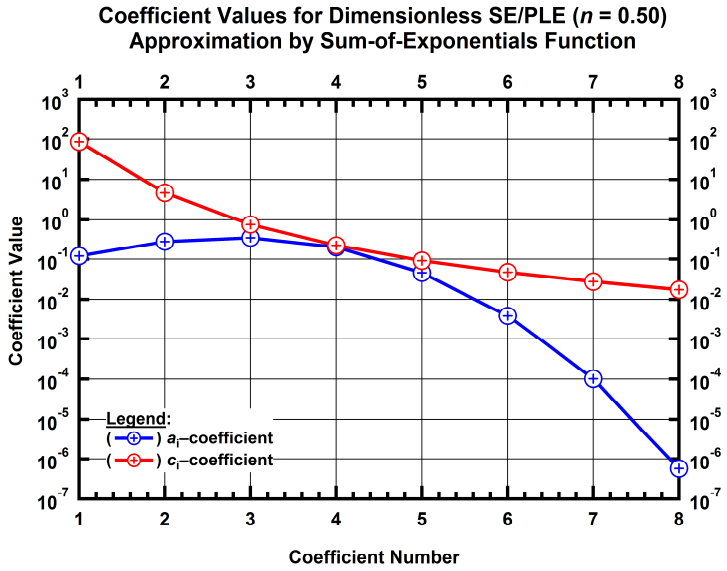

Figure 3.2 — Coefficients a_i and c_i values for the sum-of-exponentials approximation for the n = 0.5 SE/PLE case.

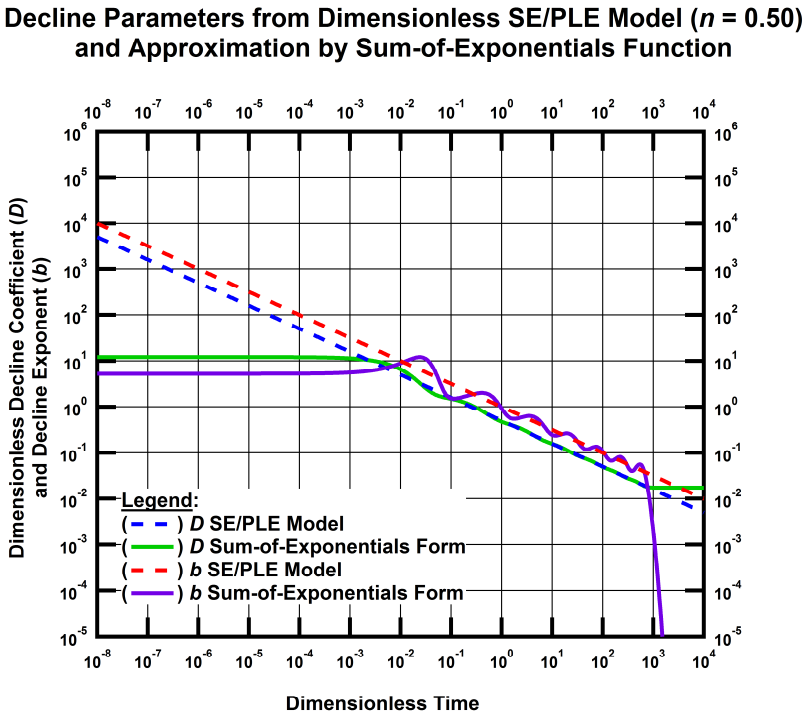

Figure 3.3 — Arps $D_D(t_D)$ and $b_D(t_D)$ functions for the sum-of-exponentials approximation for the n = 0.5 SE/PLE case.

In addition, we can use the convolution identity to try to establish if the SE/PLE decline model has some unique relationship with either a constant rate or constant pressure formulation.

In particular, the constant rate/constant pressure formulation in the Laplace domain is given as,

$$\bar{p}_{Dcr}(u) = \frac{1}{u^2 \bar{q}_{Dcp}(u)} \quad \text{.....(3.8)}$$

In simple language, there is no direct Laplace transform of the general form of Eq. 3.1 (*i.e.*, for a general value of the time exponent, n) — except for very specific cases (*e.g.*, n = 1/2 or 1). To develop a comprehensive understanding of the behavior of Eq. 3.1 in the Laplace domain, we will test three different numerical approaches in order to find an approximation:

- Approximate the SE/PLE relation by Taylor series expansion, and then take the Laplace transform.
- Use the Laguerre quadrature formulation to transform a general function into the Laplace domain.
- Use the Blasingame (1995) approach to take the Laplace transform of a piecewise power-law function.

In this sense, our first approach will be to develop, analytically, the specific case for n = 0.50 or 1/2 to find the Laplace transform and subsequent mathematical analysis as an initial reference for the numerical approaches. Eq. 3.1; hence, becomes,

$$q_D(t_D) = \exp[-t_D^{1/2}] \quad \text{.....(3.9)}$$

Using standard tables, he Laplace transform of Eq. 3.9 is,

$$\bar{q}_D(u) = \frac{1}{u} - \frac{e^{\frac{1}{4u}} \sqrt{\pi}\, \mathrm{Erfc}\left[\frac{1}{2\sqrt{u}}\right]}{2\,u^{3/2}}, \quad \text{.....(3.10)}$$

where Erfc (x) is the complementary error function. Eq. 3.10 is the dimensionless SE/PLE flowrate in Laplace domain for n = 1/2. Appendix B describes in detail how we get to the previous expression. As stated previously, we attempt to resolve the SE/PLE decline model in Laplace domain; therefore, we replace Eq. 3.10 into the "convolution" integral in Laplace domain (Eq.3.8) to obtain the following expression,

$$\bar{p}_D(u) = \frac{2}{2u - e^{\frac{1}{4u}} \sqrt{\pi} \sqrt{u}\, \mathrm{Erfc}\left[\frac{1}{2\sqrt{u}}\right]} \quad \text{.....(3.11)}$$

At this point we have resolve the SE/PLE decline model for the case n = 1/2 in Laplace domain. This problem is not suitable for direct analytical inversion; hence, we use the traditional Stehfest (1970) numerical Laplace inversion algorithm to find the results for the "constant rate" pressure and pressure derivative

functions. We present these results in **Fig. 3.4.**

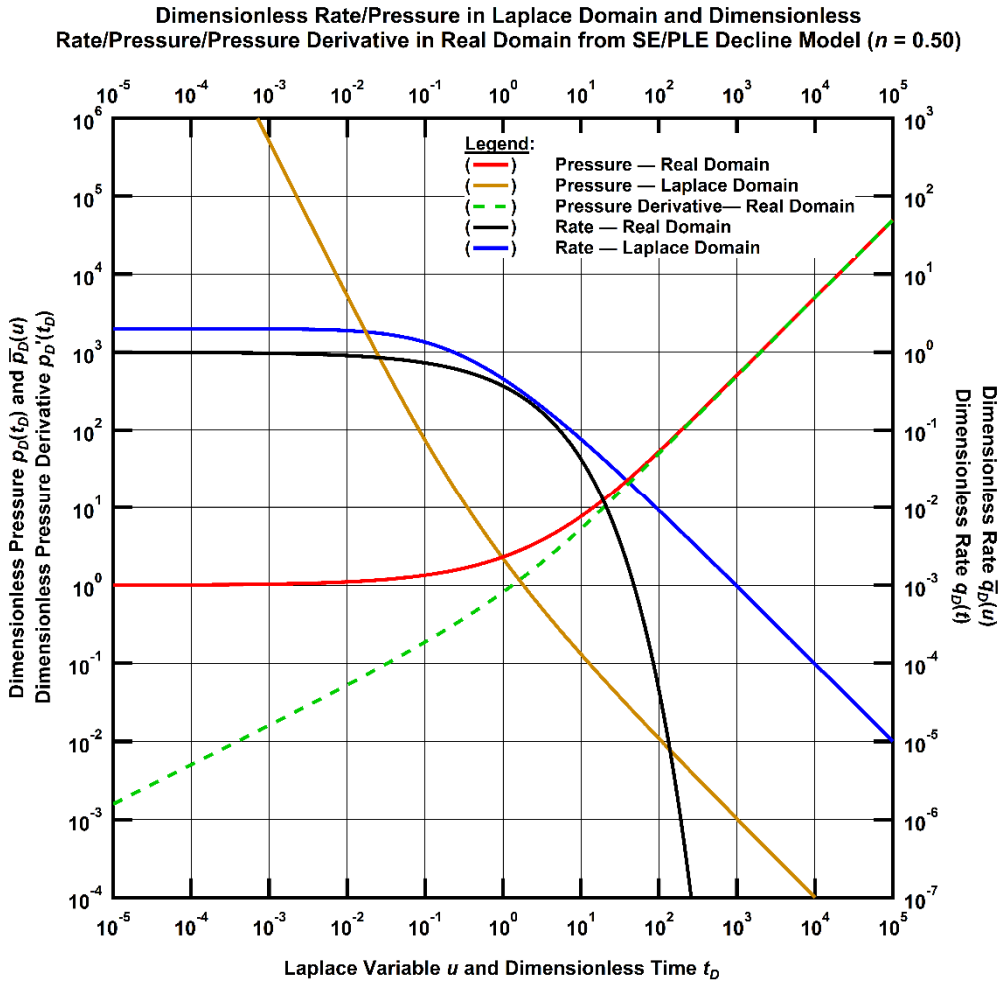

Figure 3.4 — Various functions obtained by using the Laplace transform of the SE/PLE relation (n = 0.50).

As an aside, by observation of Fig. 3.4, it seems that the dimensionless rate in Laplace domain exhibits a hyperbolic trend. In this sense, we raise the question if Eq. 3.10 may be approximated with a simpler mathematical expression for computational purposes. To test this idea, we propose two approximating models: a hyperbolic type function and a rational polynomial function, given as follows,

$$\bar{q}_D(u) \approx \frac{a_1}{[1+a_2 u]^{1/a_3}}, \quad \text{.....(3.12)}$$

$$\bar{q}_D(u) \approx \frac{b_1 + b_2 u}{1 + b_3 u + b_4 u^2}, \quad \text{.....(3.13)}$$

where the a_i and b_i constants are arbitrary regression coefficients used to match the models to the exact solution. The approximation results are presented in **Fig. 3.5** and in more detail in Appendix B. Since these results are fairly good, we extend our work to solve analytically the SE/PLE approximating functions we propose in Eq. 3.12 and Eq. 3.13 substituting them into the "convolution" integral (Eq. 3.8) and inverting the resulting expressions to real domain without the need for a numerical algorithm. The resulting "constant rate" pressure expressions for the hyperbolic and rational polynomial functions are given in Eq. 3.14 and Eq. 3.15, respectively.

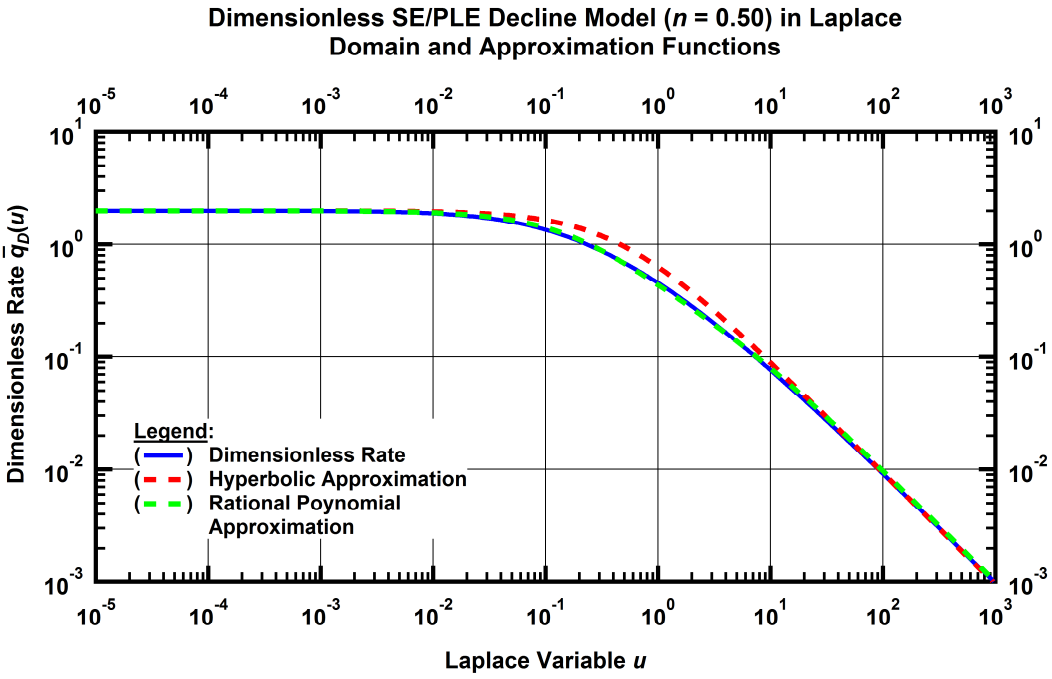

Figure 3.5 — Dimensionless SE/PLE decline model flowrate for the case $n = 0.50$ and approximating hyperbolic and rational polynomial functions.

$$p_D(t_D) \approx \frac{[a_2 + a_3 t_D]\Gamma\left[-\frac{1}{a_3}\right] + a_3\left[a_2\Gamma\left[\frac{a_3 - 1}{a_3}, \frac{t_D}{a_2}\right] - t_D\Gamma\left[-\frac{1}{a_3}, \frac{t_D}{a_2}\right]\right]}{a_1 a_3 \Gamma\left[-\frac{1}{a_3}\right]} \quad \text{(from Eq. 3.12)} \quad \ldots\ldots (3.14)$$

$$p_D(t_D) \approx \left[\frac{b_3}{b_1} - \frac{b_2}{b_1^2}\right] + \frac{[b_2^2 - b_1 b_2 b_3 + b_1^2 b_4]e^{-\frac{b_1 t_D}{b_2}}}{b_1^2 b_2} + \frac{t_D}{b_1} \quad \text{(from Eq. 3.13)} \quad \ldots\ldots (3.15)$$

Finally, real domain pressure generated from the approximating functions is computed and plotted along

with the one obtained with numerical Laplace inversion using the exact "convolved" pressure in Laplace domain (*i.e.*, Eq. 3.11). These results are presented in **Fig. 3.6** and in more detail in Appendix B.

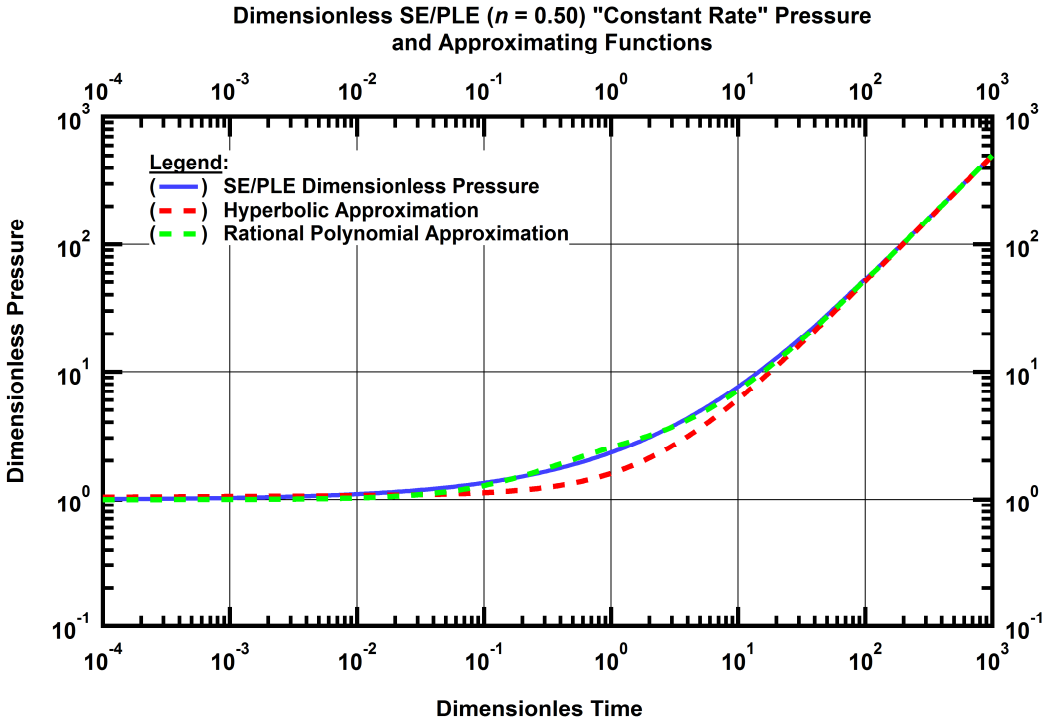

Figure 3.6 — Dimensionless SE/PLE decline model "constant rate" pressure for the case n = 0.50 and approximating hyperbolic and rational polynomial functions.

At this point we have resolved the SE/PLE model for the special case of n = 0.50 or 1/2. From our observations on **Figs.** 3.5 and 3.6 we believe that the best approximation for $\bar{q}_D(u)$ is the rational polynomial given by Eq. 3.13. For reference, we present the coefficients a_i and b_i in **Table 3.1.**

We recall that for the general SE/PLE expression there is no direct Laplace transform. Therefore, as commented previously, we test three different numerical approaches in order to find an approximation in Laplace domain. The first approach we use is that of the Taylor series expansion, followed by Laguerre quadrature, and finally, using the Blasingame (piecewise power-law function) method. The complete details of the mathematical derivation is provided in Appendix C. We present the general approximating functions as follows,

Table 3.1 — Regression coefficients, a_i and b_i, values for the hyperbolic and rational polynomial approximating functions of $\overline{q}_D(u)$.

Hyperbolic Approximating Function		Rational Polynomial Approximating Function	
Coefficient	Value	Coefficient	Value
a_1	1.99995	b_1	2.00
a_2	2.194587	b_2	0.893318
a_3	1.005188	b_3	4.758922
		b_4	0.894517

Taylor Series Expansion: we first approximate the dimensionless SE/PLE decline model using the Taylor series expansion of a real function $f(x)$, in our case $q_D(t_D)$; then, we are able to compute the Laplace transform of the series expression to give,

$$\overline{q}_D(u) \approx \frac{1}{u}\sum_{i=0}^{\infty}\frac{\Gamma(1+ni)}{i!}\left[-\frac{1}{u^n}\right]^i \qquad (3.16)$$

Laguerre Quadrature: also called Gauss-Laguerre quadrature, with this approach we approximate the Laplace transform integral definition using a series expansion. With our working variables, we obtain,

$$\overline{q}_D(u) \approx \frac{1}{u}\sum_{i=1}^{m} w_i \exp\left[-\left(\frac{x_i}{u}\right)^n\right] \qquad (3.17)$$

where, for this equation, n, is the time exponent from the SE/PLE model and m is the quadrature order of the abscissas. The x_i coefficients are the abscissas (the i^{th} zero of the Laguerre polynomials, $L_m(x)$) and w_i coefficients are the weights obtained the from the Laguerre polynomials.

Blasingame Method: this approach, idealized by Blasingame (1995), considers the Laplace transform as a series of a continuous piecewise power-law function of the form $f_i(t) = \alpha_i t^{v_i - 1}$, where we finally get,

$$\overline{q}_D(u) \approx \frac{\alpha_1}{u^{v_1}}\gamma(v_1, ut_{D1}) + \sum_{i=2}^{k-1}\left[\frac{\alpha_i}{u^{v_i}}\gamma(v_i, ut_{Di}) - \frac{\alpha_i}{u^{v_i}}\gamma(v_i, ut_{Di-1})\right] + \frac{\alpha_k}{u^{v_k}}\Gamma(v_k) - \frac{\alpha_k}{u^{v_k}}\gamma(v_k, ut_{Dk-1}) \qquad (3.18)$$

where $\Gamma(z)$ is the gamma function, $\gamma(a,x)$ is the lower incomplete gamma function, and α_i and v_i are the coefficients of Blasingame's continuous data function.

Appendix C provide the results obtained from the three methods previously commented. We tested these

three approaches exhaustively, with a wide range of time exponent, n, values, to find that the Blasingame method yields the best results and is, therefore, going to be presented in this section. The results obtained are as follows,

- **Figure 3.7** In **Fig. 3.7** we present the dimensionless SE/PLE time-rate model in Laplace domain using the Blasingame method approximation, where the trends for a specific time exponent value are each shown. This plot shows quite clearly that the approximation is well-behaved and no numerical issues are presented along the logarithmic scale of the Laplace variable.
- **Figure 3.8** In **Fig. 3.8** we present the "constant rate" pressure in real domain for various time exponent values. We obtained these results from the "convolved" approximation of $\bar{q}_D(u)$ (*i.e.*, $\bar{p}_D(u)$); then, we use the Stehfest algorithm to invert numerically the Laplace domain solution to get $p_D(t_D)$. We observe that the trends follow a close converging path until $t_D \approx 2$ and then diverge drastically with a slope depending on the time exponent value.
- **Figure 3.9** In **Fig. 3.9** we present the "constant rate" pressure derivative (the well-test pressure derivative, to be accurate) in real domain. At small dimensionless time values, the pressure derivative trend is dominated by the value of the time exponent suggesting some sort of dependency with the flow geometry; however, this is just an observation from a "constant rate" result.

III.3 Prediction of Bottomhole Flowing Pressure

Using numerical reservoir simulation, we attempt to "reverse engineer" the bottomhole flowing pressure that a specific SE/PLE model flowrate would generate. As commented before, this is a "reverse engineering" problem because we know the properties of the reservoir model, and our efforts are directed to determine if there are any unique features of the bottomhole pressure response. As a starting point example, we recall the oil material balance relation and the oil pseudosteady-state (PSS) flow relation, given by,

$$\bar{p} = p_i - m_{o,pss}\, N_p \quad \left[\text{where } m_{o,pss} = \frac{B_o}{B_{oi}} \frac{1}{Nc_t} \right] \text{ (oil material balance relation)} \quad \text{.....(3.19)}$$

$$\bar{p} = p_{wf} + b_{o,pss}\, q_o \quad \left[\text{where } b_{o,pss} = 141.2 \frac{\mu_o B_o}{kh} \left[\frac{1}{2} \ln \left[\frac{4}{e^{\gamma}} \frac{1}{C_A} \frac{A}{r_w^2} \right] + s \right] \right] \text{(oil PSS flow relation)} \quad \text{.....(3.20)}$$

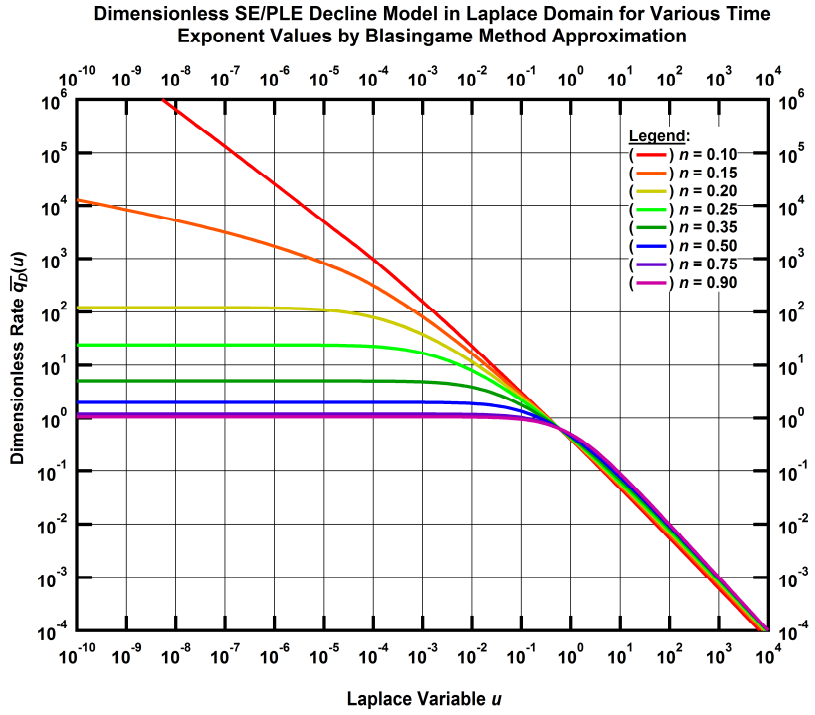

Figure 3.7 — Dimensionless SE/PLE decline model in Laplace domain for various time exponent values, n, by Blasingame method approximation.

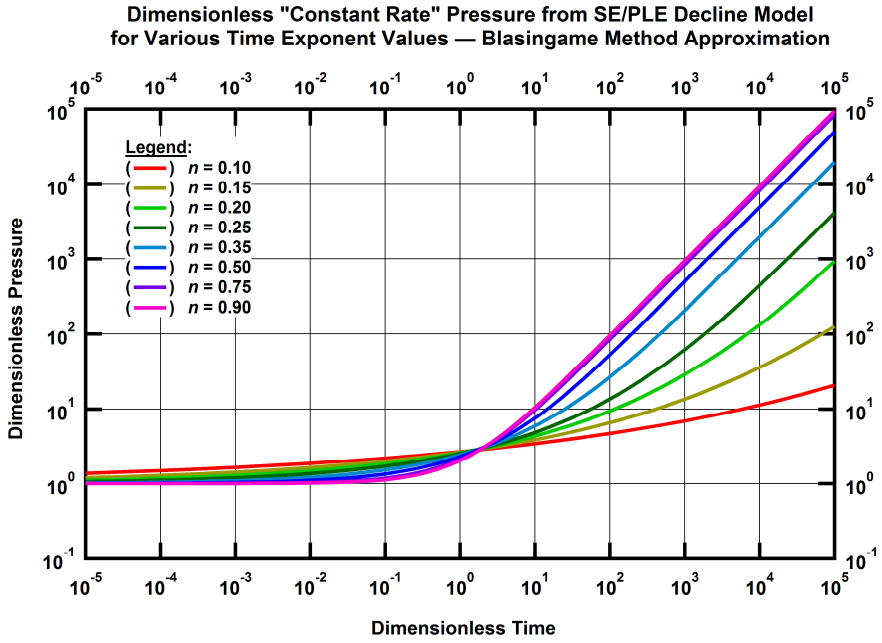

Figure 3.8 — Dimensionless "constant rate" pressure from SE/PLE decline model for various time exponent values, n — Blasingame method approximation.

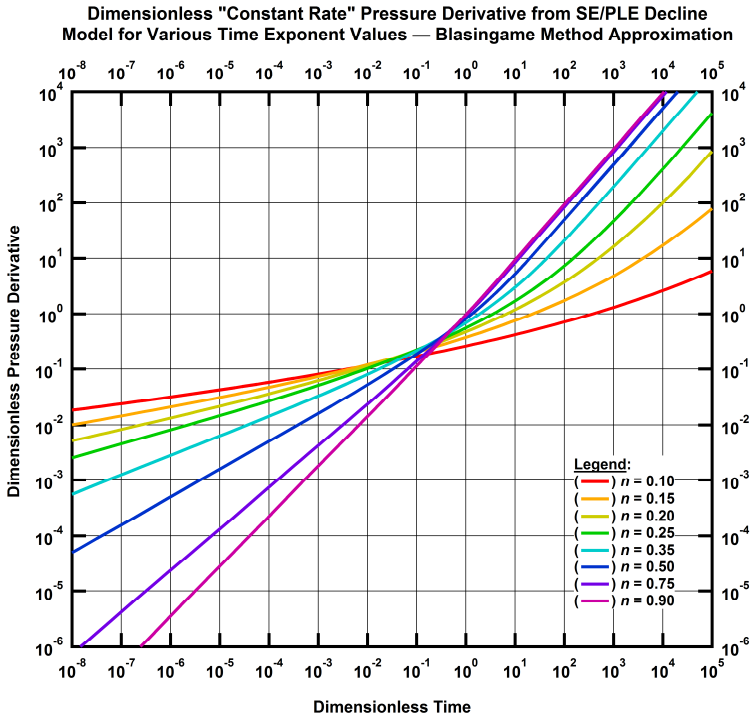

Figure 3.9 — Dimensionless "constant rate" pressure derivative from SE/PLE decline model for various time exponent values, n — Blasingame method approximation.

Combining Eq. 3.19 and Eq. 3.20 we obtain,

$$p_{wf} = p_i - b_{o,pss}\, q_o - m_{o,pss}\, N_p \quad \text{.....(3.21)}$$

For the case of a constant bottomhole pressure (*i.e.*, $dp_{wf}/dt = 0$), the derived flowrate model is exponential during pseudosteady-state (this can be easily derived from Eq. 3.19 and Eq. 3.20. See Appendix D). The resulting derived exponential time-rate model is,

$$q_o(t) = q_{oi}\, \exp[-D_i\, t] \quad \text{.....(3.22)}$$

Eq. 3.21 and Eq. 3.22 are rigorous for pseudosteady-state flow in an undersaturated black-oil reservoir. Following similar steps in the previous approach, we can implement a strategy to "prove" a given time-rate relation that is not derived from fundamental principles (*e.g.*, the power-law exponential decline model). The obvious test would be to compute the flowing bottomhole pressure (p_{wf}) using Eq. 3.21 and compare these results to the pressures from observed field data or from a numerical reservoir simulation generated using a prescribed reservoir model. For cases other than the constant bottomhole flowing pressure (generated from an exponential decline), Eq. 3.21 could be used — with the appropriate substitutions of q_o and N_p from a prescribed model — as a regression relation to validate the input time-rate model. Such a

"proof" would be somewhat disingenuous given that one would just be proving that the input rate matches the concepts of pseudosteady-state flow, but this could be one approach to proving the consistency of a given time-rate model.

Another "proof" could be to use the prescribed time-rate model in the pseudosteady-state flow equation (Eq. 3.20) and compare its performance against numerical reservoir simulation results when solving for ($\bar{p} - p_{wf}$). Again, this would be slightly weak as a "proof" of a given model, but it could be used to prove consistency. As an example, for the constant pressure case, we substitute the flowrate expression of the exponential decline model into Eq. 3.20 to obtain,

$$(\bar{p} - p_{wf}) = b_{o,pss}\, q_i \exp[-D_i\, t] \quad \text{.....(3.23)}$$

At this point, our approach is to solve for the flowing bottomhole pressure functional form (p_{wf} (t)) for pseudosteady-state flow (*i.e.*, Eq. 3.21), with a prescribed time-rate model so that it can be compared against measured or simulated well performance data. We will test two time-rate models: the traditional hyperbolic and the power-law exponential. We now need to develop the pressure functional form of these decline models.

Hyperbolic Time-Rate Model: the hyperbolic time-rate model, derived from empirical observations, and its cumulative production form are replaced into Eq. 3.21 to give,

$$p_{wf}(t) = p_i - b_{o,pss}\left[\frac{q_{oi}}{[1+bD_i t]^{1/b}}\right] - m_{o,pss}\left[\frac{q_{oi}}{(1-b)D_i}[1-(1+bD_i t)^{1-1/b}]\right] \quad \text{.....(3.24)}$$

Eq. 3.24 is the functional form of the bottomhole pressure using the hyperbolic decline as the prescribed time-rate model. Recasting Eq. 3.24 into a regression relation (*i.e.*, assigning arbitrary parameters for the model coefficients) we obtain,

$$p_{wf}(t) = a_1 - a_2\frac{1}{[1+a_3 t]^{1/a_4}} - a_5[1-(1+a_3 t)^{1-1/a_4}] \quad \text{.....(3.25)}$$

Eq. 3.25 represents the generic bottomhole pressure profile that should be obtained for the case of a well produced at a rate specified by the hyperbolic time-rate relation. The parameters a_1, a_2, a_3, a_4, and a_5 are arbitrary coefficients to be determined by regression. As an aside, we can replace the hyperbolic decline model into the pseudosteady-state flow equation to give,

$$(\bar{p} - p_{wf}) = b_{o,pss}\, q_{oi}[1+bD_i t]^{-1/b} \quad \text{.....(3.26)}$$

Reforming Eq. 3.26 into a regression relation we get,

$$(\bar{p} - p_{wf}) = m_1[1 + m_2 t]^{-1/m_3} \quad \text{.....(3.27)}$$

Eq. 3.27 represents the generic ($\bar{p}$ – p_{wf}) pressure profile that should be obtained for the case of a well produced at a rate specified by the hyperbolic time-rate relation. The parameters m_1, m_2, and m_3 are arbitrary coefficients to be determined by regression. Details on the above derivations are presented in Appendix D.

Power-Law Exponential Time-Rate Model: the power-law exponential (PLE) time-rate model, derived from empirical observations, and its cumulative production form are replaced into Eq. 3.21 (we must assume $D_\infty = 0$ in this case) to obtain,

$$p_{wf} = p_i - b_{o,pss}\, \hat{q}_{oi} \exp[-\hat{D}_i t^n] - m_{o,pss}\, \hat{q}_{oi} \frac{\hat{D}_i^{-1/n}}{n} \left[\Gamma\left[\frac{1}{n}\right] - \Gamma\left[\frac{1}{n}, \hat{D}_i t^n\right] \right] \quad \text{.....(3.28)}$$

Eq. 3.28 is the functional form of the bottomhole pressure using the PLE decline as the prescribed time-rate model. Reforming Eq. 3.28 into a regression relation (*i.e.*, assigning arbitrary parameters for the model coefficients) we obtain,

$$p_{wf}(t) = c_1 - c_2 \exp[-c_3 t^{c_4}] - c_5 \left[\Gamma\left[\frac{1}{c_4}\right] - \Gamma\left[\frac{1}{c_4}, c_3 t^{c_4}\right] \right] \quad \text{.....(3.29)}$$

Eq. 3.29 represents the generic bottomhole pressure profile that should be obtained for the case of a well produced at a rate specified by the PLE time-rate relation. The parameters c_1, c_2, c_3, c_4, and c_5 are arbitrary coefficients to be determined by regression. As an aside, we can replace the PLE decline model into the pseudosteady-state flow equation to give,

$$(\bar{p} - p_{wf}) = b_{o,pss}\, \hat{q}_{oi} \exp[-\hat{D}_i t^n - D_\infty t] \quad \text{.....(3.30)}$$

Reforming Eq. 3.30 into a regression relation we get,

$$(\bar{p} - p_{wf}) = d_1 \exp[-d_2 t^{d_3} - d_4 t] \quad \text{.....(3.31)}$$

Eq. 3.31 represents the generic ($\bar{p}$ – p_{wf}) pressure profile that should be obtained for the case of a well produced at a rate specified by the PLE relation. The parameters d_1, d_2, d_3, and d_4 are arbitrary coefficients to be determined by regression — coefficient d_4 (*i.e.*, D_∞) can be assumed to be zero. Details on the above derivations are presented in Appendix D.

Numerical Reservoir Simulation Results: as stated above, we are to "reverse engineer" the functional form of $p_{wf}(t)$ from a prescribed time-rate model by comparing simulated well performance data with the regression expressions obtained previously. To validate this concept, we have prepared a numerical

simulation case — to obtain $p_{wf}(t)$ by providing prescribed flowrates — where the reservoir is circular in shape with an area of 100 acres and the reservoir thickness is constant with a pay zone of 200 ft., the permeability and porosity are constant with a value of 6.1% and 0.10 md, respectively. The well is vertical with no skin factor and located in the center of the reservoir. We assume an initial pressure, p_i, of 10,000 psia, an initial reservoir temperature of 400°F. The fluid in the reservoir model is dry gas with no non-hydrocarbon impurities and a specific gravity of 0.633. The gas deviation factor (z-factor) is computed with Dranchuk-Abou-Kassem (DAK) correlation and viscosity with Lee, et al. correlation. We have elected to utilize a gas reservoir case because it violates the "black oil" assumptions used to derive Eq. 3.21; and hence, provides a more stringent test of Eq. 3.25 and Eq. 3.29.

We start by generating three cases of synthetic flowrates from prescribed time-rate models — these data are going to be feed to the numerical simulator to obtain their bottomhole pressure response. The synthetic flowrates generated are presented graphically as follows: in **Figs. 3.10** we have the exponential decline flowrates, in **Fig. 3.11** we have the hyperbolic decline flowrates, and finally in **Fig. 3.12** the power-law exponential decline flowrates. For reference, the decline parameters of each time-rate model are presented in **Table 3.2.** Recalling the mathematical expressions for the exponential, hyperbolic, and power-law exponential decline models, for gas flowrate, we have,

$$q_g(t) = q_{gi} \exp[-D_i t] \quad \text{(exponential)} \tag{3.32}$$

$$q_g(t) = \frac{q_{gi}}{[1 + bD_i t]^{1/b}} \quad \text{(hyperbolic)} \tag{3.33}$$

$$q_g(t) = \hat{q}_{gi} \exp[-\hat{D}_i t^n - D_\infty t] \quad \text{(power-law exponential)} \tag{3.34}$$

As commented above, the bottomhole pressure response from an exponential decline flowrate, theoretically, should yield a constant value, which is what we expect to find with our numerical reservoir simulation. This is our "calibration" step before obtaining the pressure profile from the hyperbolic and power-law exponential time-rate models. The exponential decline bottomhole pressure profiles are presented in **Fig. 3.13.** As we can observe, the pressure trends stabilize in near constant value after the transient period is over and pseudosteady state flow becomes the dominant regime. At this point, we have "reverse engineered" the flowing bottomhole pressure profiles that the hyperbolic and power-law exponential time-rate models generate using the numerical reservoir simulation case prepared.

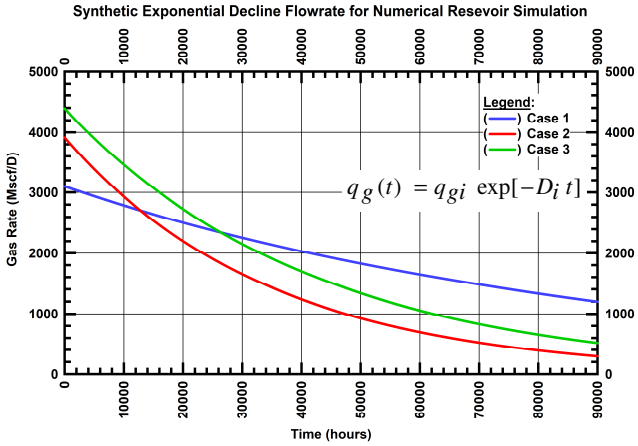

Figure 3.10 — Synthetic gas flowrates from exponential decline model.

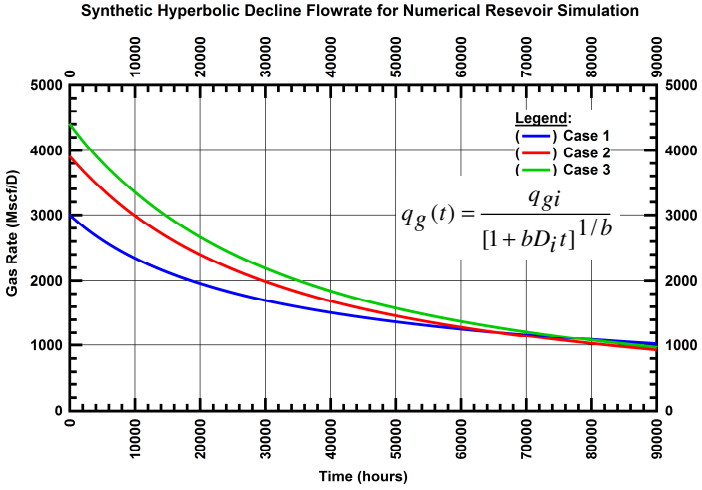

Figure 3.11 — Synthetic gas flowrates from hyperbolic decline model.

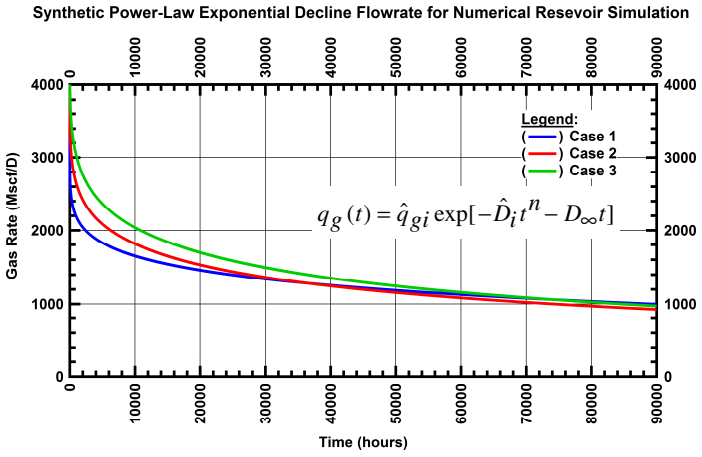

Figure 3.12 — Synthetic gas flowrates from power-law exponential decline model.

Table 3.2 — Decline parameters for the exponential, hyperbolic, and power-law exponential decline models used in numerical reservoir simulation.

		Case 1	Case 2	Case 3
Exponential Decline	q_{gi}, Mscf/D	3099	3913	4392
	D_i, 1/D	1.06×10^{-5}	2.88×10^{-5}	2.38×10^{-5}
Hyperbolic Decline	q_{gi}, Mscf/D	3000	3912	4400
	D_i, 1/D	3.00×10^{-5}	2.88×10^{-5}	2.70×10^{-5}
	b	1.5	0.8	0.7
Power-law Exponential Decline	$\hat{q}_{gi}$, Mscf/D	3300	4000	4500
	$\hat{D}_i$, 1/D	0.09	0.06	0.05
	n	0.22	0.28	0.30
	D_∞, 1/D	1.00×10^{-6}	1.00×10^{-10}	1.00×10^{-10}

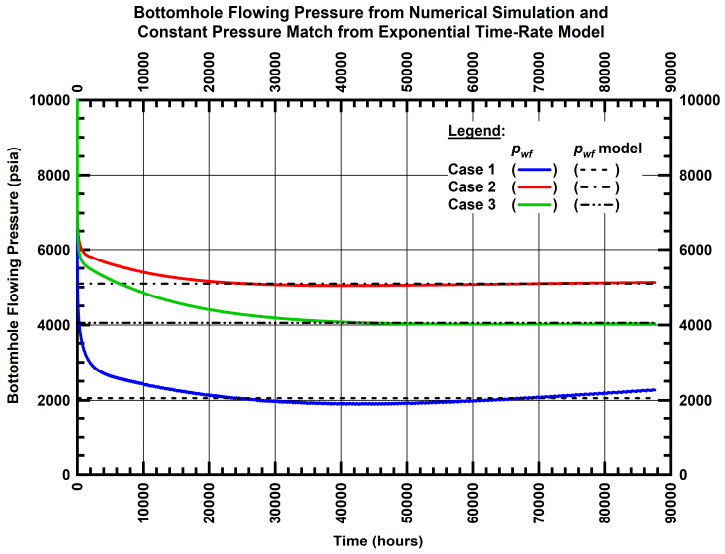

Figure 3.13 — Exponential decline bottomhole flowing pressure from numerical reservoir simulation (solid trends) and constant approximation (dashed trends).

These results are presented in **Fig. 3.14** and **Fig. 3.15** in solid color trends. Now, we face the problem of matching the simulated bottomhole pressures with the functional form obtained in Eq. 3.25 and Eq.3.29. We recall Eq. 3.25 and Eq. 3.29 for reference,

$$p_{wf}(t) = a_1 - a_2 \frac{1}{[1+a_3 t]^{1/a_4}} - a_5 [1-(1+a_3 t)^{1-1/a_4}] \quad \text{(hyperbolic)} \qquad (3.25)$$

$$p_{wf}(t) = c_1 - c_2 \exp[-c_3 t^{c_4}] - c_5 \left[\Gamma\left[\frac{1}{c_4}\right] - \Gamma\left[\frac{1}{c_4}, c_3 t^{c_4}\right] \right] \quad \text{(power-law exponential)} \qquad (3.29)$$

Using a global minimization algorithm as the regression approach, we were able to match the simulated flowing bottomhole pressure with the functional forms given in Eq. 3.25 and Eq. 3.29. The results are presented in Fig. 3.14 and Fig. 3.15 in dashed black trends. As can be observed, the match agrees very well for the cases presented. We believe that, at least conceptually, this validates our efforts to corroborate the hyperbolic and power-law exponential time-rate models for a generic flowing bottomhole pressure profile. The regression coefficients found for every analysis are presented in **Table 3.3.**

Table 3.3 — Regression coefficients for the functional form of the bottomhole pressure using the hyperbolic and power-law exponential decline models.

Model	Coefficient	Case 1	Case 2	Case 3
Hyperbolic Time-Rate Model	a_1	8000.0	6076.5	5544.1
	a_2	1.642×10^{-4}	1.721×10^{2}	1.270×10^{2}
	a_3	1.255×10^{-5}	2.524×10^{-5}	4.224×10^{-5}
	a_4	0.803568	0.747904	0.781929
	a_5	14272.5	8996.4	9263.2
Power-law Exponential Time-Rate Model	c_1	8520.3	9231.4	7231.7
	c_2	0.01000	9.5194830	9.5233723
	c_3	7.881×10^{-6}	5.488×10^{-4}	5.633×10^{-4}
	c_4	0.6479819	0.6473913	0.6402972
	c_5	3.245×10^{6}	1.204×10^{4}	1.040×10^{4}

For completeness, we present the numerical simulation results for the pressure difference ($\bar{p} - p_{wf}$) from the prescribed hyperbolic and power-law exponential decline models flowrates in **Fig. 3.16** and **Fig 3.17** (solid color trends). Again, we need to find the coefficient values, through regression, of Eq. 3.27 and Eq. 3.31, which are the functional forms from pseudosteady state flow equation and the prescribed time-rate model. For reference, we recall Eq. 3.27 and Eq. 3.31:

$$(\bar{p} - p_{wf}) = m_1 [1+m_2 t]^{-1/m_3} \qquad (3.27)$$

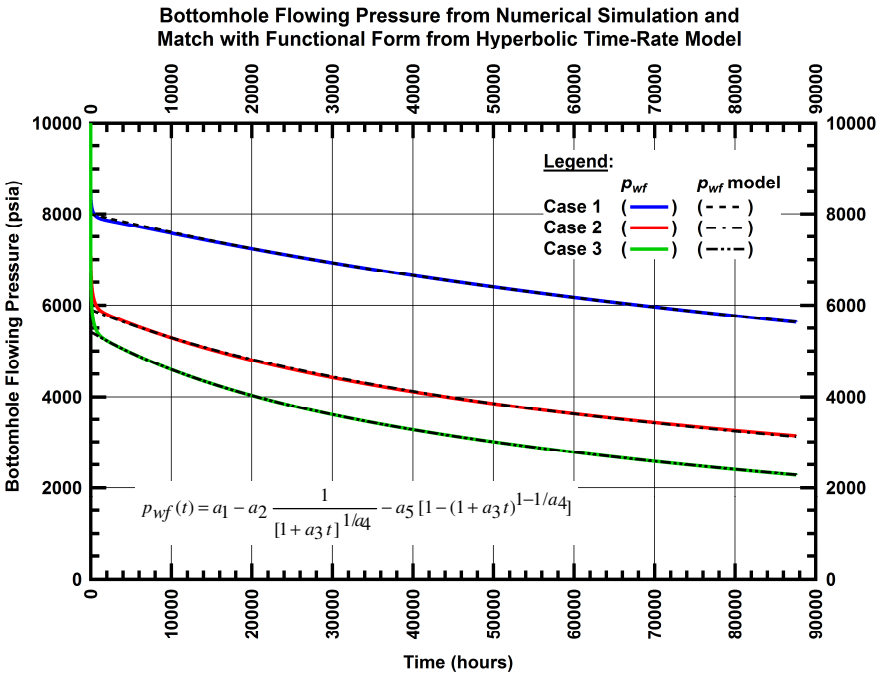

Figure 3.14 — Bottomhole flowing pressure from numerical reservoir simulation (solid trends) and match with functional form $p_{wf}(t)$ (dashed trends) from hyperbolic time-rate model.

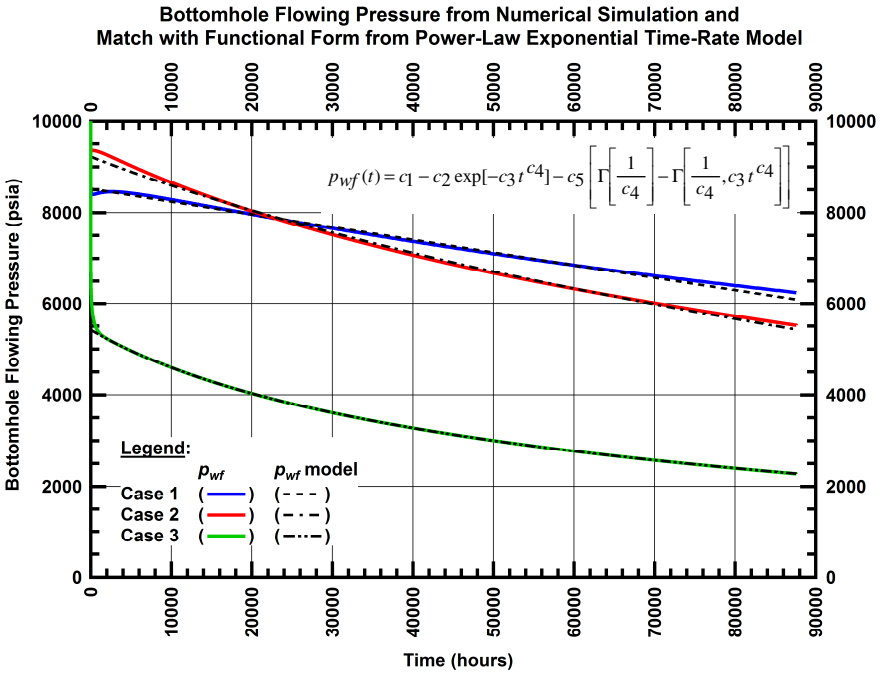

Figure 3.15 — Bottomhole flowing pressure from numerical reservoir simulation (solid trends) and match with functional form $p_{wf}(t)$ (dashed trends) from power-law exponential time-rate model.

$$(\bar{p} - p_{wf}) = d_1 \exp[-d_2 t^{d_3} - d_4 t] \quad \text{.....(3.31)}$$

The regression results are presented in Fig. 3.16 and Fig. 3.17 in black dashed trends. The regression coefficients found for this part of the study are presented in **Table 3.4.** As observed, the simulated data and their corresponding model function match very well for both hyperbolic and power-law exponential time-rate models. This additional "proof" give some support to the previous work but still it is not a derivation from fundamental principles that strictly validates the time-rate models under analysis.

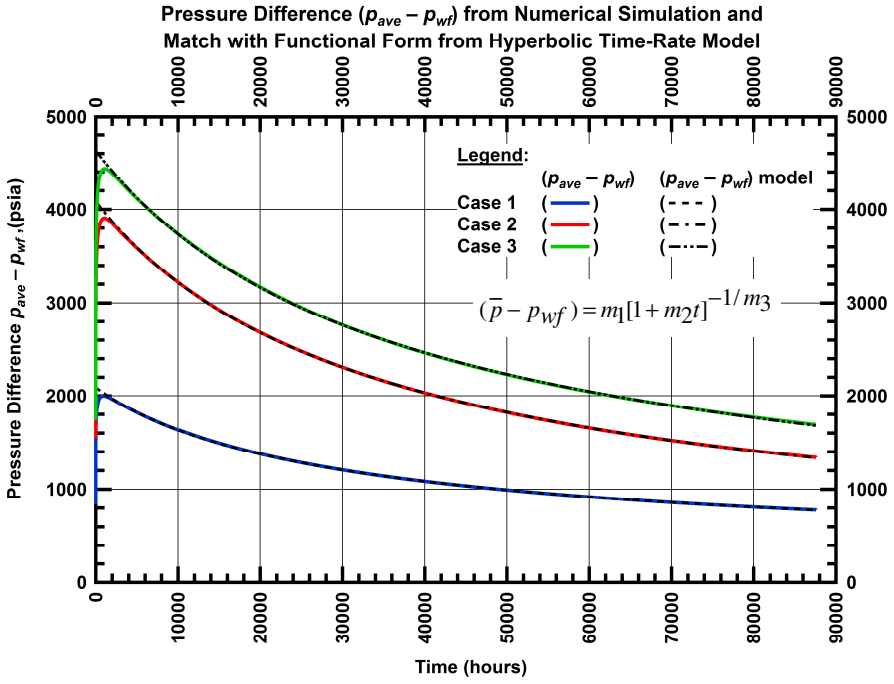

Figure 3.16 — Pressure difference $(\bar{p} - p_{wf})$ from numerical reservoir simulation (solid trends) and match with functional form $(\bar{p} - p_{wf})(t)$ (dashed trends) from hyperbolic time-rate model.

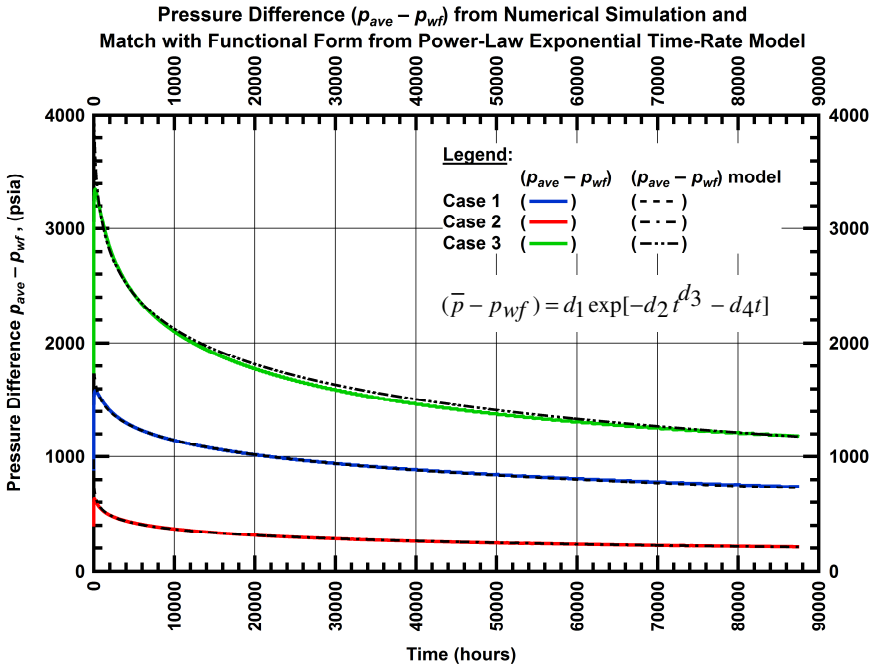

Figure 3.17 — Pressure difference ($\bar{p} - p_{wf}$) from numerical reservoir simulation (solid trends) and match with functional form ($\bar{p} - p_{wf}$)(t) (dashed trends) from power-law exponential time-rate model.

Table 3.4 — Regression coefficients for the functional form of the pressure difference ($\bar{p} - p_{wf}$) using the hyperbolic and power-law exponential decline models.

Model	Coefficient	Case 1	Case 2	Case 3
Hyperbolic Time-Rate Model	m_1	2088.37	4084.89	4629.28
	m_2	5.506×10^{-5}	3.447×10^{-5}	3.404×10^{-5}
	m_3	1.779046	1.242329	1.363027
Power-law Exponential Time-Rate Model	d_1	2019.32	1136.09	5091.35
	d_2	0.0468328	0.2063091	0.0978511
	d_3	0.2710893	0.1851144	0.2377925
	d_4	1.000×10^{-9}	1.000×10^{-10}	1.000×10^{-8}

CHAPTER IV

SUMMARY, CONCLUSIONS, AND RECOMMENDATIONS

IV.1 Summary

The stated goal of this work is to establish some theoretical basis of the stretched exponential/power-law exponential (SE/PLE) flowrate model; unfortunately, there is no clear path to a theoretical "proof." However, using the concept of a sum-of-exponentials approximation we were able to demonstrate that such an approximation is viable for a number of time exponent values. As an aside, using the same concept we were able to approximate the hyperbolic and modify hyperbolic decline models.

In addition, although we were not able to uniquely resolve each case of the SE/PLE analytically using the Laplace transform, we were able to demonstrate the behavior of the $n = 0.5$ case and we also demonstrated the use of numerical approaches to represent the SE/PLE in the Laplace domain. This work may lead to an eventual understanding of the "analytic" behavior of the SE/PLE relation.

Lastly, we demonstrated a "reverse engineering" approach to predict and/or interpret the pressure behavior for the case of an SE/PLE flowrate model imposed on a given reservoir model. While this is also not a "proof," this work does provide insight into the pressure behavior of this system, particularly for the case of an undersaturated black oil reservoir produced at pseudosteady-state flow conditions.

IV.2 Conclusions

- The SE/PLE approximation by "sum-of-exponentials" is proven by "brute force" — that is, the proposed 8-term approximations yield reasonably accurate correlations for the specified SE/PLE functions for almost all cases that were considered. However, the $D_D(t_D)$ and $b_D(t_D)$ functions show the oscillating behavior of the "sum-of-exponentials" formulations that would be expected when more terms are required.
- There is no direct Laplace transform of the SE/PLE decline model (except for the case of $n = 0.50$) — however; this work clearly shows that very accurate approximations can be developed in the Laplace domain using numerical approaches, the Blasingame method being the best one.
- The "reverse engineering" approach of predicting the bottomhole flowing pressure profile for an SE/PLE flowrate model imposed on a given reservoir model (numerical or analytical) was shown to be successful. For this work, only the case of an undersaturated black oil reservoir produced to pseudosteady-state flow conditions were shown to uniquely match the conceptual model. In addition, other empirical models were considered.

IV.3 Recommendations

- This work on the SE/PLE approximation should be continued for dry gas reservoir systems. While it is not obvious that there is a clear path to an analytical (or semi-analytical) solution for the SE/PLE for the gas case, there exists a possibility of developing an approximate solution.
- Efforts should be continued on finding a semi-analytical expression for the SE/PLE decline model from the standard hyperbolic/modified hyperbolic relation. This can provide some justification for the SE/PLE as a "special case" of the hyperbolic relation.

NOMENCLATURE

Field Variables:

b = Hyperbolic decline exponent, dimensionless
$b_{o,pss}$ = Pseudosteady-state flow coefficient, psia/STB/D
B = Oil formation volume factor, RB/STB
c_t = Total compressibility, $psia^{-1}$
$\hat{D}_i$ = Power-law exponential model initial decline parameter, $(1/D)^n$
D_∞ = Power-law exponential model terminal decline parameter, 1/D
h = Reservoir net pay, ft
k = Permeability, md
m = Quadrature order of the abscissa for the Laguerre polynomials, dimensionless
$m_{o,pss}$ = Material balance coefficient, psia/STB
n = Power-law exponential model time exponent parameter, dimensionless
N_p = Cumulative oil production, STB
$\overline{p}$ = Average pressure, psia
p = Pressure, psia
p_{wf} = Bottomhole flowing pressure, psia
q = Flowrate, STB/D or MSCF/D
$\hat{q}i$ = Stretched exponential/power-law exponential model initial flowrate parameter, MSCF/D
r_w = Wellbore radius, ft
t = Production time, D or hr

Subscripts:

g = Gas
i = Initial or integral
o = Oil

Greek:

Δ = Difference
Γ = Gamma function
γ = Lower incomplete gamma function
τ = Stretched exponential model time coefficient, dimensionless
μ = Viscosity, cp

REFERENCES

Arps, J.J. 1945. Analysis of Decline Curves. *Transactions of the AIME* **160** (01). SPE-945228-G. http://dx.doi.org/10.2118/945228-G.

Blasingame, T.A. 1995. *Math Lecture 5 — The Laplace Transform*, Petroleum Engineering 620 Lecture Notes. College Station, TX: Texas A&M University.

Chamberlin, R.V., Mozurkewich, G., Orbach, R. 1984. Time Decay of the Remanent Magnetization in Spin-Glasses. *Physical Review Letters* **52** (10): 86–870. 10.1103/PhysRevLett.52.867.

Clark, A.J., Lake, L.W., Patzek, T.W. 2011. Production Forecasting with Logistic Growth Models. SPE Annual Technical Conference and Exhibition, Denver, Colorado, USA, 30 October-2 November. SPE-144790-MS. http://dx.doi.org/10.2118/144790-MS.

Cutler, W.W. 1924. Estimation of Underground Oil Reserves by Oil-well Production Curves. DOI/USBM Bulletin 228, US Bureau of Mines, Washington, DC.

Duong, A.N. 2011. Rate-Decline Analysis for Fracture-Dominated Shale Reservoirs. *SPE Reservoir Evaluation & Engineering* **14** (03): 377–387. SPE-137748-PA. http://dx.doi.org/10.2118/137748-PA.

Fulford, D.S., Blasingame, T.A. 2013. Evaluation of Time-Rate Performance of Shale Wells using the Transient Hyperbolic Relation. SPE Unconventional Resources Conference Canada, Calgary, Alberta, Canada, 5-7 November. SPE-167242-MS. http://dx.doi.org/10.2118/167242-MS.

Gentry, R.W., McCray, A.W. 1978. The Effect of Reservoir and Fluid Properties on Production Decline Curves. *Journal of Petroleum Technology* **30** (09): 1327-1341. SPE-6341-PA. http://dx.doi.org/10.2118/6341-PA.

Ilk, D., Currie, S.M., Symmons, D. et al. 2010. Hybrid Rate-Decline Models for the Analysis of Production Performance in Unconventional Reservoirs. SPE Annual Technical Conference and Exhibition, Florence, Italy, 19–22 September. SPE-135616-MS. https://doi.org/10.2118/135616-MS.

Ilk, D., Rushing, J.A., Perego, A.D. et al. 2008. Exponential vs. Hyperbolic Decline in Tight Gas Sands: Understanding the Origin and Implications for Reserve Estimates Using Arps' Decline Curves. SPE Annual Technical Conference and Exhibition, Denver, Colorado, 21–24 September. SPE-116731-MS. http://dx.doi.org/10.2118/116731-MS.

Johnson, R.H., Bollens, A.L. 1927. The Loss Ratio Method of Extrapolating Oil Well Decline Curves.

Transactions of the AIME **77** (01): 771-778. SPE-927771-G. http://dx.doi.org/10.2118/927771-G.

Jones, P.J. 1942. Estimating Oil Reserves from Production-Decline Rates. *Oil and Gas Journal* **40** (35): 43–44.

Kohlrausch, F. 1863. Ueber die elastische Nachwirkung bei der Torsion. *Annalen der Physik* **195** (7): 337–368. andp.18631950702. http://dx.doi.org/10.1002/andp.18631950702.

Kohlrausch, R. 1847. Ueber das Dellmann'sche Elektrometer. *Annalen der Physik* **148** (11): 353–393. http://dx.doi.org/10.1002/andp.18471481102.

Kohlrausch, R. 1854. Theorie des elektrischen Rückstandes in der Leidener Flasche. *Annalen der Physik* **167** (2): 179–214. 10.1002/andp.18541670203.

Lewis, J.O., Beal, C.H. 1918. Some New Methods for Estimating the Future Production of Oil Wells. *Transactions of the AIME* **59** (01): 492–520. SPE-918492-G. http://dx.doi.org/10.2118/918492-G.

Maley, S. 1985. The Use of Conventional Decline Curve Analysis in Tight Gas Well Applications. SPE/DOE Low Permeability Gas Reservoirs Symposium, Denver, Colorado, May 19–22. SPE-13898-MS. http://dx.doi.org/10.2118/13898-MS.

Palmer, R.G., Stein, D.L., Abrahams, E. et al. 1984. Models of Hierarchically Constrained Dynamics for Glassy Relaxation. *Physical Review Letters* **53** (10): 958–961. 10.1103/PhysRevLett.53.958.

Robertson, S. 1988. Generalized Hyperbolic Equation. SPE-18731-MS.

Stehfest, H. 1970. Algorithm 368: Numerical inversion of Laplace transforms [D5]. *Communications of the ACM* **13** (1): 47-49. ACM-361969. http://dx.doi.org/10.1145/361953.361969.

Valkó, P.P. 2009. Assigning value to stimulation in the Barnett Shale: a simultaneous analysis of 7000 plus production hystories and well completion records. SPE Hydraulic Fracturing Technology Conference, The Woodlands, Texas, 19-21 January. SPE-119369-MS. http://dx.doi.org/10.2118/119369-MS.

Weibull, W. 1951. A Statistical Distribution Function of Wide Applicability. *Journal of Applied Mechanics-Transactions of the Asme* **18** (3): 293-297.

Williams, G., Watts, D.C. 1970. Non-symmetrical dielectric relaxation behaviour arising from a simple empirical decay function. *Transactions of the Faraday Society* **66** (0): 80–85. http://dx.doi.org/10.1039/TF9706600080.

APPENDIX A

DIMENSIONLESS HYPERBOLIC, MODIFY HYPERBOLIC, AND POWER-LAW EXPONENTIAL DECLINE MODELS APPROXIMATION BY A SUM-OF-EXPONENTIALS FUNCTION

Recalling the mathematical expression for the Power-Law Exponential (PLE) decline model we have,

$$q(t) = \hat{q}_i \exp[-D_\infty t - \hat{D}_i t^n] \quad \text{.....(A-1)}$$

Where:

$\hat{q}_i$ = initial flowrate coefficient,

D_∞ = terminal decline coefficient,

D_i = decline coefficient,

n = time exponent.

Neglecting boundary-dominated effects — which means that the terminal decline coefficient is zero — Eq. A-1 becomes,

$$q(t) = \hat{q}_i \exp[-\hat{D}_i t^n] \quad \text{.....(A-2)}$$

We select appropriate dimensionless variables for rate and time presented in Eq. A-3 and Eq. A-4, respectively,

$$q_D = \frac{q(t)}{\hat{q}_i} \quad \text{.....(A-3)}$$

$$t_D = \frac{t}{\hat{D}_i^{-1/n}} \quad \text{.....(A-4)}$$

Replacing time and rate dimensionless variables into Eq. A-2 yields the dimensionless PLE decline model as follows,

$$q_D(t_D) = \exp[-t_D^n] \quad \text{.....(A-5)}$$

For different time exponent (n) values, the dimensionless PLE decline model is calculated and presented graphically in **Fig. A-1.**

Recalling the mathematical expression for the Hyperbolic (HYP) (Eq. A-6) and Modify Hyperbolic (MH) (Eq. A-7) decline models we have,

$$q(t) = \frac{q_i}{[1 + bD_i t]^{1/b}}, \quad \text{(A-6)}$$

$$q(t) = \begin{cases} \dfrac{q_i}{[1 + bD_i t]^{1/b}}, & D > D_{lim} \\ q_{lim} \exp[-D_{lim}[t - t_{lim}], & D \le D_{lim} \end{cases}, \quad \text{(A-7)}$$

Where:

q_i = initial flowrate,

D_i = initial nominal decline rate,

b = decline exponent,

and, for the MH decline model,

$$q_{lim} = q_i \left[\frac{D_{lim}}{a_i} \right]^{1/b}, \quad \text{(A-8)}$$

$$t_{lim} = \frac{[q_i / q_{lim}]^b - 1}{bD_i} \quad \text{(A-9)}$$

Using appropriate dimensionless variables for rate and time (Eq. A-10 and Eq. A-11), we can represent the HYP and MH decline models in dimensionless terms, mathematically presented in Eq. A-12 and Eq.A-13, respectively, to give,

$$qD = \frac{q(t)}{q_i} \quad \text{(A-10)}$$

$$t_D = \frac{t}{D_i} \quad \text{(A-11)}$$

$$q_D(t_D) = \frac{1}{[1 + bt_D]^{1/b}} \quad \text{(A-12)}$$

$$q_D(t_D) = \begin{cases} \dfrac{1}{[1 + bt_D]^{1/b}}, & D_D < D_{Dlim} \\ q_{Dlim} \exp[-D_{Dlim}[t_D - t_{Dlim}], & D_D \ge D_{Dlim} \end{cases}, \quad \text{(A-13)}$$

where, for the dimensionless MH decline model,

$$D_{Dlim} = D_{lim} / D_i, \quad \text{(A-14)}$$

$$q_{Dlim} = \frac{q_{lim}}{q_i} = [D_{Dlim}]^{1/b}, \quad \text{(A-15)}$$

$$t_{Dlim} = \frac{t_{lim}}{D_i} = \frac{[1/q_{Dlim}]^b - 1}{b} \quad \text{(A-16)}$$

A graphical representation of the dimensionless decline models offered in this section is presented in **Fig. A-2,** including the dimensionless exponential decline mode.

Our goal is to approximate the dimensionless HYP, MH, and PLE decline models with a sum-of-exponential function as presented in Eq. A-17.

$$q_D(t_D) \approx \sum_{i=1}^{\infty} a_i \exp[-c_i t_D] \quad \text{(A-17)}$$

The sum allows an infinite number of terms but for our purposes, we develop an 8-term sum. With this consideration, Eq. A-17 becomes,

$$q_D(t_D) \approx \sum_{i=1}^{8} a_i \exp[-c_i t] \approx a_1 \exp[-c_1 t_D] + a_2 \exp[-c_2 t_D] + ... + a_8 \exp[-c_8 t_D] \quad \text{(A-18)}$$

Recalling the mathematical expressions for the loss ratio, $D(t)$, and the loss ratio derivative, $b(t)$, we have,

$$D(t) = -\frac{1}{q(t)} \frac{dq(t)}{dt}, \quad \text{(A-19)}$$

and,

$$b(t) = \frac{d}{dt}\left[\frac{1}{D(t)}\right] = -\frac{d}{dt}\left[\frac{q(t)}{dq(t)/dt}\right] \quad \text{(A-20)}$$

We transform $D(t)$, and $b(t)$ (Eq. A-19 and Eq. A-20) to a dimensionless form to have,

$$D_D(t_D) = -\frac{1}{q_D(t_D)} \frac{dq_D(t_D)}{dt_D}, \quad \text{(A-21)}$$

and,

$$b_D(t_D) = \frac{d}{dt_D}\left[\frac{1}{D_D(t_D)}\right] \quad \text{(A-22)}$$

Where,

$$D_D(t_D) = D(t)/D^{1/n}$$

$$b_D(t_D) = b(t)$$

Now we compute the specific mathematical expressions for $D_D(t_D)$, and $b_D(t_D)$ substituting $q_D(t_D)$ with a prescribed decline model. For the dimensionless HYP decline model we have,

$$D_{D_{HYP}}(t_D) = [1+bt_D]^{-1}, \text{ and} \quad \text{(A-23)}$$

$$b_{D_{HYP}}(t_D) = b \quad \text{(A-24)}$$

For the dimensionless MH decline model we get,

$$D_{D_{MH}}(t_D) = \begin{cases} [1+bt_D]^{-1}, & t_D < t_{D_{lim}} \\ D_{D_{lim}}, & t_D \geq t_{D_{lim}} \end{cases}, \text{ and} \quad \text{(A-25)}$$

$$b_{D_{MH}}(t_D) = \begin{cases} b, & t_D < t_{D_{lim}} \\ 0, & t_D \geq t_{D_{lim}} \end{cases} \quad \text{(A-26)}$$

For the dimensionless PLE decline model we have,

$$D_{D_{PLE}}(t_D) = nt_D{}^{-1+n}, \text{ and} \quad \text{(A-27)}$$

$$b_{D_{PLE}} = \frac{(1-n)}{n} t_D{}^{-n}, \quad \text{(A-28)}$$

Additionally, if we replace the 8-term sum-of-exponentials function approximation as a prescribed decline model we get,

$$D_D(t_D) = \frac{\sum_{i=1}^{8} -a_i c_i \exp[-c_i t_D]}{\sum_{i=1}^{8} a_i \exp[-c_i t_D]}, \text{ and} \quad \text{(A-29)}$$

$$b_D(t_D) = 1 - \frac{\sum_{i=1}^{8} a_i \exp[-c_i t_D] \sum_{i=1}^{8} a_i c_i{}^2 \exp[-c_i t_D]}{\sum_{i=1}^{8} -a_i c_i \exp[-c_i t_D]} \quad \text{(A-30)}$$

The results for the sum-of-exponentials function approximations are presented graphically in **Fig. A-3** for the HYP model (b = 0.5), **Fig. A-4** for the MH model (b = 0.5, and D_{Dlim} = 0.3), and in **Figs. A-5 through A-9** for the PLE model (n = 0.10, 0.25, 0.50, 0.75, and 0.90). The regression coefficients a, and c for each of the dimensionless decline models used in the analyses, are presented in **Tables A-1** and **A-2.** The

goodness of fit is quantified using statistical analysis including the calculation of the coefficient of determination (R^2), the root-mean-squared error (RMSE), and the mean absolute percentage error (MAPE). **Table A-3** presents the values of these parameters for the cases analyzed.

Table A-1 — Sum-of-exponentials function approximation regression coefficients a, and c for the dimensionless power-law exponential model — all time exponent (n) values.

	n = 0.10		n = 0.25	
i	a-coefficient	c-coefficient	a-coefficient	c-coefficient
1	9.841353×10^{-2}	6.573365×10^{5}	1.097850×10^{-1}	1.334994×10^{4}
2	1.098894×10^{-1}	6.641112×10^{3}	1.999069×10^{-1}	1.074632×10^{2}
3	1.094840×10^{-1}	1.534101×10^{2}	2.542623×10^{-1}	3.632678×10^{0}
4	1.087172×10^{-1}	6.528884×10^{0}	2.214290×10^{-1}	2.694054×10^{-1}
5	1.068735×10^{-1}	3.399521×10^{-1}	1.297597×10^{-1}	3.377798×10^{-2}
6	9.472461×10^{-2}	2.063725×10^{-2}	4.808604×10^{-2}	6.032813×10^{-3}
7	7.859471×10^{-2}	1.476507×10^{-3}	1.067426×10^{-2}	1.390193×10^{-3}
8	1.229141×10^{-1}	4.626721×10^{-5}	1.188956×10^{-3}	3.404229×10^{-4}

	n = 0.50		n = 0.75	
i	a-coefficient	c-coefficient	a-coefficient	c-coefficient
1	1.200419×10^{-1}	8.605042×10^{1}	1.418404×10^{-1}	9.964773×10^{0}
2	2.752668×10^{-1}	4.684082×10^{0}	4.217645×10^{-1}	1.315927×10^{0}
3	3.446412×10^{-1}	7.588249×10^{-1}	3.586537×10^{-1}	5.590372×10^{-1}
4	1.987149×10^{-1}	2.208953×10^{-1}	7.236349×10^{-2}	3.561238×10^{-1}
5	4.600016×10^{-2}	9.176576×10^{-2}	3.014942×10^{-3}	2.659094×10^{-1}
6	3.851469×10^{-3}	4.728950×10^{-2}	1.292699×10^{-5}	2.106522×10^{-1}
7	1.014553×10^{-4}	2.776573×10^{-2}	1.292699×10^{-8}	1.642442×10^{-1}
8	5.736669×10^{-7}	1.740180×10^{-2}	1.326987×10^{-12}	1.301183×10^{-1}

	n = 0.90	
i	a-coefficient	c-coefficient
1	2.113351×10^{-1}	2.422184×10^{0}
2	5.461201×10^{-1}	8.984480×10^{-1}
3	2.275310×10^{-1}	6.831430×10^{-1}
4	1.398680×10^{-2}	5.952928×10^{-1}
5	2.462382×10^{-5}	5.312010×10^{-1}
6	1.246238×10^{-9}	4.721902×10^{-1}
7	1.246200×10^{-14}	4.204995×10^{-1}
8	8.000000×10^{-20}	3.700010×10^{-1}

Table A-2 — Sum-of-exponentials function approximation regression coefficients a, and c for the dimensionless hyperbolic and modify hyperbolic decline models.

Dimensionless Hyperbolic Decline Model

i	a-coefficient	c-coefficient
1	1.17841×10^{-2}	6.10804×10^{0}
2	6.17862×10^{-1}	1.26462×10^{0}
3	3.30120×10^{-1}	3.53039×10^{-1}
4	3.73554×10^{-2}	8.99971×10^{-2}
5	2.68488×10^{-3}	2.24989×10^{-2}
6	1.73898×10^{-4}	5.64919×10^{-3}
7	1.13722×10^{-5}	1.42398×10^{-3}
8	6.63933×10^{-7}	2.94248×10^{-4}

Dimensionless Modify Hyperbolic Decline Model

i	a-coefficient	c-coefficient
1	1.22538×10^{-1}	1.50609
2	2.66159×10^{-1}	1.12335
3	3.64880×10^{-1}	0.30000
4	1.96120×10^{-1}	1.32032
5	4.63397×10^{-2}	2.12372
6	3.85836×10^{-3}	7.84564
7	1.01461×10^{-4}	19.9908
8	5.73667×10^{-7}	79.9997

Table A-3 — Goodness of fit parameters for all dimensionless decline models approximation by sum-of-exponentials function.

	HYP	MH	PLE (n = 0.10)	PLE (n = 0.25)
R^2	0.999996	0.999998	0.999637	0.999717
RMSE	0.818375	0.000838	0.006587	0.009032
MAPE	0.001301	0.119020	0.969736	1.459380

	PLE (n = 0.50)	PLE (n = 0.75)	PLE (n = 0.90)
R^2	0.999933	0.999963	0.999971
RMSE	0.004784	0.003251	0.002917
MAPE	0.801292	0.419920	0.350549

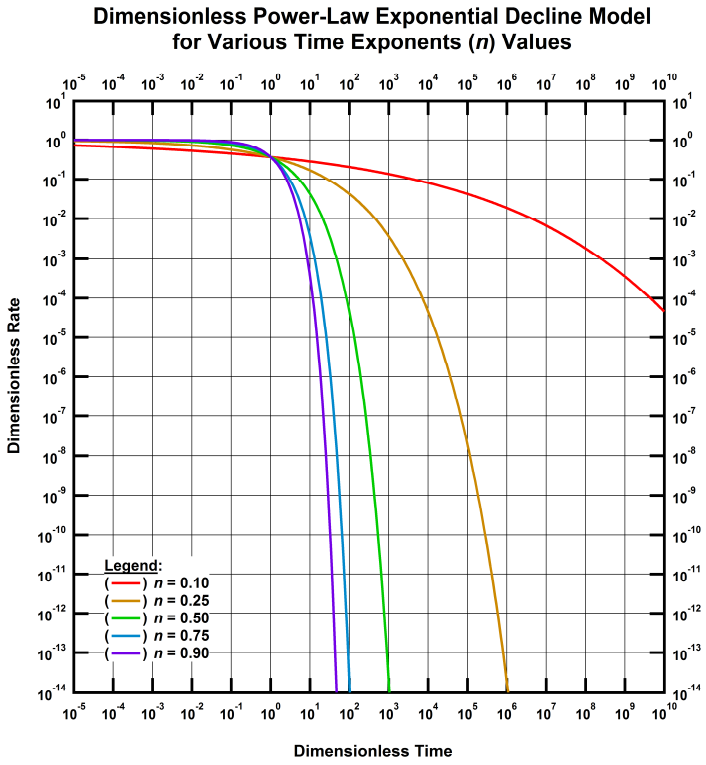

Figure A-1 — Dimensionless rate functions, various SE/PLE cases.

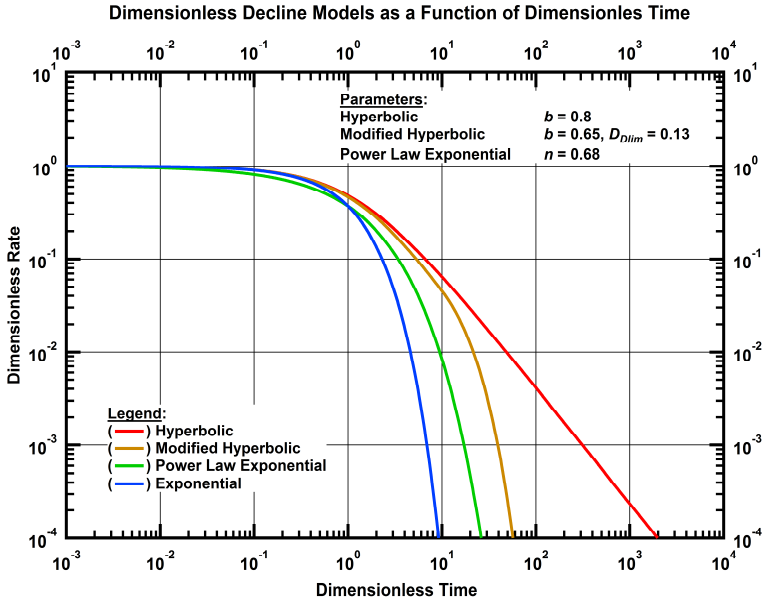

Figure A-2 — Dimensionless rate function, various rate-time models (exponential, hyperbolic, modified-hyperbolic, and power-law exponential).

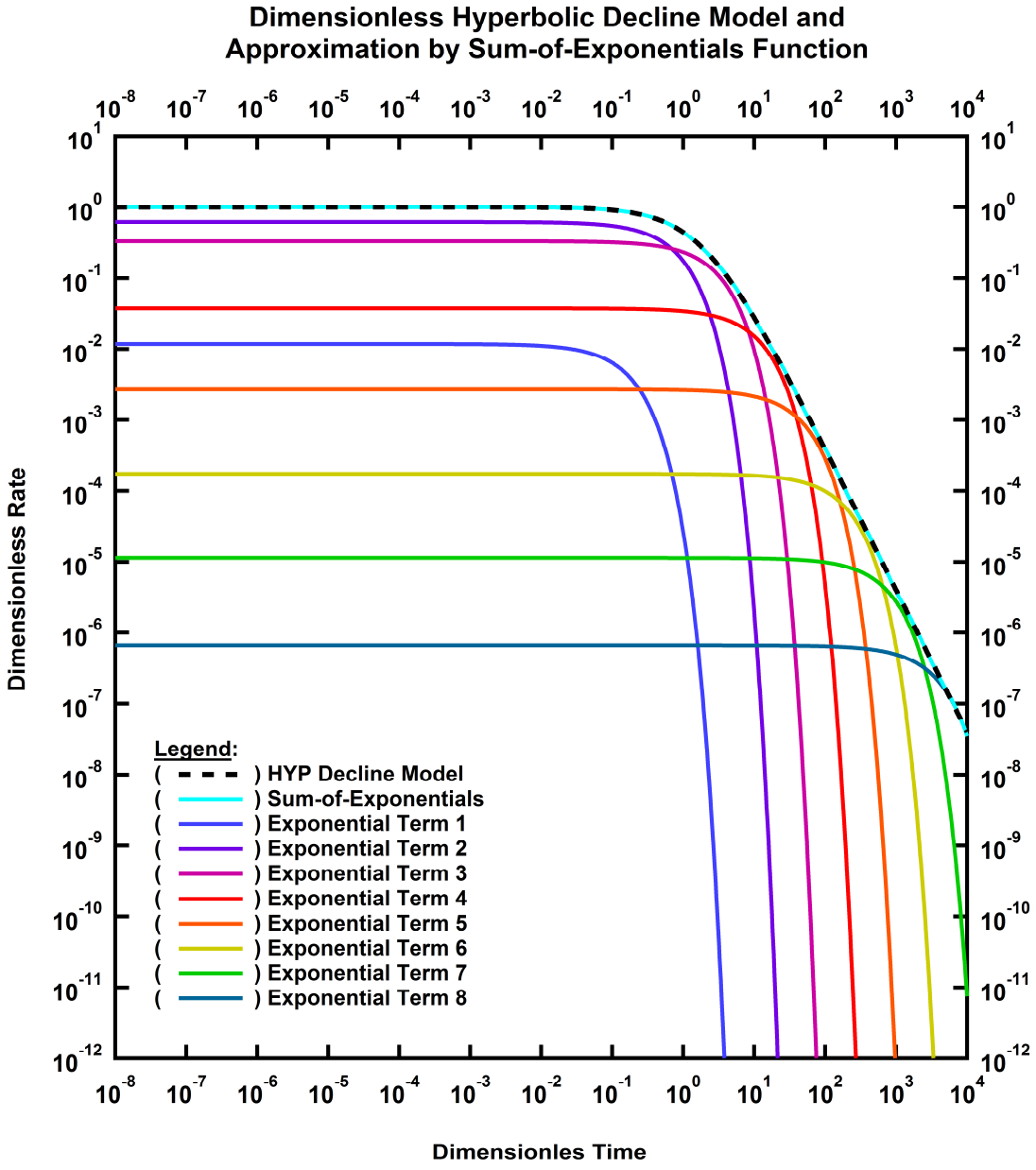

Figure A-3a — Dimensionless rate functions for the sum-of-exponentials approximation for the hyperbolic decline model.

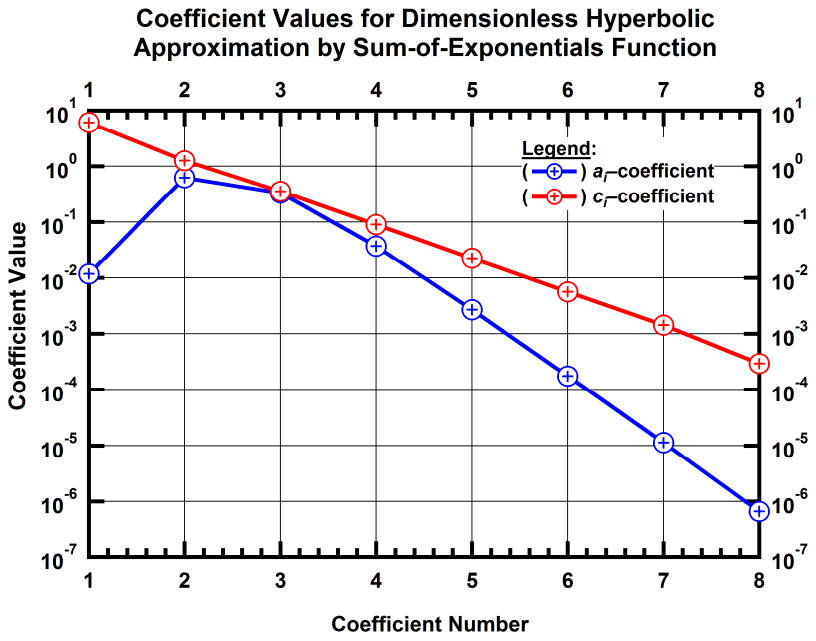

Figure A-3b — Coefficient values for the sum-of-exponentials approximation for the hyperbolic decline model.

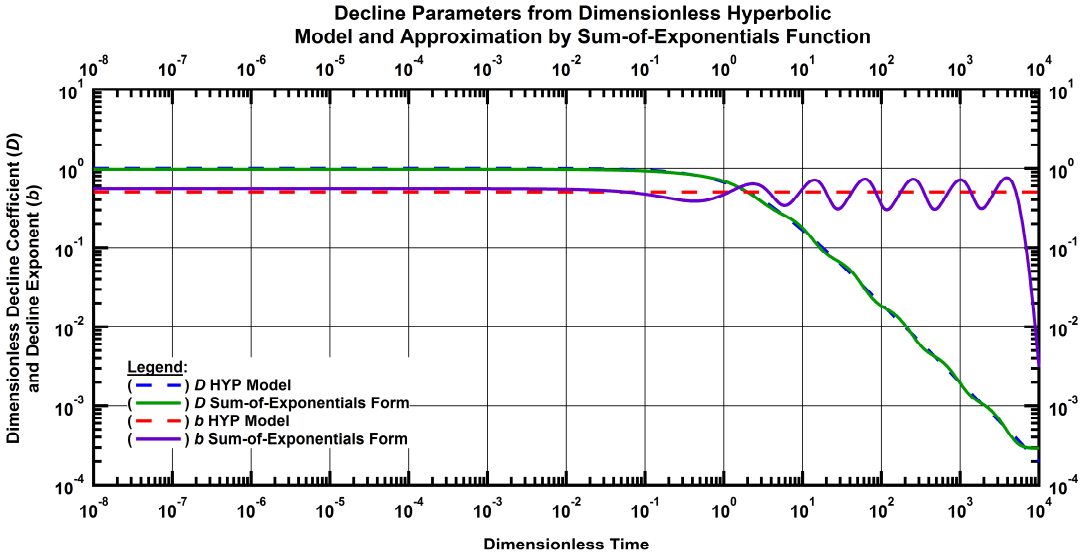

Figure A-3c — Arps $D_D(t_D)$ and $b_D(t_D)$ functions for the sum-of-exponentials approximation for the hyperbolic decline case.

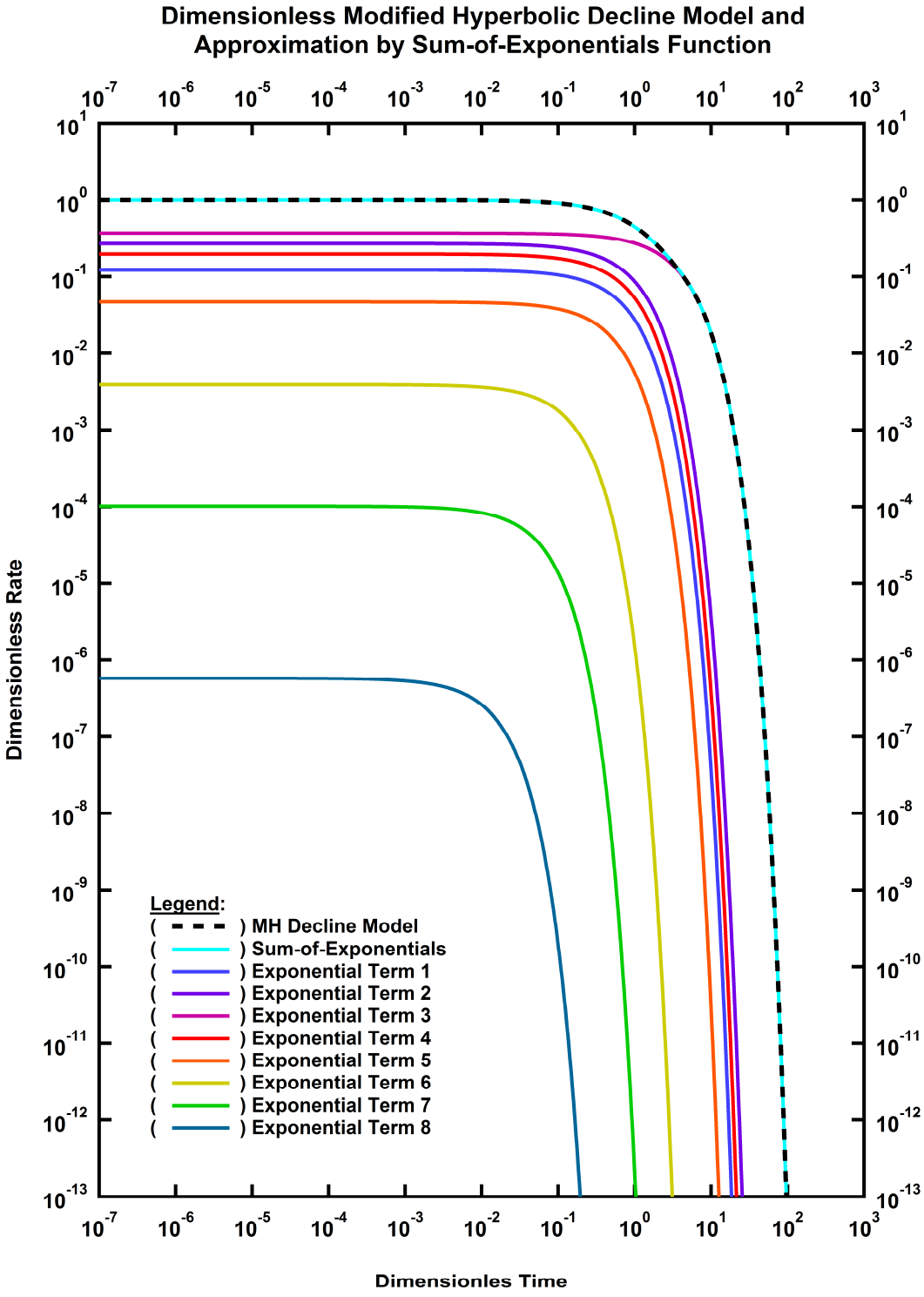

Figure A-4a — Dimensionless rate functions for the sum-of-exponentials approximation for the modified hyperbolic decline model.

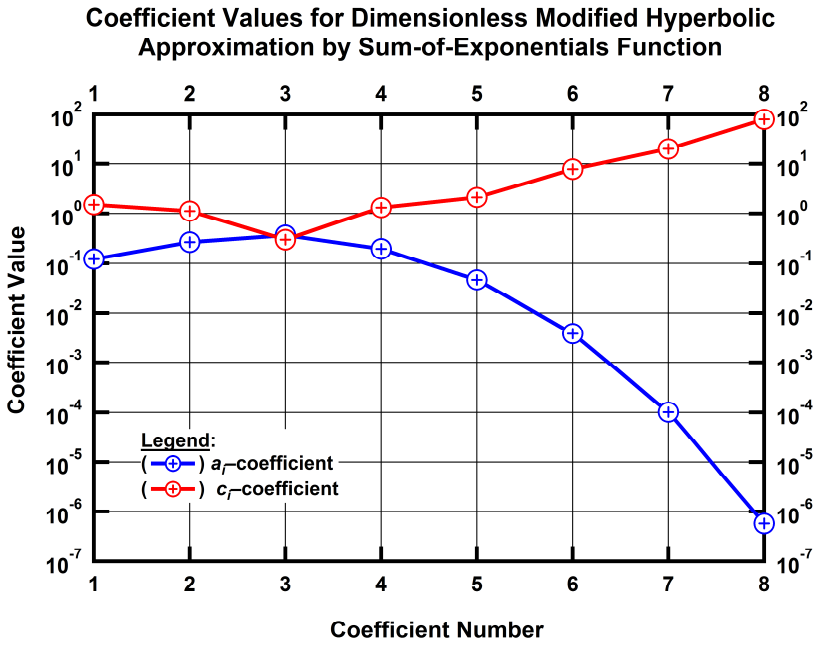

Figure A-4b — Coefficient values for the sum-of-exponentials approximation for the modified hyperbolic decline model.

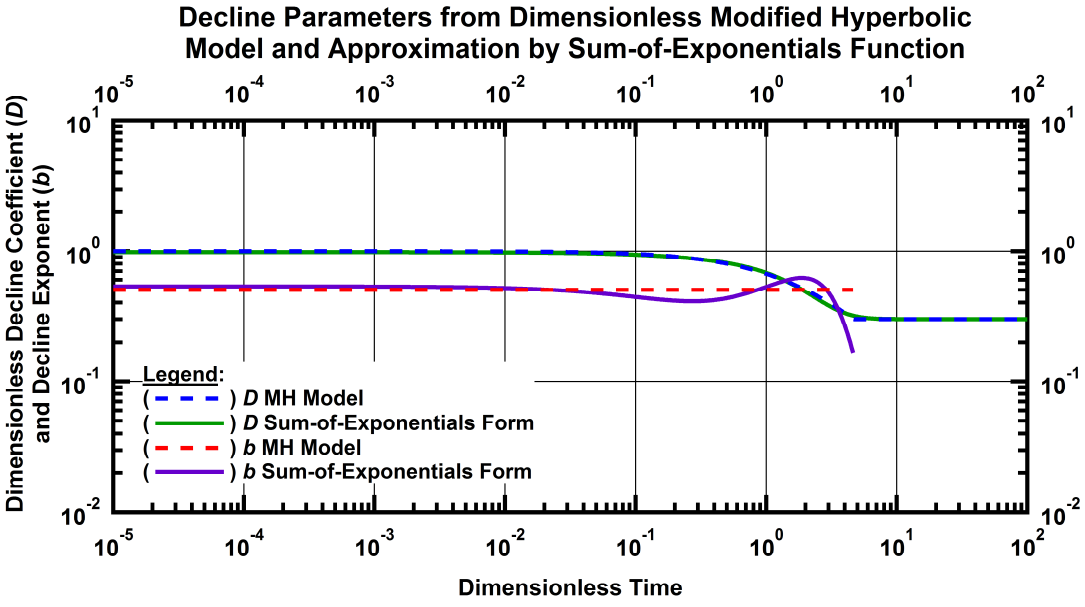

Figure A-4c — Arps $D_D(t_D)$ and $b_D(t_D)$ functions for the sum-of-exponentials approximation for the modified hyperbolic decline case.

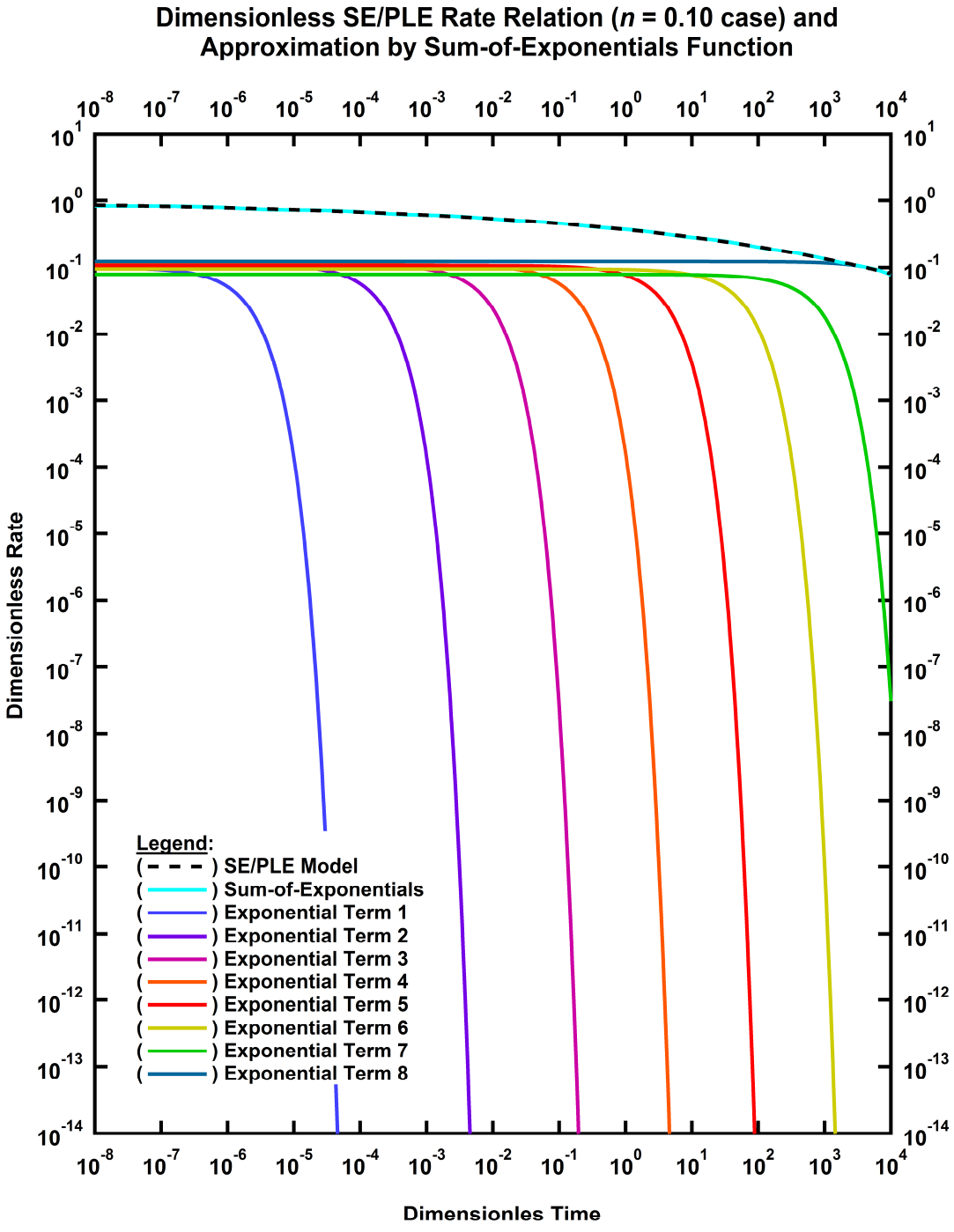

Figure A-5a — Dimensionless rate functions for the sum-of-exponentials approximation for the n = 0.10 SE/PLE case.

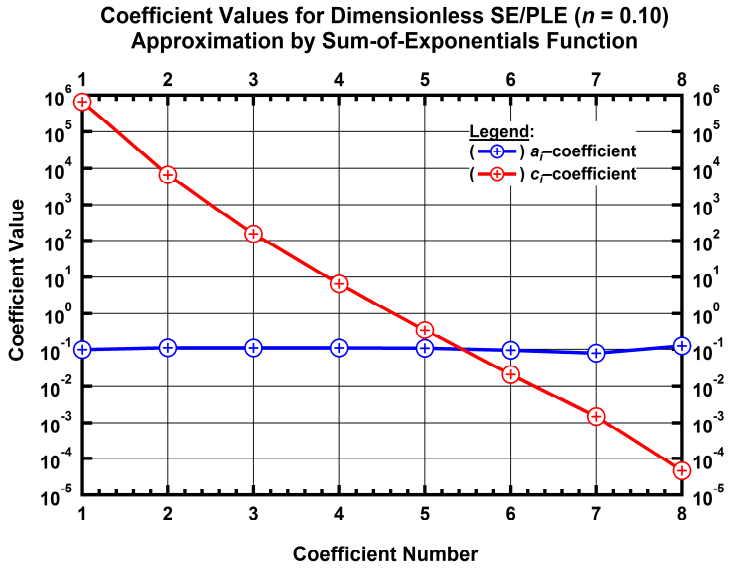

Figure A-5b — Coefficients a_i and c_i values for the sum-of-exponentials approximation for the n = 10 SE/PLE case.

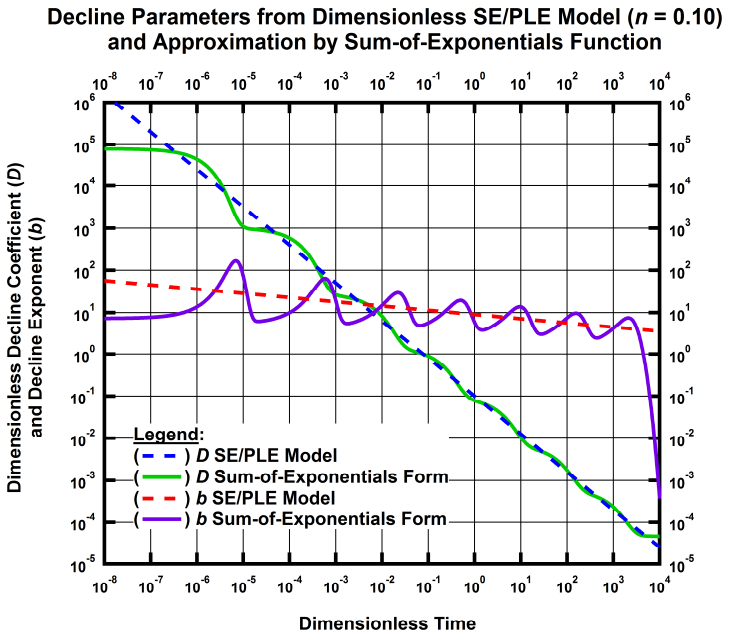

Figure A-5c — Arps $D_D(t_D)$ and $b_D(t_D)$ functions for the sum-of-exponentials approximation for the n = 0.10 SE/PLE case.

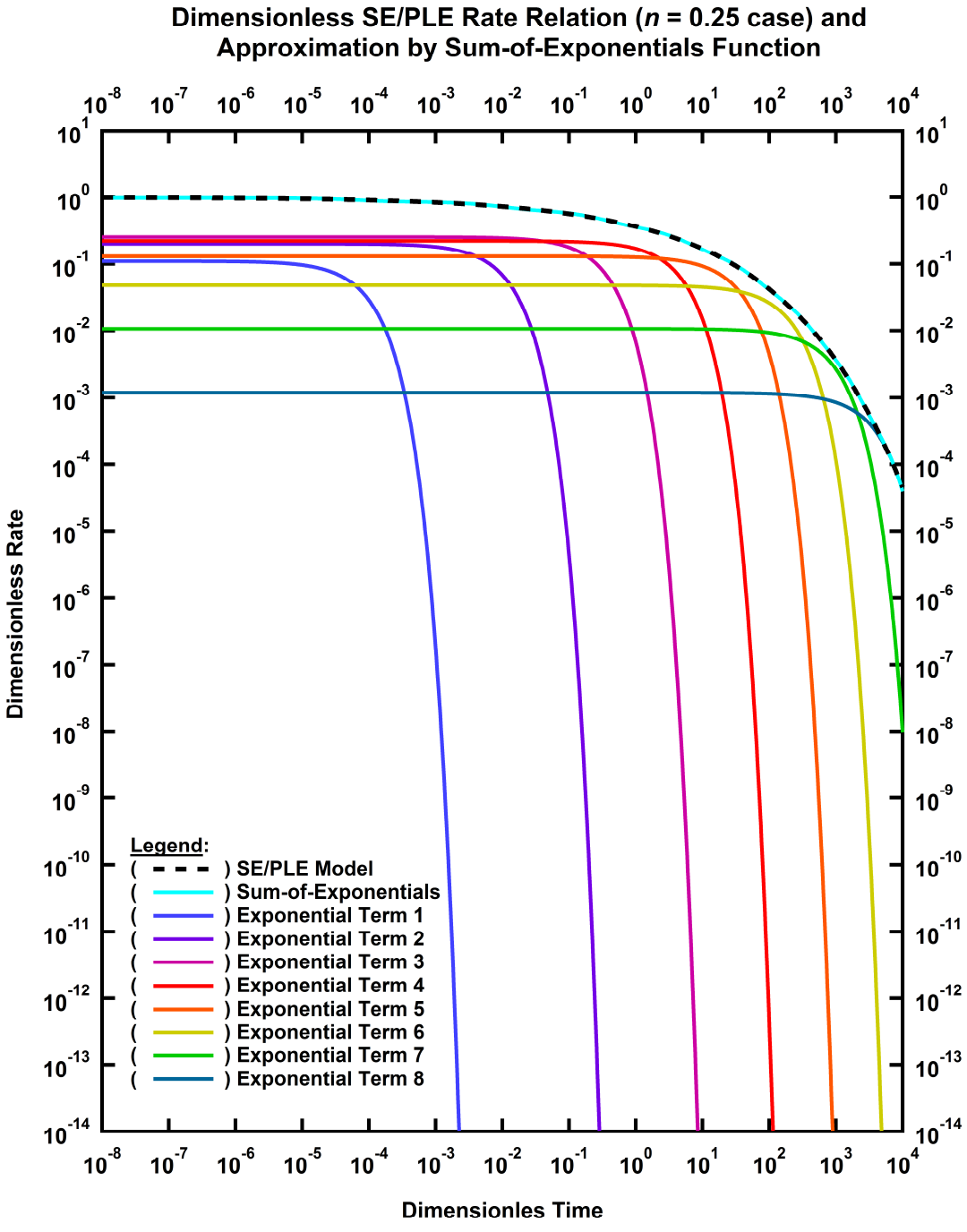

Figure A-6a — Dimensionless rate functions for the sum-of-exponentials approximation for the n = 0.25 SE/PLE case.

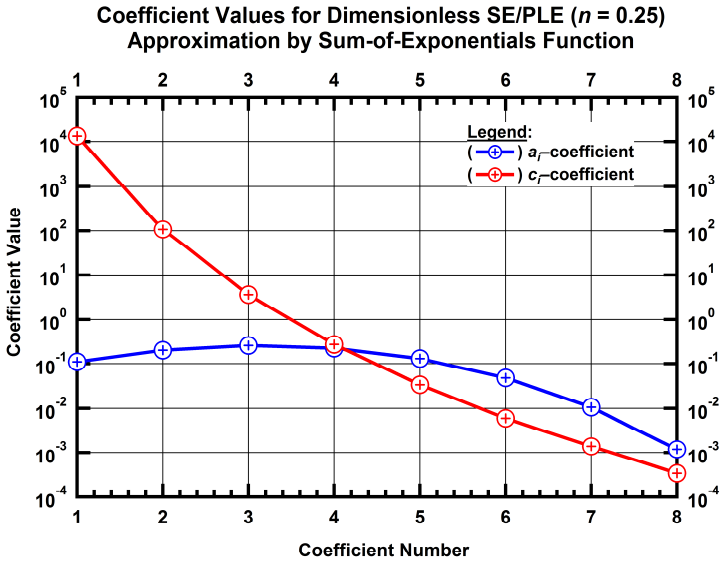

Figure A-6b — Coefficients a_i and c_i values for the sum-of-exponentials approximation for the n = 25 SE/PLE case.

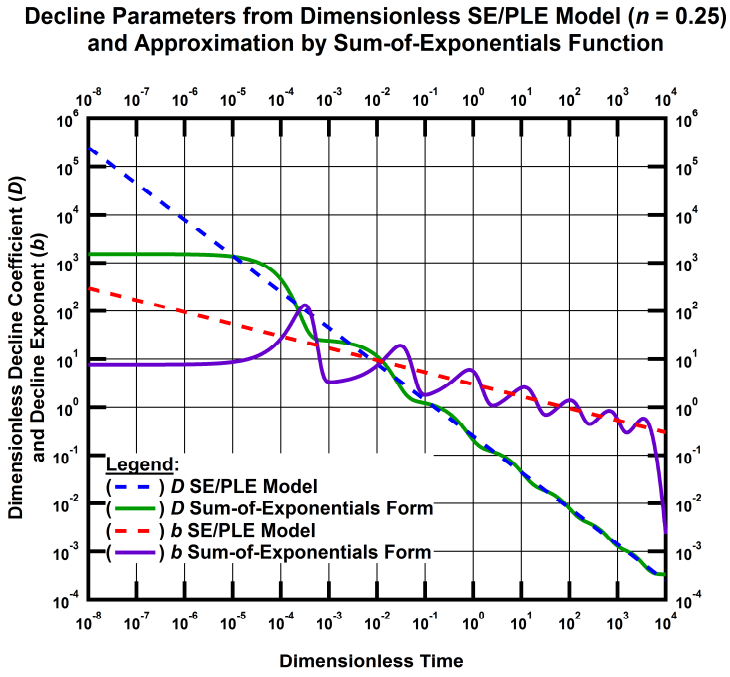

Figure A-6c — Arps $D_D(t_D)$ and $b_D(t_D)$ functions for the sum-of-exponentials approximation for the n = 0.25 SE/PLE case.

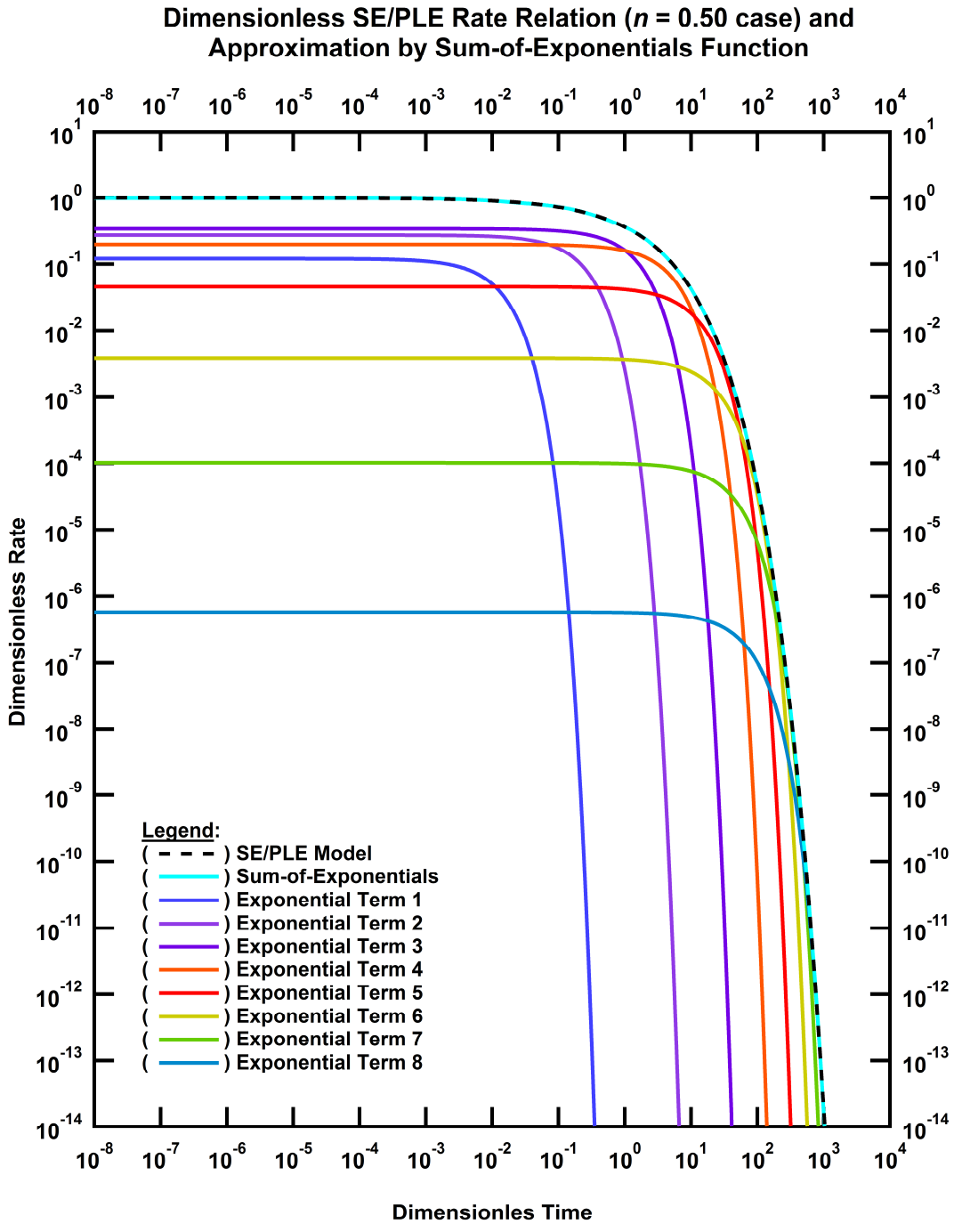

Figure A-7a — Dimensionless rate functions for the sum-of-exponentials approximation for the n = 0.50 SE/PLE case.

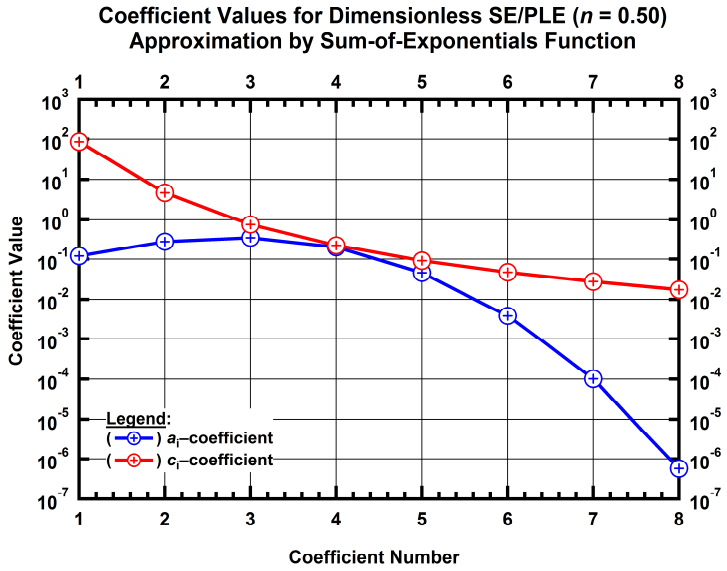

Figure A-7b — Coefficients a_i and c_i values for the sum-of-exponentials approximation for the n = 50 SE/PLE case.

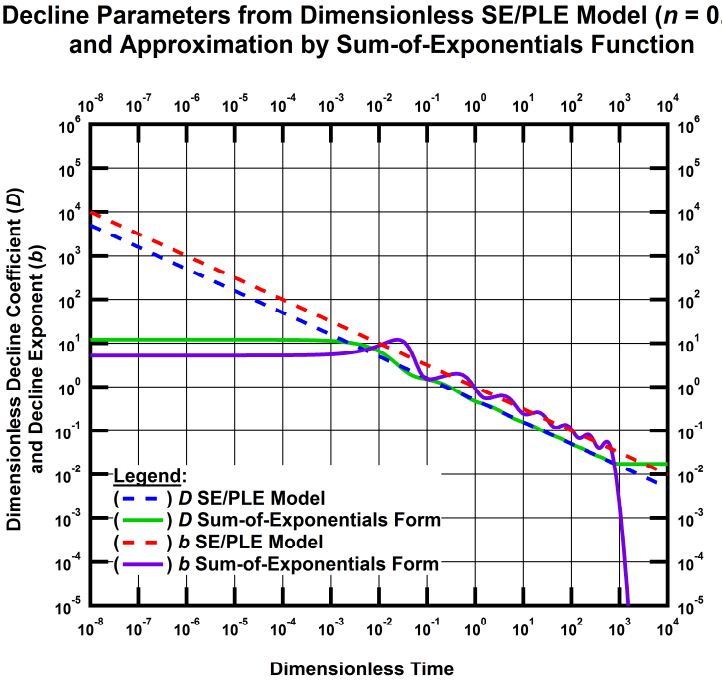

Figure A-7c — Arps $D_D(t_D)$ and $b_D(t_D)$ functions for the sum-of-exponentials approximation for the n = 0.50 SE/PLE case.

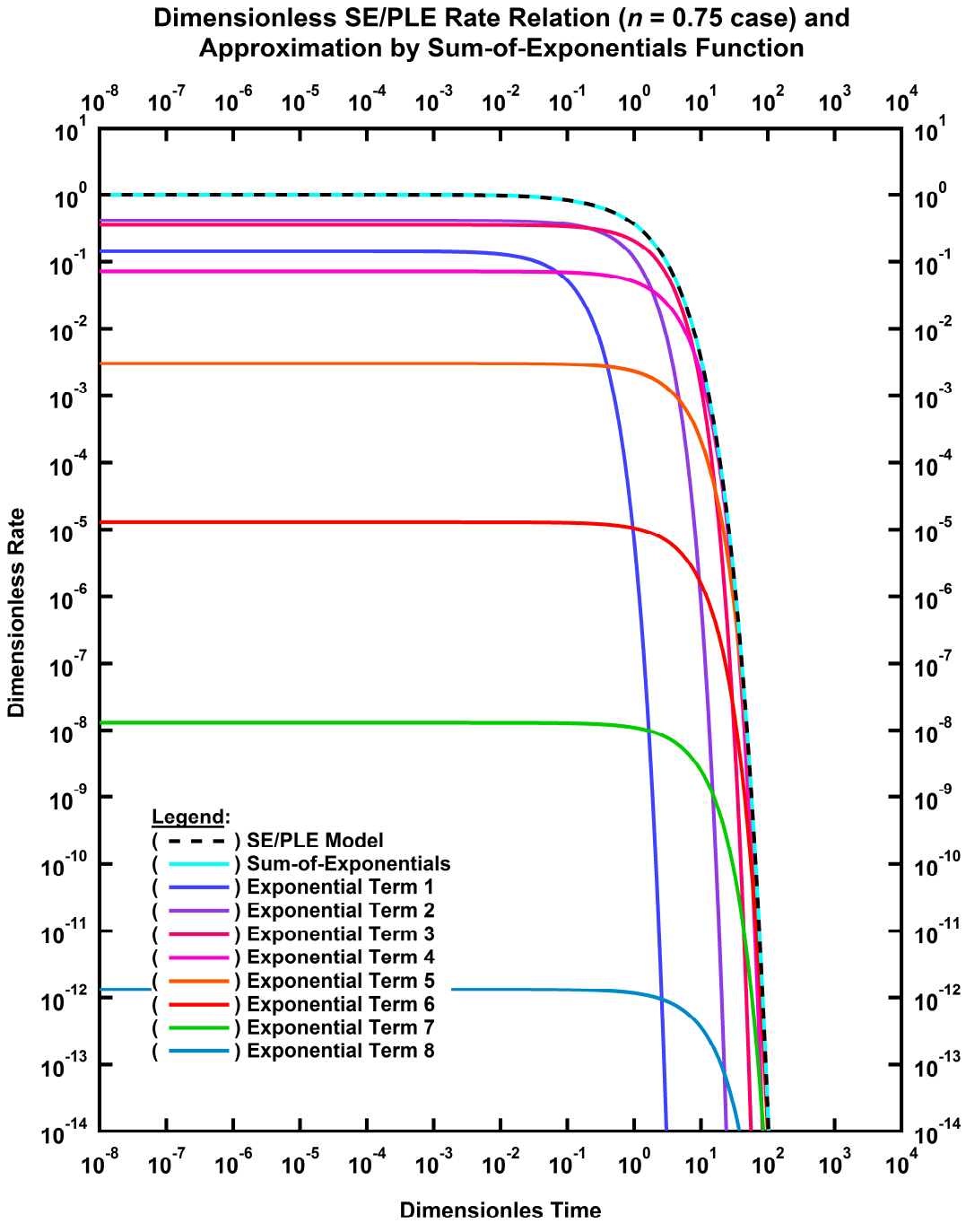

Figure A-8a — Dimensionless rate functions for the sum-of-exponentials approximation for the n = 0.75 SE/PLE case.

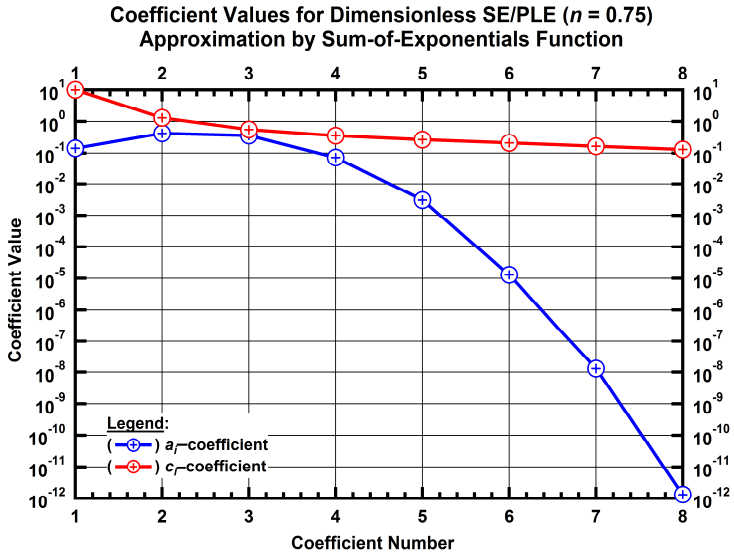

Figure A-8b — Coefficients a_i and c_i values for the sum-of-exponentials approximation for the n = 75 SE/PLE case.

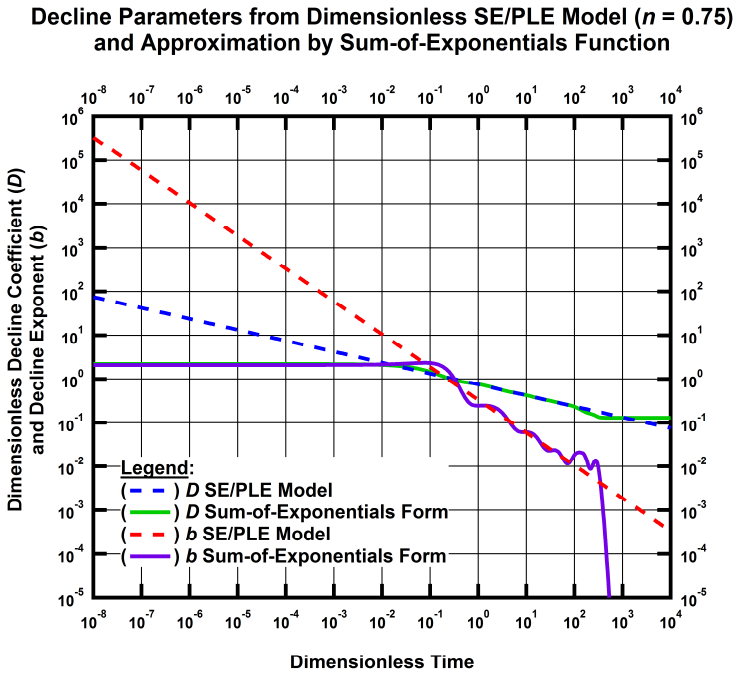

Figure A-8c — Arps $D_D(t_D)$ and $b_D(t_D)$ functions for the sum-of-exponentials approximation for the n = 0.75 SE/PLE case.

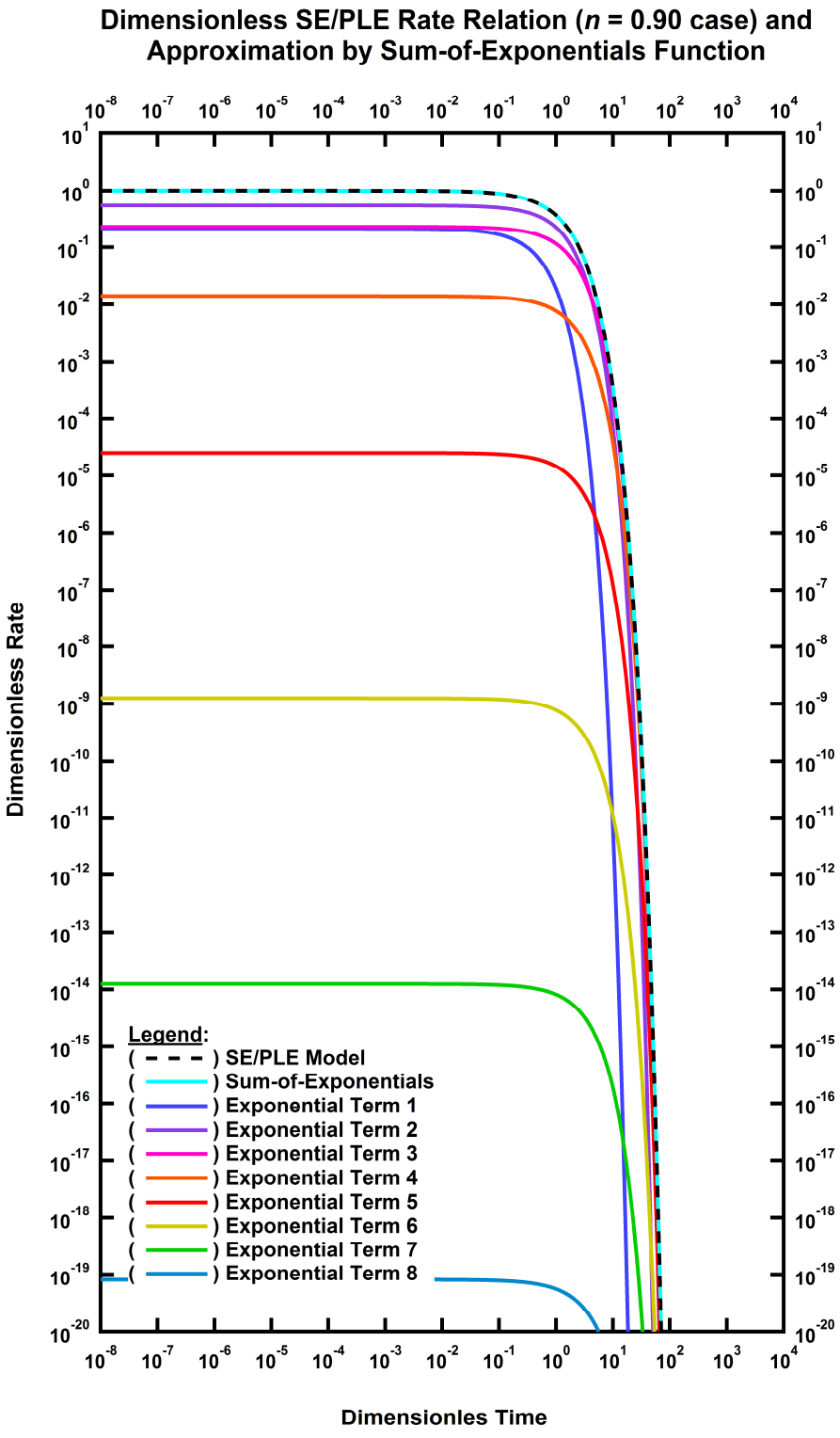

Figure A-9a — Dimensionless rate functions for the sum-of-exponentials approximation for the n = 0.90 SE/PLE case.

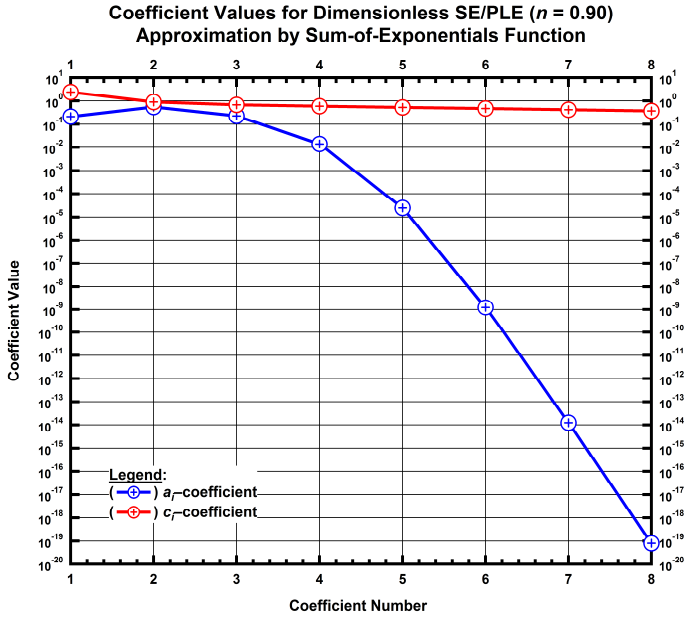

Figure A-9b — Coefficients a_i and c_i values for the sum-of-exponentials approximation for the n = 90 SE/PLE case.

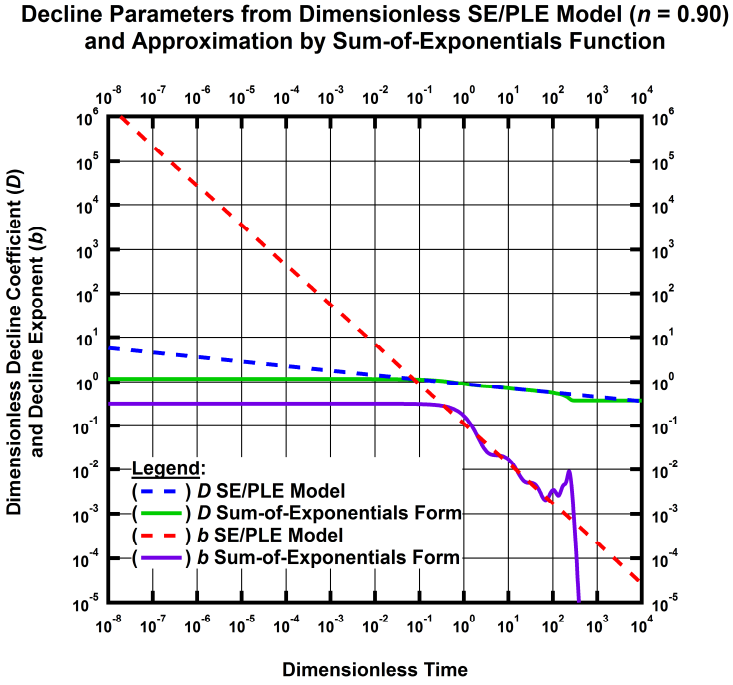

Figure A-9c — Arps $D_D(t_D)$ and $b_D(t_D)$ functions for the sum-of-exponentials approximation for the n = 0.90 SE/PLE case.

APPENDIX B

LAPLACE TRANSFORM OF THE DIMENSIONLESS STRETCHED EXPONENTIAL/POWER-LAW EXPONENTIAL DECLINE MODEL WITH $n = 0.50$

Recalling the expression for the dimensionless stretched exponential/power-law exponential (SE/PLE) decline model we have,

$$q_D(t_D) = \exp[-t_D^{\,n}] \,, \qquad \text{(B-1)}$$

where n is the time exponent. For this specific case, we make $n = 0.50$ or 1/2; therefore, we get,

$$q_D(t_D) = \exp[-t_D^{\,1/2}] \qquad \text{(B-2)}$$

From Laplace transform tables (Oberhettinger and Badii, 1973, *Tables of Laplace Transform*) we found that for the function,

$$f(t) = \exp[-at^{1/2}] \,, \qquad \text{(B-3)}$$

the Laplace transform is,

$$\bar{g}(u) = \int_0^\infty f(t)e^{-ut}dt = \frac{1}{u} - \frac{a\, e^{\frac{a^2}{4u}}\sqrt{\pi}\,\mathrm{Erfc}\left[\frac{a}{2\sqrt{u}}\right]}{2\,\mathrm{u}^{3/2}} \qquad \mathrm{Re}\ u > 0 \,, \qquad \text{(B-4)}$$

where Erfc is the complementary error function, defined as,

$$\mathrm{Erfc}(x) = \frac{2}{\sqrt{\pi}}\int_x^\infty e^{-t^2}\,dt \qquad \text{(B-5)}$$

Using Eq. B-4, and making $a = 1$, we get the Laplace transform for the dimensionless SE/PLE decline model for the case $n = 0.50$ as follows,

$$\bar{q}_D(u) = \frac{1}{u} - \frac{e^{\frac{1}{4u}}\sqrt{\pi}\,\mathrm{Erfc}\left[\frac{1}{2\sqrt{u}}\right]}{2\,\mathrm{u}^{3/2}} \qquad \text{(B-6)}$$

We compute Eq. B-6 for a logarithmic time range and the results are presented graphically in **Fig. B-1.** We use the "convolution" integral in Laplace domain to obtain the "constant rate" pressure response from the dimensionless SE/PLE time-rate model. Recalling the convolution integral in Laplace domain we have,

$$\bar{p}_{Dcr}(u) = \frac{1}{u^2 \bar{q}_{Dcp}(u)} \quad \text{.....(B-7)}$$

Therefore, replacing Eq. B-6 into Eq. B-7 we get a dimensionless pressure expression in Laplace domain as,

$$\bar{p}_D(u) = \frac{2}{2u - e^{\frac{1}{4u}} \sqrt{\pi} \sqrt{u} \operatorname{Erfc}\left[\frac{1}{2\sqrt{u}}\right]} \quad \text{.....(B-8)}$$

We compute Eq. B-8 for a logarithmic time range and the results are presented graphically in **Fig. B-2.** Since there is no direct Laplace transform of Eq. B-8, we use a numerical inversion algorithm to obtain the pressure response in real time. We select the traditional Stehfest algorithm for this section of the work; for completeness, we compute the well test pressure derivative as well. These results are presented graphically in **Fig. B-3.**

By observation of Fig. B-1, it seems noticeable that the trend of the dimensionless SE/PLE rate in Laplace domain may be approximated with a hyperbolic function to simplify the mathematical form of Eq. B-6. Therefore, an expression with regression coefficients is used to make such approximation, as follows,

$$\bar{q}_D(u) \approx \frac{a_1}{[1 + a_2 u]^{1/a_3}} \text{ ,} \quad \text{.....(B-9)}$$

where a_1, a_2 and a_3 are the regression coefficients used to match the exact rate-time solution. Performing a regression analysis, we obtain the approximation as is presented graphically in **Fig. B-4.** The coefficient values for the best fit are: a_1 = 1.99995, a_2 = 2.194587, and a_3 = 1.005188. Furthermore, we obtain the dimensionless "constant rate" pressure approximation by substituting Eq. B-9 into Eq. B-7, giving,

$$\bar{p}_D(u) \approx \frac{[1 + a_2 u]^{1/a_3}}{a_1 u^2} \quad \text{.....(B-10)}$$

We compare the results of the dimensionless pressure approximation with the exact pressure solution as can be observed graphically in **Fig. B-5.** We are able to compute the real time dimensionless pressure response from Eq. B-10 since there is a direct inverse Laplace transform expression for this functional form, to give,

$$p_D(t) \approx \frac{[a_2 + a_3 t]\Gamma\left[-\frac{1}{a_3}\right] + a_3\left[a_2 \Gamma\left[\frac{a_3 - 1}{a_3}, \frac{t}{a_2}\right] - t\Gamma\left[-\frac{1}{a_3}, \frac{t}{a_2}\right]\right]}{a_1 a_3 \Gamma\left[-\frac{1}{a_3}\right]} \quad \text{.....(B-11)}$$

which was computed using Wolfram Mathematica. For completeness, we compute the well test pressure

derivative from Eq. B-11. The mathematical expression is given by,

$$p_D'(t) \approx \frac{t\left[\Gamma\left[-\frac{1}{a_3},\frac{t}{a_2}\right]-\Gamma\left[-\frac{1}{a_3}\right]\right]}{a_1\Gamma\left[-\frac{1}{a_3},\frac{t}{a_2}\right]} \quad \text{.....(B-12)}$$

In Eq. B-11 and Eq. B-12, $\Gamma(s)$ is the gamma function and $\Gamma(s,x)$ is the upper incomplete gamma function. The results computed from the pressure and pressure derivative approximations can be observed in **Fig. B-6.**

As an additional test, we developed a rational polynomial expression to match the dimensionless SE/PLE flowrate trend, observed in Fig. B-1, in the form of,

$$\bar{q}_D(u) \approx \frac{b_1 + b_2 u}{1 + b_3 u + b_4 u^2}, \quad \text{.....(B-13)}$$

where b_1, b_2, b_3, and b_4, are regression coefficients. Performing the regression analysis, we found that the values of these coefficients are: $b_1 = 2.0$, $b_2 = 0.893318$, $b_3 = 4.758922$, and $b_4 = 0.894517$. The results are presented graphically in **Fig. B-7.** As with the hyperbolic function approximation, we obtain the functional forms of the pressure in Laplace domain (Eq. B-14) and in real time (Eq. B-15) (there is a direct Laplace inversion expression), and for completeness the well test pressure derivative (Eq. B-16) is calculated. These mathematical expressions are presented below:

$$\bar{p}_D(u) \approx \frac{1 + b_3 u + b_4 u^2}{u^2[b_1 + b_2 u]} \quad \text{.....(B-14)}$$

$$p_D(t) \approx \left[\frac{b_3}{b_1} - \frac{b_2}{b_1^2}\right] + \frac{[b_2^2 - b_1 b_2 b_3 + b_1^2 b_4]e^{-\frac{b_1 t}{b_2}}}{b_1^2 b_2} + \frac{t}{b_1} \quad \text{.....(B-15)}$$

$$p_D'(t) \approx \frac{t}{b_1} - \frac{[b_2^2 - b_1 b_2 b_3 + b_1^2 b_4]e^{-\frac{b_1 t}{b_2}} t}{b_1 b_2^2} \quad \text{.....(B-16)}$$

The pressure results from the rational polynomial approximation are presented graphically in **Fig. B-8** and **Fig. B-9**.

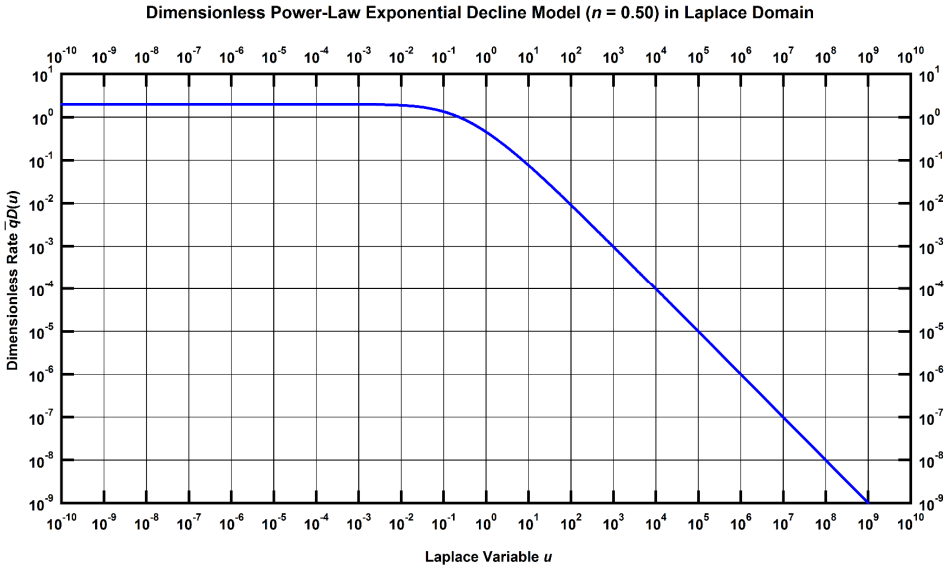

Figure B-1 — Dimensionless SE/PLE decline model (n = 0.50) in Laplace domain.

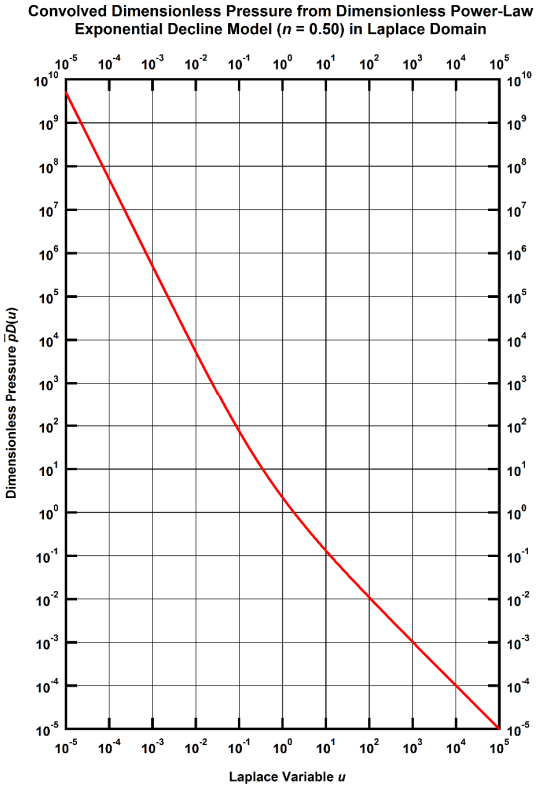

Figure B-2 — Dimensionless "constant rate" pressure from the dimensionless SE/PLE decline model (n = 0.50) in Laplace domain.

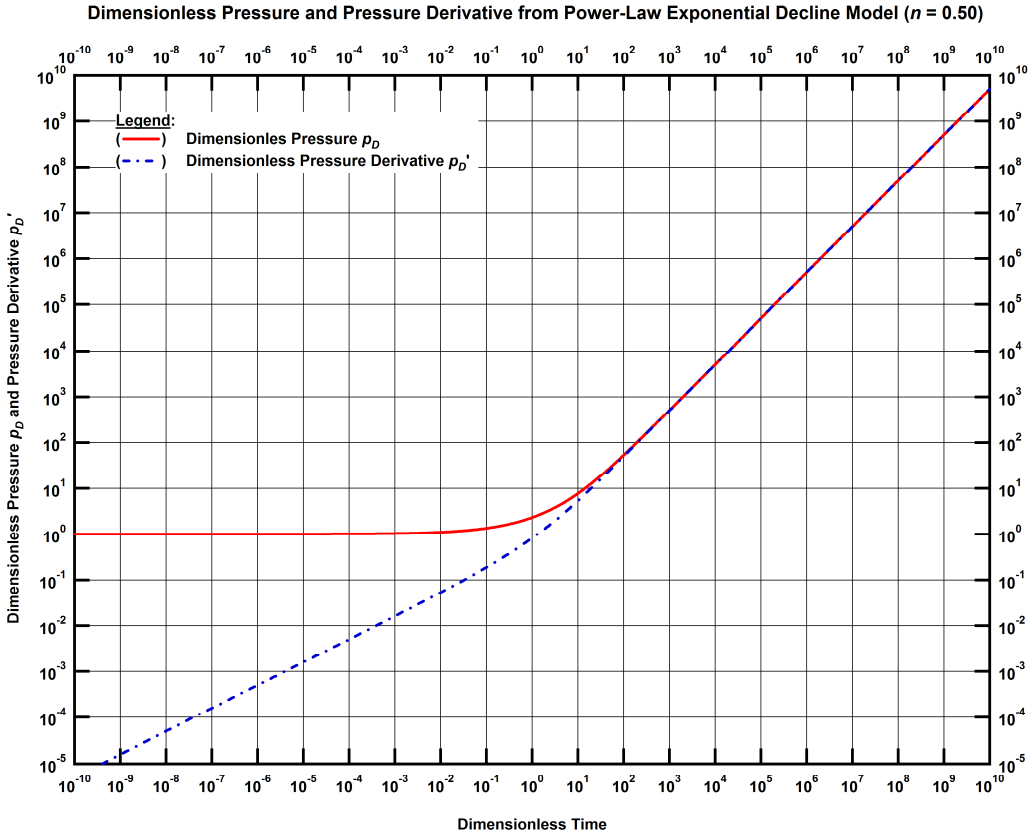

Figure B-3 — Dimensionless pressure and pressure derivative from the dimensionless SE/PLE decline model (n = 0.5) – numerical Laplace inversion using Stehfest algorithm.

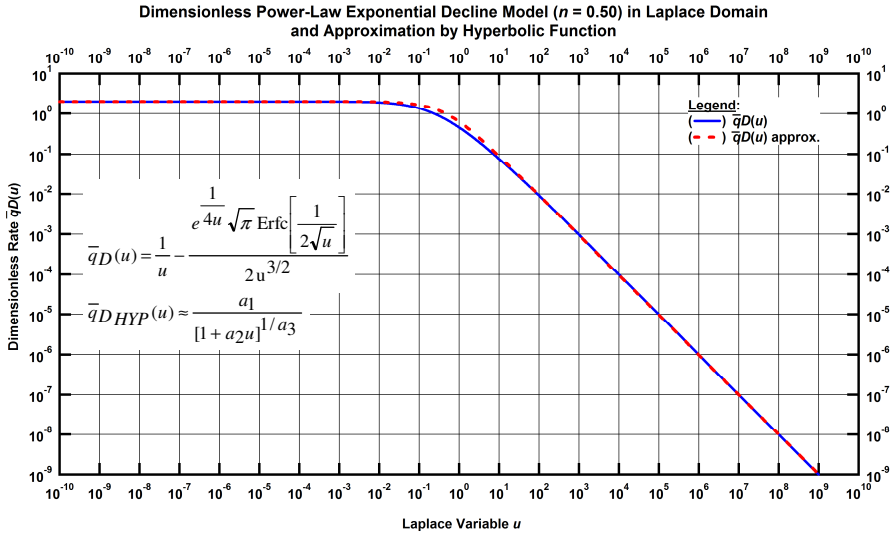

Figure B-4 — Dimensionless SE/PLE decline model (n = 0.50) in Laplace Domain and approximation by hyperbolic function.

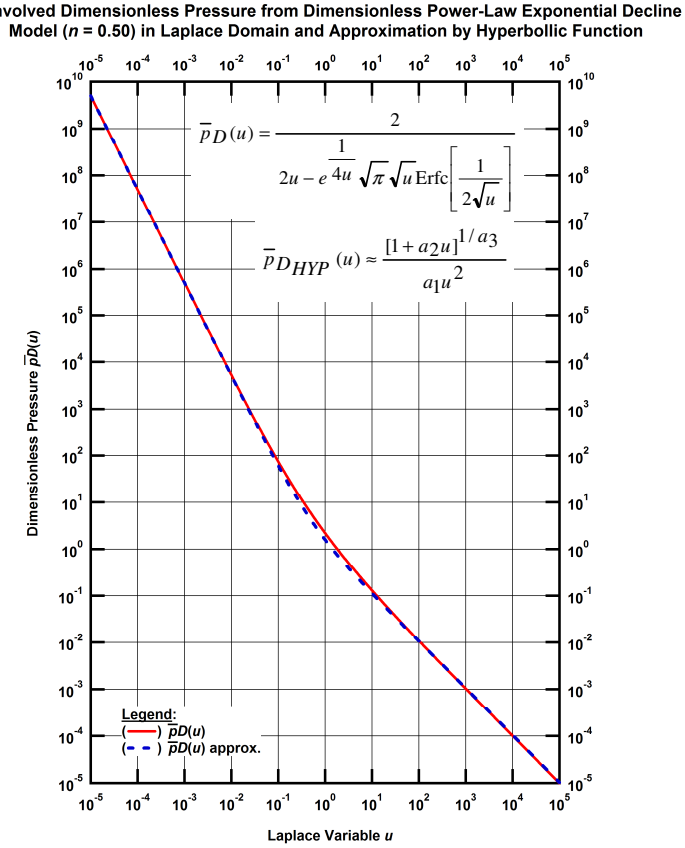

Figure B-5 — Dimensionless "constant rate" pressure from the SE/PLE decline model (n = 0.50) in Laplace domain and approximation by hyperbolic function.

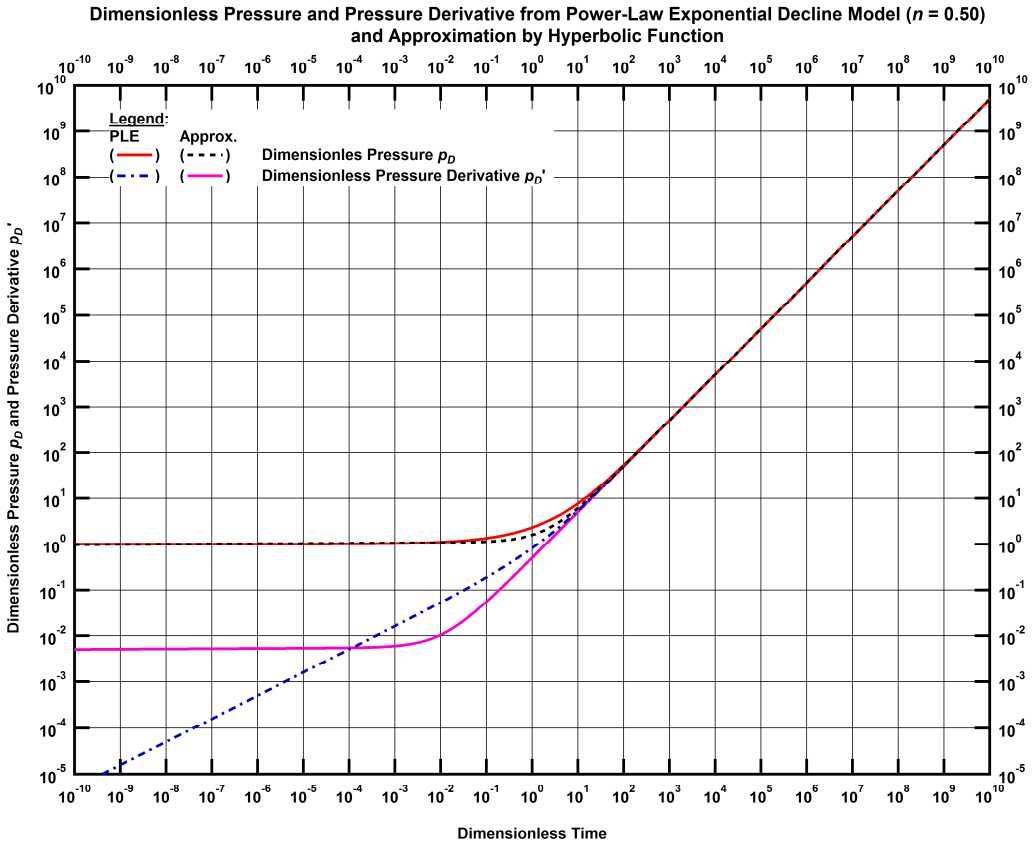

Figure B-6 — Dimensionless pressure and pressure derivative in real domain from the SE/PLE decline model (n = 0.5) and approximation by hyperbolic function.

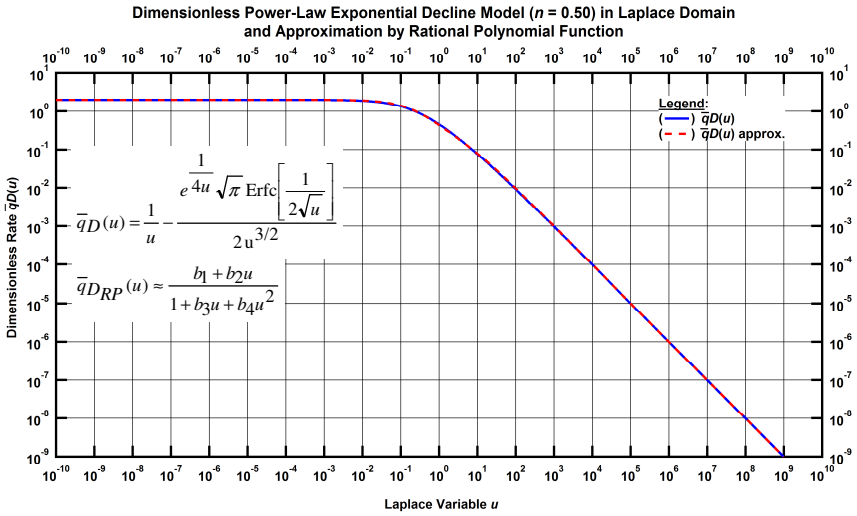

Figure B-7 — Dimensionless SE/PLE decline model (n = 0.50) in Laplace Domain and approximation by rational polynomial function.

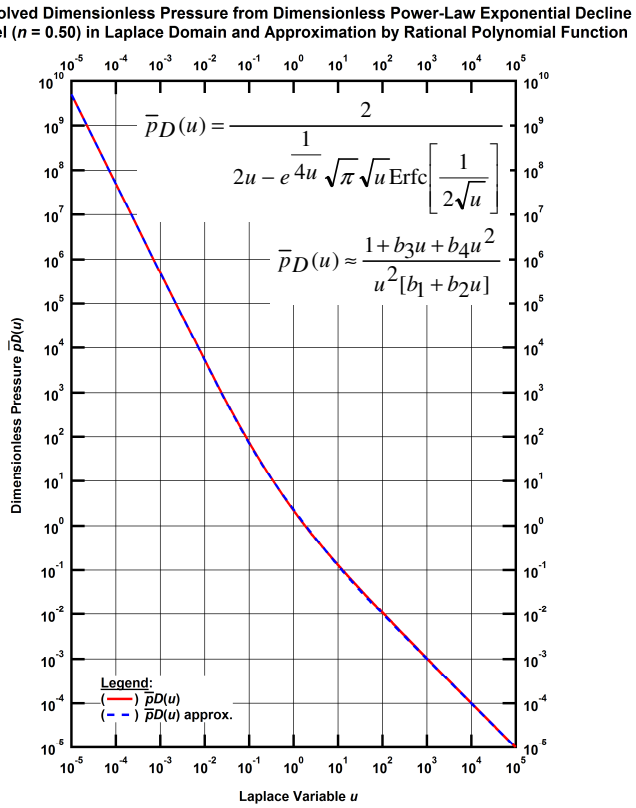

Figure B-8 — Dimensionless "constant rate" pressure from the SE/PLE decline model (n = 0.50) in Laplace domain and approximation by rational polynomial function.

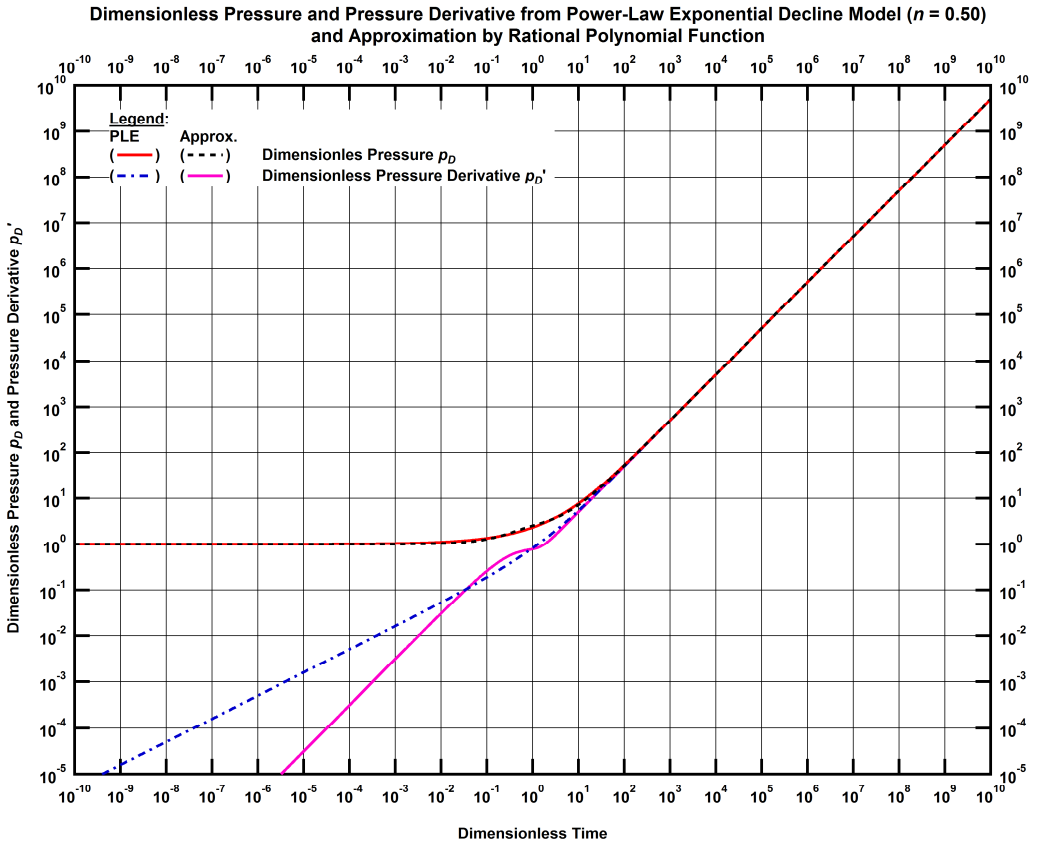

Figure B-9 — Dimensionless pressure and pressure derivative in real domain from the SE/PLE decline model (n = 0.5) and approximation by rational polynomial function.

APPENDIX C

DIMENSIONLESS POWER-LAW EXPONENTIAL DECLINE MODEL IN LAPLACE DOMAIN APPROXIMATIONS

Recalling the dimensionless form of the Stretched Exponential/Power Law Exponential (SE/PLE) decline model — presented in appendix A — we have:

$$q_D(t_D) = \exp[-t_D{}^n] \quad \text{(C-1)}$$

There is no direct Laplace transform of Eq. C-1 (*i.e.*, for a general value of the time exponent, n) — except for very specific cases (*e.g.*, n = 1/2 or 1). To develop a comprehensive understanding of the behavior of Eq. C-1 in the Laplace domain, we will test three different numerical approaches in order to find an approximation in Laplace domain:

- Approximate the SE/PLE relation by Taylor series expansion, and then take this approximating function directly into the Laplace domain.
- Use the Laguerre quadrature formulation to transform a general function into the Laplace domain.
- Use methodology proposed by Blasingame (1995) to determine the Laplace transform of a piecewise power-law function.

Taylor Series Expansion Approach:

Recalling the Taylor series expansion of a real function $f(x)$ about a point $x = a$, we have:

$$f(x) = f(a) + f'(a)(x-a) + \frac{f''(a)}{2!}(x-a)^2 + \frac{f^{(3)}(a)}{3!}(x-a)^3 + \ldots + \frac{f^{(n)}(a)}{n!}(x-a)^n \quad \text{(C-2)}$$

or,

$$f(x) = \sum_{i=0}^{\infty} \frac{f^{(i)}(a)}{i!}(x-a)^i \quad \text{(C-3)}$$

Recalling the dimensionless SE/PLE decline model and making a variable of substitution, $y = -t_D{}^n$, we get:

$$q_D(y) = \exp[y] \quad \text{(C-4)}$$

Replacing the real function in Eq. C-3 with Eq. C-4, and making $a = 0$ gives:

$$q_D(y) \approx \sum_{i=0}^{\infty} \frac{1}{i!}\left[\frac{d^{(i)}\exp[y]}{dy^{(i)}}\right] y^i = \sum_{i=0}^{\infty} \frac{y^i}{i!} \quad \text{(C-5)}$$

Replacing the variable of substation $y = -t_D{}^n$ into Eq. C-5 we get the Taylor series expansion approximation

of the dimensionless SE/PLE decline model as follows:

$$q_D(t_D) \approx \sum_{i=0}^{\infty} \frac{[-1]^i}{i!} t_D{}^{ni} \qquad \text{(C-6)}$$

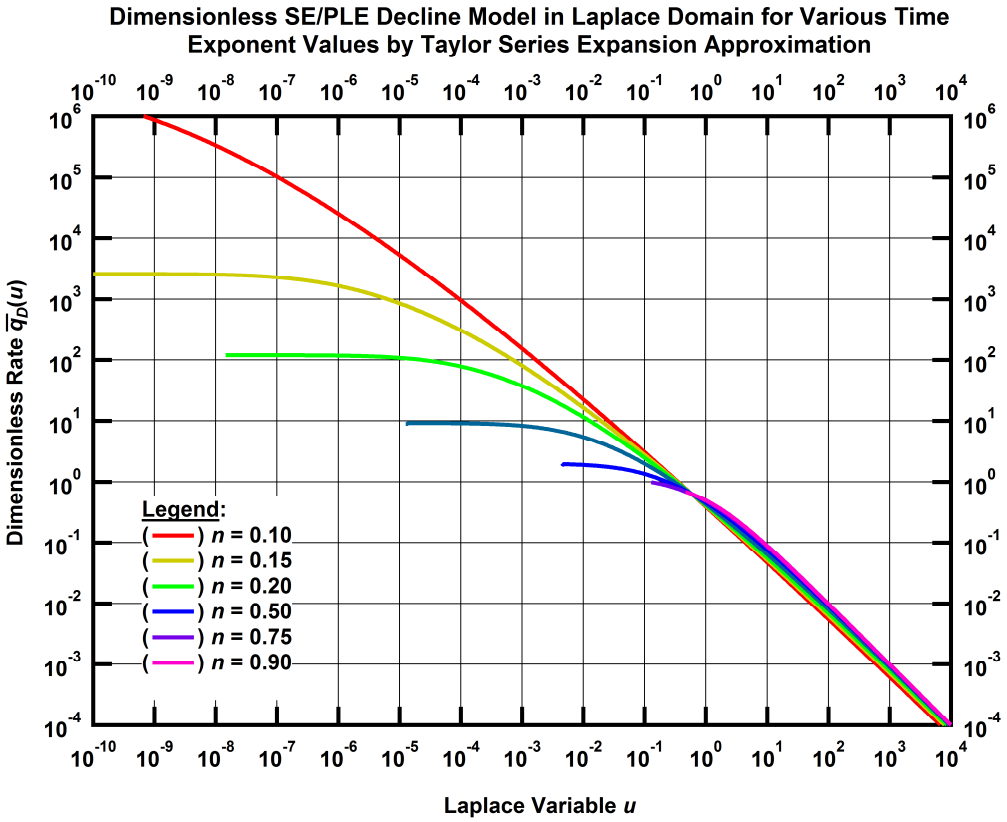

Figure C-1 — Dimensionless SE/PLE decline model in Laplace domain for various time exponent values, *n*, by Taylor series expansion approximation.

From Laplace transform tables (Oberhettinger and Badii, 1973, *Tables of Laplace Transform*) we found that for the function:

$$f(t) = t^v \qquad \mathrm{Re}\, v > -1 \qquad \text{(C-7)}$$

the Laplace transform is,

$$\bar{g}(u) = \int_0^{\infty} f(t) e^{-ut} dt = u^{-v-1} \Gamma(v+1) \qquad \mathrm{Re}\ u > 0 \qquad \text{(C-8)}$$

where $\Gamma(v+1)$ is the gamma function, defined as,

$$\Gamma(x) = \int_0^\infty x^{z-1} e^{-x} dx \quad \text{(C-9)}$$

By inspection of Eq. C-6 and Eq. C-7, we identify that $t_D{}^n \equiv t^v$. Therefore, using Eq. C-8 we get the Laplace transform for the dimensionless SE/PLE by Taylor series approximation, as follows:

$$\bar{q}_D(u) \approx \frac{1}{u} \sum_{i=0}^{\infty} \frac{\Gamma(1+ni)}{i!} \left[-\frac{1}{u^n} \right]^i \quad \text{(C-10)}$$

The results obtained from Eq. C-10 — for different SE/PLE time exponent values, n — are presented graphically in **Fig. C-1.** We observed failed trends that can be attributed to numerical instability at small values of dimensionless time.

Laguerre Quadrature Approach:
Recalling the definition of the Laplace transform we have:

$$\bar{f}(u) = \int_0^\infty f(t) e^{-ut} dt \quad \text{(C-11)}$$

We use a variable of substitution $x = ut$, and we know that $dx = udt$. Reviewing the limits of Eq. C-11 as well as our variable of substitution we get that $t = x/u$ and $dt = dx/u$, and that at $t = 0$, $x = 0$, and at $t = \infty$, x = ∞. These changes yields:

$$\bar{f}(u) = \frac{1}{u} \int_0^\infty f(x/u) e^{-x} dx, \quad \text{(C-12)}$$

which is of the form,

$$\bar{f}(u) = \frac{1}{u} \int_0^\infty g(x) dx, \quad \text{(C-13)}$$

where,

$$g(x) = f(x/u) e^{-x} \quad \text{(C-14)}$$

From the Laguerre quadrature definition we have:

$$\int_0^{\infty} g(x)dx \approx \sum_{i=1}^{m} w_i e^{x_i}\, g(x_i)\ , \quad \text{(C-15)}$$

where x_i , the abscissa, is the i^{th} zero of the Laguerre polynomials, $L_m(x)$,and the w_i are the weights. The Laguerre polynomials are given by the sum:

$$L_m(x) = \sum_{k=0}^{m} \frac{(-1)^k}{k!}\binom{m}{k} x^k\ , \quad \text{(C-16)}$$

and the weights,

$$w_i = \frac{x_i}{(m+1)^2 [L_{m+1}(x_i)]^2} \quad \text{(C-17)}$$

Combining Eq. C-13 and Eq. C-15 we get,

$$\bar{f}(u) = \frac{1}{u}\sum_{i=1}^{m} w_i e^{x_i}\left[f\left(\frac{x_i}{u}\right) e^{-x_i} \right]$$

or,

$$\bar{f}(u) = \frac{1}{u}\sum_{i=1}^{m} w_i f\left(\frac{x_i}{u}\right) \quad \text{(C-18)}$$

Eq. C-18 is a completely general relation for taking the Laplace transform of a function $f(u)$. Recalling the dimensionless SE/PLE decline model we have:

$$q_D(t_D) = \exp[-t_D{}^n] \quad \text{(C-1)}$$

Replacing Eq. C-1 into Eq. C-18 and changing the equation to our working variables yields:

$$\bar{q}_D(u) \approx \frac{1}{u}\sum_{i=1}^{m} w_i \exp\left[-\left(\frac{x_i}{u}\right)^n \right], \quad \text{(C-19)}$$

Where n is the time exponent from the SE/PLE model and m is the quadrature order of the abscissas. We compute Eq. C-19 for various time exponent values. The weights, w_i, and roots, x_i, of the Laguerre polynomials are calculated for a quadrature order of m = 1000. The results are presented graphically in **Fig. C-2.** We observed failed trends that can be attributed to numerical instability at small values of dimensionless time.

Blasingame Method Approach:

The first step is to take the Laplace transform of data points as a piecewise power-law continuous function. A schematic plot for this approach is shown in **Fig. C-3.** The Laplace transform of a piecewise data function is given by:

$$\overline{f}(u) = \sum_{i=1}^{k} \overline{f_i}(u) = \sum_{i=1}^{k} \int_{t_{i-1}}^{t_i} f_i(t) e^{-ut} dt, \qquad 0 = t_0 < t_1 \ldots < t_{k-1} < t_k \equiv \infty, \quad \text{(C-20)}$$

where the continuous data function, $f_i(t)$, is as follows:

$$f_i(t) = \alpha_i t^{\beta_i} = \alpha_i t^{\nu_i - 1} \quad \text{(C-21)}$$

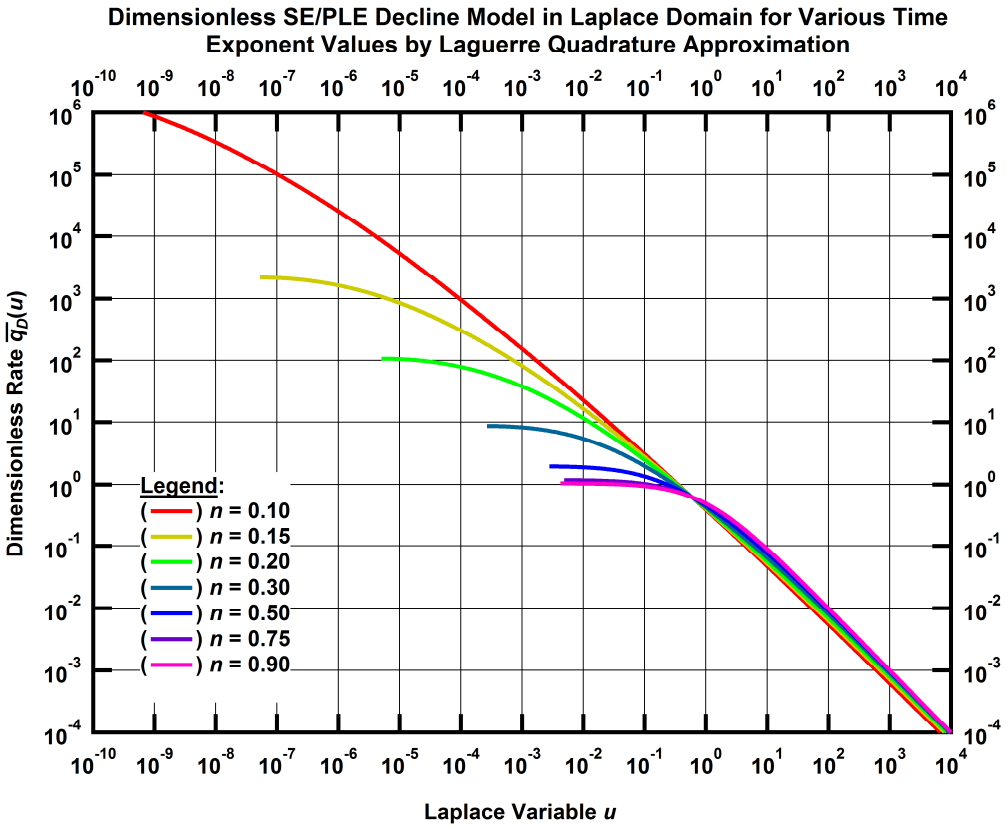

Figure C-2 — Dimensionless SE/PLE decline model in Laplace domain for various time exponent values, n, by Laguerre quadrature approximation.

Considering an arbitrary partition, $t_{i-1} < t < t_i$, and combining Eqs. C-20 and C-21 we have:

$$\overline{f_i}(u) = \alpha_i \int_{t_{i-1}}^{t_i} t^{v_i - 1} e^{-ut}\, dt \quad \text{(C-22)}$$

Considering the limits in Eq. C-22, as well as an arbitrary integrand, $i(t)$, we can write:

$$\int_{t_{i-1}}^{t_i} i(t)dt = \int_0^{\infty} i(t)dt - \int_{t_i}^{\infty} i(t)dt - \int_0^{t_{i-1}} i(t)dt \quad \text{(C-23)}$$

The integrals in Eq. C-23 can be replaced analytically. From Gradshteyn and Ryzhik (2014. *Table of integrals, series, and products*. Saint Louis, US: Academic Press.), we have:

$$\int_0^{\infty} x^m \exp[-\beta x^n]dx = \frac{\Gamma(\gamma)}{n\beta^{\gamma}}, \quad \gamma = \frac{m+1}{n} \quad [\mathrm{Re}\,\beta > 0,\ \mathrm{Re}\,m > 0,\ \mathrm{Re}\,n > 0], \quad \text{(C-24)}$$

$$\int_u^{\infty} x^n \exp[-\mu x]dx = \mu^{-n-1}\Gamma(n+1, \mu u) \quad [u > 0, \mathrm{Re}\,\mu > 0, n = 0,1,2,\ldots], \quad \text{(C-25)}$$

$$\int_0^{u} x^n \exp[-\mu x]dx = \mu^{-n-1}\gamma(n+1, \mu u) \quad [u > 0, \mathrm{Re}\,\mu > 0, n = 0,1,2,\ldots] \quad \text{(C-26)}$$

Which for our variables, Eq. C-24 through Eq. C-26 become:

$$\int_0^{\infty} t^{v_i - 1} e^{-ut}\, dt = u^{-v_i}\Gamma(v_i), \quad \text{(C-27)}$$

$$\int_{t_i}^{\infty} t^{v_i - 1} e^{-ut}\, dt = u^{-v_i}\Gamma(v_i, ut_i), \quad \text{(C-28)}$$

$$\int_0^{t_{i-1}} t^{v_i - 1} e^{-ut}\, dt = u^{-v_i}\gamma(v_i, ut_{i-1}) \quad \text{(C-29)}$$

Substituting Eq. C-27 through Eq. C-29 into Eq. C-23 we get:

$$\int_{t_{i-1}}^{t_i} t^{v_i - 1} e^{-ut}\, dt = \frac{1}{u^{v_i}}[\Gamma(v_i) - \Gamma(v_i, ut_i) - \gamma(v_i, ut_{i-1})] \quad \text{(C-30)}$$

Substituting Eq. C-30 into Eq. C-22 we have:

$$\overline{f_i}(u) = \frac{\alpha_i}{u^{v_i}}[\Gamma(v_i) - \Gamma(v_i, ut_i) - \gamma(v_i, ut_{i-1})] \text{ , } \quad \text{(C-31)}$$

where:

$$\Gamma(z) = \int_0^\infty t^{z-1} e^{-t} dt \text{ is the gamma function, } \quad \text{(C-32)}$$

$$\gamma(a,x) = \int_0^x e^{-t} t^{a-1} dt \text{ is the lower incomplete gamma function, and } \quad \text{(C-33)}$$

$$\Gamma(a,x) = \Gamma(a) - \gamma(a,x) = \int_x^\infty e^{-t} t^{a-1} dt \text{ is the upper incomplete gamma function. } \quad \text{(C-34)}$$

Substituting Eq. C-34 into Eq. C-31 we have,

$$\overline{f_i}(u) = \frac{\alpha_i}{u^{v_i}}[\gamma(v_i, ut_i) - \gamma(v_i, ut_{i-1})] \quad \text{(C-35)}$$

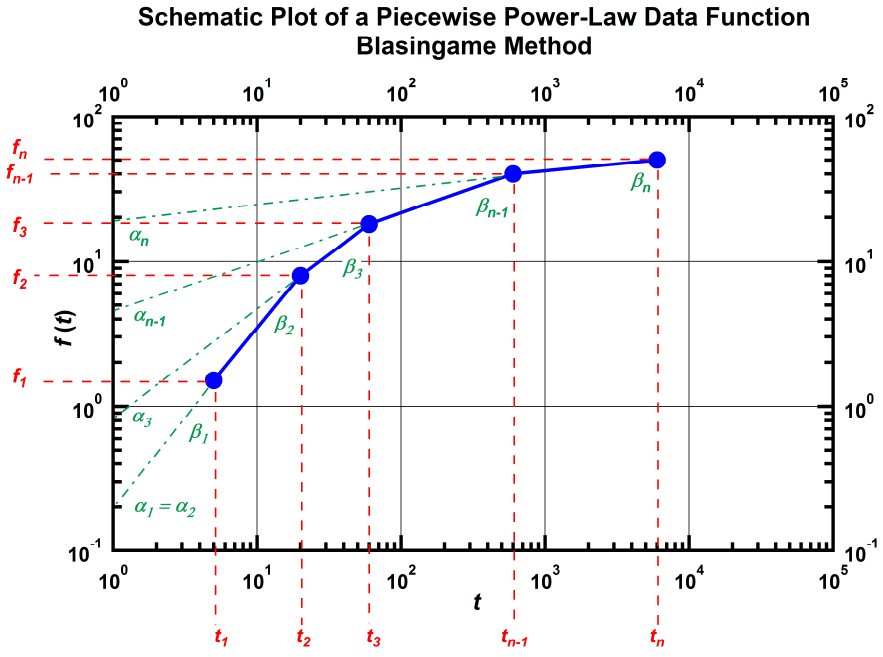

Figure C-3 — Schematic plot of a piecewise power-law data function used for Blasingame method numerical Laplace transform.

Presenting the first two and last two terms using Eq. C-35 yields:

$$i=1 \qquad \overline{f_1}(u)=\frac{\alpha_1}{u^{v1}}[\gamma(v_1,ut_1)]\,, \quad \text{(C-36)}$$

$$i=2 \qquad \overline{f_2}(u)=\frac{\alpha_2}{u^{v2}}[\gamma(v_2,ut_2)-\gamma(v_2,ut_1)]\,, \quad \text{(C-37)}$$

$$i=k-1 \qquad \overline{f}_{k-1}(u)=\frac{\alpha_{k-1}}{u^{vk-1}}[\gamma(v_{k-1},ut_{k-1})-\gamma(v_{k-1},ut_{k-2})]\,, \quad \text{(C-38)}$$

$$i=k \qquad \overline{f}_{k}(u)=\frac{\alpha_k}{u^{vk}}[\gamma(v_k,ut_k)-\gamma(v_k,ut_{k-1})] \quad \text{(C-39)}$$

For the last partition, $t_k \equiv \infty$, and recalling the definition of the upper incomplete gamma function, $\Gamma(a,x) = \Gamma(a) - \gamma(a,x)$, we consider $x = \infty$; hence, $\Gamma(a,\infty) = \Gamma(a) - \gamma(a,\infty)$. But, $\Gamma(a,\infty) = 0$; therefore, Eq. C-39 becomes:

$$i=k,\ t_k \equiv \infty \qquad f_k(u)=\frac{\alpha_k}{u^{vk}}\Gamma(v_k)-\frac{\alpha_k}{u^{vk}}\gamma(v_k,ut_{k-1}) \quad \text{(C-40)}$$

Substituting Eq. C-36, Eq. C-37, and Eq. C-40, into Eq. C-20, we have the resulting Laplace transform function as follows:

$$\bar{f}(u)=\frac{\alpha_1}{u^{v1}}\gamma(v_1,ut_1)+\frac{\alpha_2}{u^{v2}}\gamma(v_2,ut_2)-\frac{\alpha_2}{u^{v2}}\gamma(v_2,ut_1)+\ldots+\frac{\alpha_{k-1}}{u^{vk-1}}\gamma(v_{k-1},ut_{k-1})$$
$$-\frac{\alpha_{k-1}}{u^{vk-1}}\gamma(v_{k-1},ut_{k-2})+\frac{\alpha_k}{u^{vk}}\Gamma(v_k)-\frac{\alpha_k}{u^{vk}}\gamma(v_k,ut_{k-1})\,, \quad \text{(C-41)}$$

or,

$$\bar{f}(u)=\frac{\alpha_1}{u^{v1}}\gamma(v_1,ut_1)+\sum_{i=2}^{k-1}\left[\frac{\alpha_i}{u^{vi}}\gamma(v_i,ut_i)-\frac{\alpha_i}{u^{vi}}\gamma(v_i,ut_{i-1})\right]+\frac{\alpha_k}{u^{vk}}\Gamma(v_k)-\frac{\alpha_k}{u^{vk}}\gamma(v_k,ut_{k-1}) \quad \text{(C-42)}$$

From the continuous data function—in terms of our working variables: dimensionless time, t_D, and dimensionless rate, q_D, from the SE/PLE decline model data points — we compute the values of α_i and v_i using Eq. C-21 with two contiguous data points as follows,

$$q_{Dj}(t_D)=\alpha_i {t_D}_j^{\,v_i-1} \text{ and,} \quad \text{(C-43)}$$

$$q_{Dj+1}(t_D)=\alpha_i {t_D}_{j+1}^{\,v_i-1} \quad \text{(C-44)}$$

Solving Eq. C-43 and C-44 we find that:

$$v_i = \frac{\ln\left[\dfrac{q_{Dj}}{q_{Dj+1}}\right]}{\ln\left[\dfrac{t_{Dj}}{t_{Dj+1}}\right]} \qquad \text{(C-45)}$$

The values of α_i are computed from Eq. C-43. We compute the numerical Laplace transform function — in the form of Eq. C-42 as follows:

$$\bar{q}_D(u) = \frac{\alpha_1}{u^{v_1}}\gamma(v_1, ut_{D1}) + \sum_{i=2}^{k-1}\left[\frac{\alpha_i}{u^{v_i}}\gamma(v_i, ut_{Di}) - \frac{\alpha_i}{u^{v_i}}\gamma(v_i, ut_{Di-1})\right]$$

$$+ \frac{\alpha_k}{u^{v_k}}\Gamma(v_k) - \frac{\alpha_k}{u^{v_k}}\gamma(v_k, ut_{Dk-1}) \qquad \text{(C-46)}$$

The results obtained from Eq. C-46 — for different time exponent, *n*, values — are presented graphically in **Fig. C-4.**

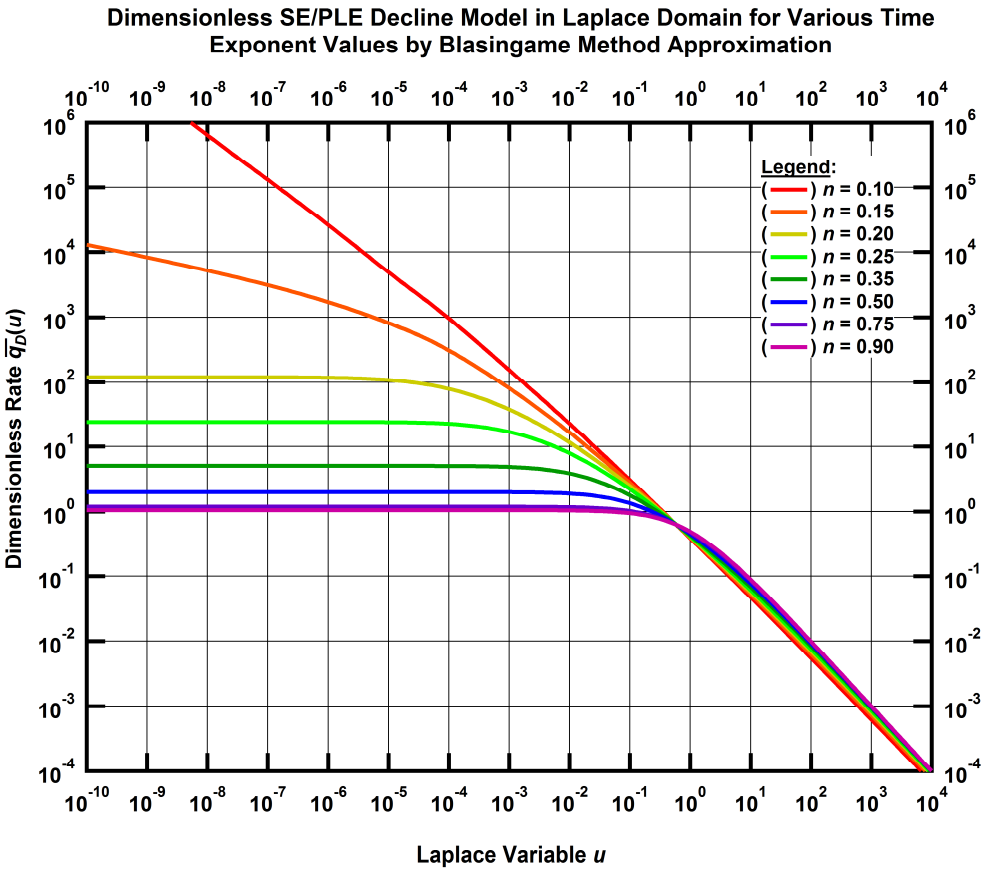

Figure C-4 — Dimensionless SE/PLE decline model in Laplace domain for various time exponent values, *n*, by Blasingame method approximation.

"Constant rate" pressure and pressure derivative from SE/PLE in Laplace domain (Blasingame method): Recalling the Laplace domain "convolution" mathematical expression, we have:

$$\overline{p}_{Dcr}(u) = \frac{1}{u^2 \overline{q}_{Dcp}(u)}, \quad \text{(C-47)}$$

where $q_{Dcp}(u)$ is the dimensionless flowrate in Laplace domain from a constant pressure solution and $p_{Dcr}(u)$ is the dimensionless pressure in Laplace domain from a constant rate solution. We attempt to resolve the dimensionless SE/PLE decline model in Laplace domain; therefore, we replace Eq. C-46 into the "convolution" integral in Laplace domain (Eq. C-47) to obtain the following expression:

$$\overline{p}_D(u) = \frac{1}{u^2}\left[\frac{\alpha_1}{u^{v_1}}\gamma(v_1, ut_{D1}) + \sum_{i=2}^{k-1}\left[\frac{\alpha_i}{u^{v_i}}\gamma(v_i, ut_{Di}) - \frac{\alpha_i}{u^{v_i}}\gamma(v_i, ut_{Di-1})\right]\right.$$

$$+\frac{\alpha_k}{u^{v_k}}\Gamma(v_k)-\frac{\alpha_k}{u^{v_k}}\gamma(v_k,ut_{Dk-1})\Bigg]^{-1} \quad \text{.....(C-48)}$$

Using Eq. C-48, we compute the "constant rate" pressure from the dimensionless SE/PLE decline model in Laplace domain approximation for different time exponent values, n, (*i.e.*: 0.10, 0.15, 0.20, 0.25, 0.35, 0.50, 0.75, and 0.90). These results are presented graphically in **Fig. C-5.**

To find the dimensionless pressure in real time domain, we use a numerical Laplace inversion algorithm because of the complexity and inability to invert analytically Eq. C-48. We choose the traditional Stehfest algorithm for the numerical Laplace inversion with 12 extrapolation coefficients, mathematically expressed as:

$$f(n,t)=\frac{\ln(2)}{t}\sum_{i=1}^{n}V_i\bar{f}\left[\frac{\ln(2)}{t}i\right] \quad \text{.....(C-49)}$$

where V_i are the Stehfest extrapolation coefficients given by:

$$V_i=(-1)^{n/2+i}\sum_{k=(i+1)/2}^{\min(i,n/2)}\frac{k^{n/2}(2k)!}{(n/2-k)!k!(k-1)!(i-k)!(2k-i)!} \quad \text{.....(C-50)}$$

These results are presented graphically in **Fig. C-6.** Additionally, it is possible to compute numerically the semi-log pressure derivative knowing that $f'(t)=L^{-1}\{uf(u)-f(t=0)\}$ and $dp/d\ln t=tdp/dt$; therefore,

$$p_D'(t)=tL^{-1}\left\{\frac{1}{u\,q_D(u)}\right\} \quad \text{.....(C-51)}$$

These results are presented graphically in **Fig. C-7.**

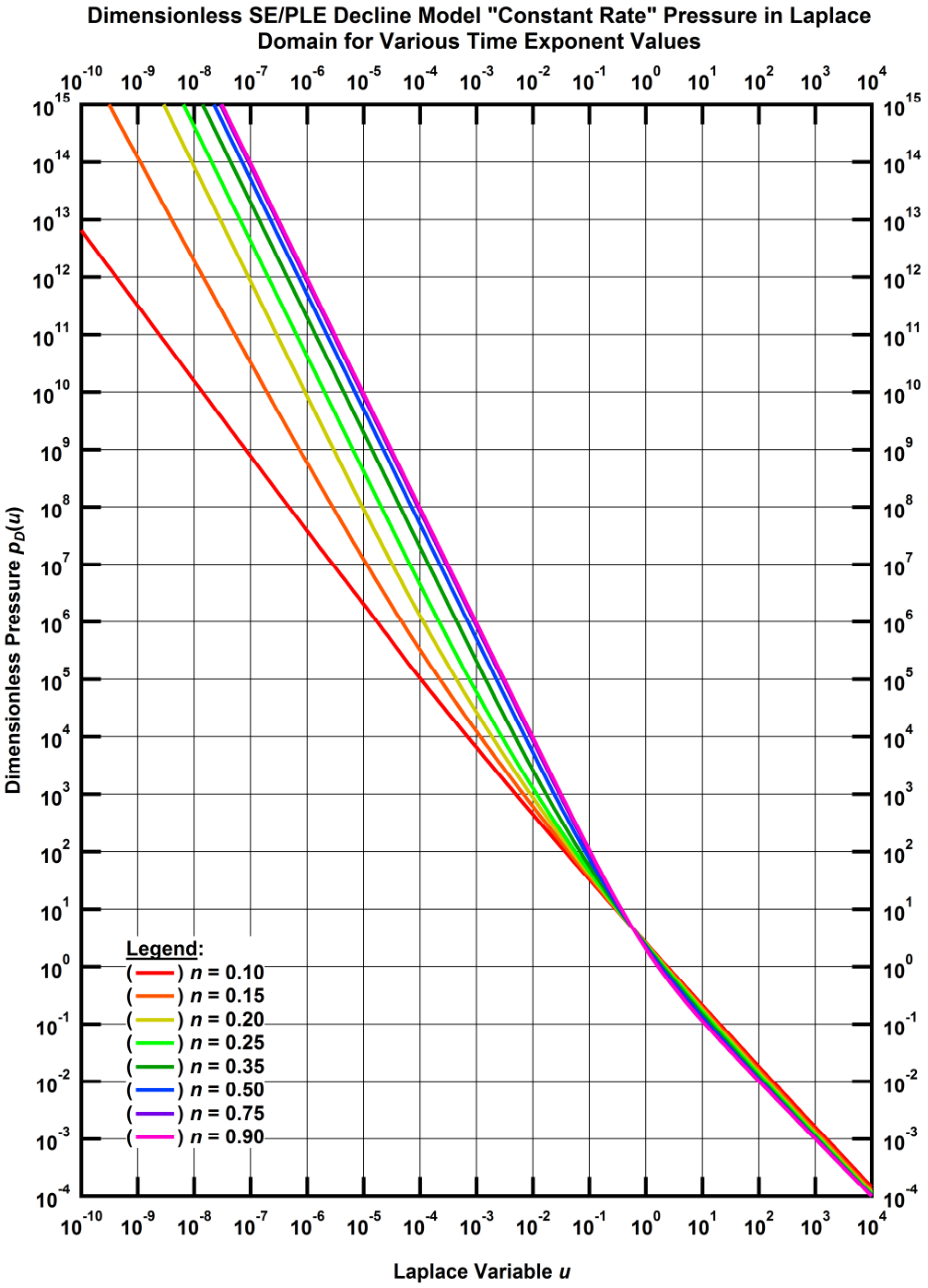

Figure C-5 — Dimensionless SE/PLE decline model "constant rate" pressure in Laplace domain for various time exponent values.

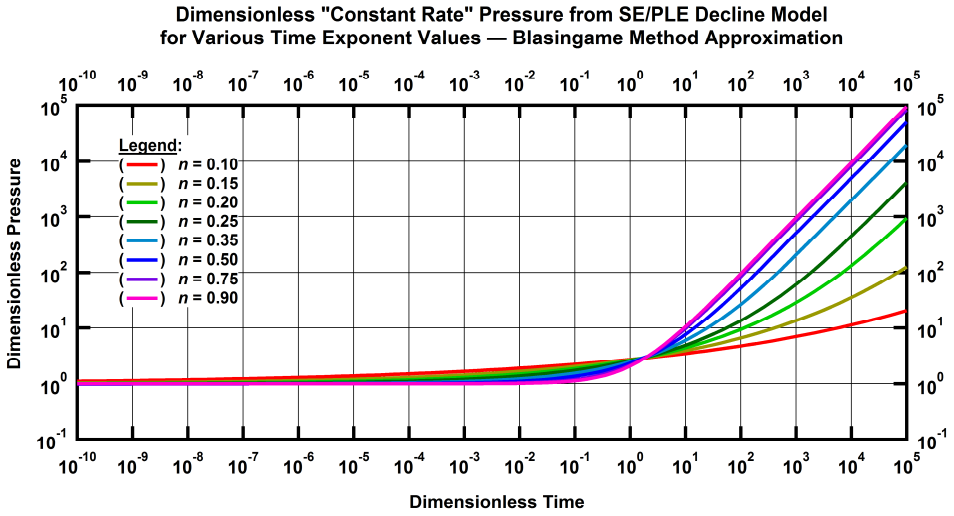

Figure C-6 — Dimensionless "constant rate" pressure from SE/PLE decline model for various time exponent values.

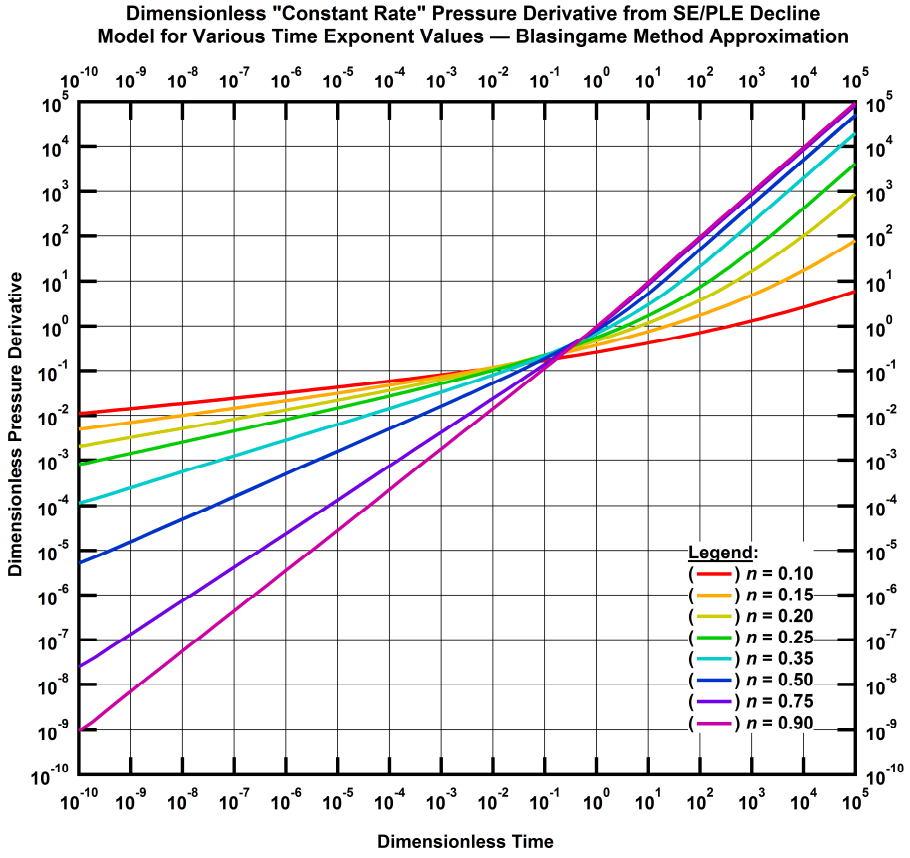

Figure C-7 — Dimensionless "constant rate" pressure derivative from SE/PLE decline model for various time exponent values.

APPENDIX D

VALIDATION OF TIME-RATE FLOW RELATIONS ASSUMING PSEUDOSTEADY-STATE FLOW BEHAVIOR: EXPONENTIAL, HYPERBOLIC, AND STRETCHED EXPONENTIAL/POWER-LAW EXPONENTIAL CASES

Constant p_{wf} Liquid Case (Exponential Decline):

The oil material balance relation is given as,

$$\overline{p} = p_i - m_{o,pss}\ N_p\ , \quad \text{.....(D-1)}$$

where the material balance coefficient is,

$$m_{o,pss} = \frac{B_o}{B_{oi}} \frac{1}{Nc_t} \quad \text{.....(D-2)}$$

The oil pseudosteady-state flow relation is given as,

$$\overline{p} = p_{wf} + b_{o,pss}\ q_o\ , \quad \text{.....(D-3)}$$

where the pseudosteady-state flow coefficient is,

$$b_{o,pss} = 141.2 \frac{\mu_o B_o}{kh} \left[\frac{1}{2} \ln \left[\frac{4}{e^{\gamma}} \frac{1}{C_A} \frac{A}{r_w^2} \right] + s \right] \quad \text{.....(D-4)}$$

Taking the derivative of the oil material balance relation (Eq. D-1) with respect to time yields,

$$\frac{d\overline{p}}{dt} = \frac{dp_i}{dt} - m_{o,pss} \frac{dN_p}{dt}\ ,$$

where we note that,

$$\frac{dp_i}{dt} = 0\ ,$$

and,

$$\frac{dN_p}{dt} = q_o\ ,$$

which reduces to the following form,

$$\frac{d\overline{p}}{dt} = -m_{o,pss}\ q_o \quad \text{.....(D-5)}$$

Similarly, taking the derivative of the oil pseudosteady-state relation (Eq. D-3) with respect to time, we have,

$$\frac{d\bar{p}}{dt} = \frac{dp_{wf}}{dt} + b_{o,pss}\,\frac{dq_o}{dt} \quad \text{.....(D-6)}$$

Substituting Eq. D-5 into Eq. D-6, yields,

$$-m_{o,pss}\,q_o = \frac{dp_{wf}}{dt} + b_{o,pss}\,\frac{dq_o}{dt}$$

Rearranging, we obtain,

$$\frac{1}{q_o}\frac{dq_o}{dt} = -\frac{m_{o,pss}}{b_{o,pss}} - \frac{1}{b_{o,pss}}\frac{1}{q_o}\frac{dp_{wf}}{dt}\,, \quad \text{.....(D-7)}$$

and for completeness, we can also solve Eq. D-7 for the dp_{wf}/dt term,

$$\frac{dp_{wf}}{dt} = -b_{o,pss}\,\frac{dq_o}{dt} - m_{o,pss}\,q_o \quad \text{.....(D-8)}$$

As an aside, setting Eq. D-1 and Eq. D-3 equal, we have,

$$\Delta p = (p_i - p_{wf}) = b_{o,pss}\,q_o + m_{o,pss}\,N_p \quad \text{.....(D-9)}$$

In addition, if we divide through Eq. D-9 by the flowrate (q_o), we obtain the identity,

$$\frac{\Delta p}{q_o} = b_{o,pss} + m_{o,pss}\,\frac{N_p}{q_o}\,, \quad \text{.....(D-10)}$$

where the form given by Eq. D-10 is the defining relationship for variable-rate, variable pressure drop production data analysis. In addition, solving Eq. D-9 for the flowing bottomhole pressure, p_{wf}, gives us,

$$p_{wf} = p_i - b_{o,pss}\,q_o - m_{o,pss}\,N_p \quad \text{.....(D-11)}$$

At this point, we return to our effort to derive a time-rate relation using Eq. D-8. To proceed, we must make an assumption regarding the behavior of p_{wf} (or more specifically dp_{wf}/dt) — in this case, we specifically assume that p_{wf} = constant (*i.e.*, $dp_{wf}/dt = 0$). Making this assumption, Eq. D-8 reduces to,

$$-b_{o,pss}\,\frac{dq_o}{dt} - m_{o,pss}\,q_o = 0 \quad \text{.....(D-12)}$$

Rearranging (*i.e.*, moving the constant terms to the right-hand-side), we have,

$$\frac{1}{q_O}\frac{dq_O}{dt} = -\frac{m_{O,pss}}{b_{O,pss}} \quad \text{.....(D-13)}$$

Considering the form given by Eq. D-13, we make the following definition for convenience,

$$D_i = \frac{m_{O,pss}}{b_{O,pss}} \quad \text{.....(D-14)}$$

Substituting Eq. D-14 into Eq. D-13 yields,

$$\frac{1}{q_O}\frac{dq_O}{dt} = -D_i \quad \text{.....(D-15)}$$

Multiplying through Eq. D-15 by the *dt* term yields our final form of the first order ordinary differential equation for time-rate behavior, which is given as,

$$\frac{1}{q_O} dq_O = -D_i \, dt \quad \text{.....(D-16)}$$

Eq. D-16 can be solved by direct integration as follows,

$$\int_{q_{oi}}^{q_O} \frac{1}{q_O} dq_O = -D_i \int_0^t dt \quad \text{.....(D-17)}$$

Completing the integration in Eq. D-17, we have,

$$\ln\left[\frac{q_O}{q_{oi}}\right] = -D_i \, t \quad \text{.....(D-18)}$$

Exponentiating both sides of Eq. D-18 and rearranging terms, we obtain the final form of the "exponential" decline relation,

$$q_O(t) = q_{oi} \, \exp[-D_i \, t] \quad \text{.....(D-19)}$$

At this point, we have demonstrated the process of deriving the exponential decline relation (*i.e.*, Eq. D-19) from basic principles. As bit of housekeeping, we need to define the "initial rate" (*i.e.*, the q_{oi} parameter). To begin, we recall Eq. D-3,

$$\overline{p} = p_{wf} + b_{O,pss} \, q_O \, , \quad \text{.....(D-3)}$$

and we note that at $t = 0$, $\overline{p} = p_i$ — hence, $q_o = q_{oi}$. Making these substitutions in Eq. D-3 yields the following result,

$$p_i = p_{wf} + b_{o,pss}\, q_{oi}$$

Solving for the q_{oi} parameter, we obtain,

$$q_{oi} = \frac{1}{b_{o,pss}}(p_i - p_{wf}) \quad \text{.....(D-20)}$$

At this point, we have clearly established the identity for q_{oi}. As an alternate form of Eq. D-20, we solve for $p_{i} - p_{wf}$, which yields,

$$(p_i - p_{wf}) = b_{o,pss}\ q_{oi} \quad \text{.....(D-21)}$$

We will now proceed to use this result in the defining relations to ensure that we have not violated any mathematics in creating Eq. D-19 — specifically, we will "test" Eq. D-19 in the governing relations that we used to define Eq. D-19 to ensure that this form is correct. Taking the derivative of Eq. D-19, we have:

$$\begin{aligned}\frac{dq_o}{dt} &= q_{oi}\ \frac{d}{dt}\left[\exp[-D_i\, t]\right] \\ &= -D_i\ q_{oi}\ \exp[-D_i\, t] \\ &= -D_i\ q_o \quad \text{.....(D-22)}\end{aligned}$$

Recalling Eq. D-8,

$$\frac{dp_{wf}}{dt} = -b_{o,pss}\ \frac{dq_o}{dt} - m_{o,pss}\ q_o \quad \text{.....(D-8)}$$

Substituting Eq. D-22 into Eq. D-8, we have,

$$\frac{dp_{wf}}{dt} = -b_{o,pss}\ (-D_i\ q_o\ ) - m_{o,pss}\ q_o \quad \text{.....(D-23)}$$

Substituting Eq. D-14 into Eq. D-23, we have our first validation of Eq. D-19 (*i.e.*, $dp_{wf}/dt = 0$)

$$\frac{dp_{wf}}{dt} = -b_{o,pss}\left[-\left[\frac{m_{o,pss}}{b_{o,pss}}\right] q_o\ \right] - m_{o,pss}\ q_o = 0 \quad \text{.....(D-24)}$$

Taking the integral of Eq. D-19, we have,

$$\begin{aligned}Np &= q_{oi} \int_0^t \exp[-D_i\, t]\, dt \\ &= -q_{oi}\ \frac{1}{D_i}[\exp[-D_i\, t] - 1]\end{aligned}$$

$$= q_{oi}\ \frac{1}{D_i}[1-\exp[-D_i\,t]]$$

$$= \frac{1}{D_i}[q_{oi}\ - q_o\ ] \quad \text{.....(D-25)}$$

Recalling Eq. D-9 for our next validation,

$$\Delta p = (\,p_i - p_{wf}\,) = b_{o,pss}\ q_o + m_{o,pss}\ N_p \quad \text{..... (D-9)}$$

Substituting Eq. D-25 and Eq. D-14 into Eq. D-9 yields,

$$(\,p_i - p_{wf}\,) = b_{o,pss}\ q_o + m_{o,pss}\ N_p$$

$$= b_{o,pss}\ q_o + m_{o,pss}\ \frac{1}{\dfrac{m_{o,pss}}{b_{o,pss}}}[q_{oi}\ - q_o\ ]$$

$$= b_{o,pss}\ q_o + b_{o,pss}\, q_{oi}\ - b_{o,pss}\, q_o$$

$$= b_{o,pss}\, q_{oi} \quad \text{.....(D-26)}$$

Substitution of Eq. D-21 into Eq. D-26, we have,

$$(\,p_i - p_{wf}\,) = (\,p_i - p_{wf}\,)$$

or,

$$p_{wf}\ = p_{wf} \quad \text{.....(D-27)}$$

While trivial, Eq. D-27 does confirm the validity of Eq. D-19.

Before proceeding to other time-rate relations, we need to establish a strategy for how to "prove" a given time-rate relation that is <u>not derived</u> from fundamental principles (*e.g.*, the power-law exponential decline model). The obvious test would be to compute the flowing <u>bottomhole</u> pressure (p_{wf}) using Eq. D-11 and compare this to the pressures from observed field data or from a simulation generated using a prescribed reservoir model. For reference, Eq. D-11 is given by,

$$p_{wf}\ = p_i - b_{o,pss}\ q_o - m_{o,pss}\ N_p \quad \text{.....(D-11)}$$

For the case of constant flowing bottomhole pressure (*i.e.*, p_{wf} = constant), Eq. D-11 has been proven (see above) to yield "$p_{wf} = p_{wf}$" which, while trivial, does validate that case. For cases other than the constant flowing bottomhole pressure, Eq. D-11 could be used (with the appropriate substitutions of the prescribed q_o and N_p from time-rate models) as a regression relation to validate the input time-rate model. Such a "proof" would be somewhat disingenuous given that one would just be proving that the input rate matches

the concepts of pseudosteady-state flow, but this could be one approach to proving the consistency of a given time-rate model.

Another "proof" could be to use the prescribed time-rate model (actually the time-cumulative form of a prescribed time-rate model) in the material balance equation (*i.e.*, Eq. D-1) to compare model performance and reservoir simulation results. Again, this would be slightly weak as a "proof" of a given model, but it could be used to prove consistency. Recalling Eq. D-1, we have,

$$\overline{p} = p_i - m_{o,pss}\ N_p \quad \text{.....(D-1)}$$

For the constant pressure case, we can substitute the appropriate form of Eq. D-25 into Eq. D-1 to obtain,

$$\overline{p} = p_i - m_{o,pss}\left[q_{oi}\ \frac{1}{D_i}[1-\exp[-D_i\ t]]\right] \quad \text{.....(D-28)}$$

Substituting Eq. D-14 into Eq. D-28, yields,

$$\overline{p} = p_i - m_{o,pss}\left[q_{oi}\ \frac{1}{\left[\frac{m_{o,pss}}{b_{o,pss}}\right]}[1-\exp[-D_i\ t]]\right]$$

$$= p_i - q_{oi}\ b_{o,pss}\,[1-\exp[-D_i\ t]] \quad \text{.....(D-29)}$$

Where the known form for $q_{oi}\,b_{o,pss}$ is given by Eq. D-21. Substituting Eq. D-21 into Eq. D-29 gives us,

$$\overline{p} = p_i - (p_i - p_{wf})\,[1-\exp[-D_i\ t]] \quad \text{.....(D-30)}$$

Continuing to reduce terms in Eq. D-30 leads to,

$$\overline{p} = p_{wf} + (p_i - p_{wf})\exp[-D_i\ t] \quad \text{.....(D-31)}$$

where it can be noted that Eq. D-31 is the result that one would obtain by directly solving this particular case starting with the pseudosteady-state flow equation (*i.e.*, Eq. D-3).

As noted above, our approach is to solve for the p_{wf} form for pseudosteady-state flow (*i.e.*, Eq. D-11), so that the model can be compared against measured or simulated well performance data.

Hyperbolic Time-Rate Model

The hyperbolic time-rate model, derived from empirical observations, is given by,

$$q_o(t) = \frac{q_{oi}}{[1+bD_i t]^{1/b}} \quad \text{.....(D-32)}$$

The starting point for this development is to establish the cumulative production form for Eq. D-32. Taking the integral of Eq. D-32, we have,

$$N_p(t) = \int_0^t \frac{q_{oi}}{[1+bD_i t]^{1/b}} dt$$

$$= \frac{q_{oi}}{(1-b)D_i}[1-(1+bD_i t)^{1-1/b}] \quad \text{.....(D-33)}$$

Recalling Eq. D-11, we have,

$$p_{wf} = p_i - b_{o,pss}\, q_o - m_{o,pss}\, N_p \quad \text{.....(D-11)}$$

Substituting Eq. D-32 and Eq. D-33 into Eq. D-11 gives us,

$$p_{wf} = p_i - b_{o,pss}\left[\frac{q_{oi}}{[1+bD_i t]^{1/b}}\right] - m_{o,pss}\left[\frac{q_{oi}}{(1-b)D_i}[1-(1+bD_i t)^{1-1/b}]\right] \quad \text{.....(D-34)}$$

Reforming Eq. D-34 into a regression relation (*i.e.*, assigning arbitrary parameters for the model coefficients), we obtain,

$$p_{wf} = a_1 - a_2 \frac{1}{[1+a_3 t]^{1/a_4}} - a_5 [1-(1+a_3 t)^{1-1/a_4}], \quad \text{.....(D-35)}$$

where in Eq. D-35 the parameters a_1, a_2, a_3, a_4, and a_5 are arbitrary coefficients, to be determined by regression. Recalling the oil pseudosteady-state flow relation,

$$\bar{p} = p_{wf} + b_{o,pss}\, q_o \quad \text{.....(D-3)}$$

Solving for $(\bar{p} - p_{wf})$ we have,

$$(\bar{p} - p_{wf}) = b_{o,pss}\, q_o \quad \text{.....(D-36)}$$

Substituting the hyperbolic time-rate relation, gives,

$$(\bar{p} - p_{wf}) = b_{o,pss}\, q_{oi}[1+bD_i t]^{-1/b} \quad \text{.....(D-37)}$$

Reforming Eq. D-37 into a regression relation (*i.e.*, assigning arbitrary parameters for the model coefficients) we obtain,

$$(\bar{p} - p_{wf}) = m_1[1+m_2 t]^{-1/m_3} \quad \text{.....(D-38)}$$

where in Eq. D-38 the parameters m_1, m_2, and m_3 are arbitrary coefficients, to be determined by regression.

Power-Law Exponential Time-Rate Model

The power-law exponential time-rate model, derived from empirical observations, is given by,

$$q_o(t) = \hat{q}_{oi} \exp[-\hat{D}_i t^n - D_\infty t] \quad \text{.....(D-39)}$$

The specific "objective" of this effort will be to establish the functional form of $p_{wf}(t)$ such that this form satisfies the power-law exponential time-rate model (*i.e.*, Eq. D-39). Recall that for the exponential decline case, the specific form of $p_{wf}(t)$ required to satisfy the relation,

$$p_{wf}(t) = \text{constant} \quad \text{.....(D-40)}$$

It is worth noting at this point that the oil material balance relation (Eq. D-1) and the oil pseudosteady-state flow relation (Eq. D-3) are rigorous — that is, these relations are not where we propose any empiricism — our objective will be to "reverse engineer" the functional form of $p_{wf}(t)$ using Eq. D-11 (which is rigorous for pseudosteady-state flow behavior), coupled mathematically with the power-law exponential time-rate model (Eq. D-39).

The starting point for this development is to establish the cumulative production form for Eq. D-39. Taking the integral of Eq. D-39, we have (we must assume $D_\infty = 0$ as the integral for the case where $D_\infty \neq 0$ does not exist),

$$\begin{aligned} N_p(t) &= \hat{q}_{oi} \int_0^t \exp[-\hat{D}_i t^n]\, dt \\ &= \hat{q}_{oi} \left[-\frac{\hat{D}_i^{-1/n}}{n} \Gamma\left[\frac{1}{n}, \hat{D}_i t^n\right] + \frac{\hat{D}_i^{-1/n}}{n} \Gamma\left[\frac{1}{n}, 0\right] \right] \\ &= \hat{q}_{oi} \frac{\hat{D}_i^{-1/n}}{n} \left[\Gamma\left[\frac{1}{n}\right] - \Gamma\left[\frac{1}{n}, \hat{D}_i t^n\right] \right] \end{aligned} \quad \text{.....(D-41)}$$

Recalling Eq. D-11, we have,

$$p_{wf} = p_i - b_{o,pss}\, q_o - m_{o,pss}\, N_p \quad \text{.....(D-11)}$$

Substituting Eq. D-39 and Eq. D-41 into Eq. D-11 (assuming $D_\infty = 0$) gives us,

$$p_{wf} = p_i - b_{o,pss}\, \hat{q}_{oi} \exp[-\hat{D}_i t^n] - m_{o,pss}\, \hat{q}_{oi} \frac{\hat{D}_i^{-1/n}}{n} \left[\Gamma\left[\frac{1}{n}\right] - \Gamma\left[\frac{1}{n}, \hat{D}_i t^n\right] \right] \quad \text{.....(D-42)}$$

Reforming Eq. D-42 into a regression relation (*i.e.*, assigning arbitrary parameters for the model coefficients), we obtain,

$$p_{wf} = c_1 - c_2 \exp[-c_3 t^{c4}] - c_5 \left[\Gamma\left[\frac{1}{c_4}\right] - \Gamma\left[\frac{1}{c_4}, c_3 t^{c4}\right] \right], \quad \text{(D-43)}$$

where in Eq. D-43 the parameters c_1, c_2, c_3, c_4, and c_5 are arbitrary coefficients, to be determined by regression.

Recalling the oil pseudosteady-state flow relation,

$$\bar{p} = p_{wf} + b_{o,pss}\, q_o \quad \text{(D-3)}$$

Recalling the solution for $(\bar{p} - p_{wf})$ we have,

$$(\bar{p} - p_{wf}) = b_{o,pss}\, q_o \quad \text{(D-36)}$$

Substituting the power-law exponential time-rate relation gives,

$$(\bar{p} - p_{wf}) = b_{o,pss}\, \hat{q}_{oi} \exp[-\hat{D}_i t^n - D_\infty t] \quad \text{(D-44)}$$

Reforming Eq. D-44 into a regression relation (*i.e.*, assigning arbitrary parameters for the model coefficients), we obtain,

$$(\bar{p} - p_{wf}) = d_1 \exp[-d_2 t^{d3} - d_4 t] \quad \text{(D-45)}$$

Where in Eq. D-45 the parameters d_1, d_2, d_3, and d_4 are arbitrary coefficients, to be determined by regression — coefficient d_4 (*i.e.*, D_∞) can be assumed to be zero.